BIOSORPTION OF Fe^{2+} FROM POTABLE WATER USING NATURAL AND MODIFIED SUGARCANE BAGASSE

Submitted in fulfilment of the requirements of the degree of Master of Engineering in the Faculty of Engineering and the Built Environment at the Durban University of Technology

Nompumelelo Lindi Gelsiah Ndebele

2022

Supervisor: Prof P. Musonge

Co-Supervisor: Prof B.F. Bakare

DEDICATION

I would like to dedicate this work to my daughter, Senamile Lubanzi Zenande Khumalo and my mother- the phenomenal woman, my pillar of strength, Mrs Sibongile Margaret Ndebele.

DECLARATION

I, **Nompumelelo Lindi Gelsiah Ndebele**, declare that

(i) The research reported in this thesis is my original work, except otherwise indicated.

(ii) This thesis has not been submitted for any degree or examination at any other university.

(iii) This thesis does not contain other persons' data, pictures, graphs or other information, unless expressly acknowledged as being sourced from other persons.

(iv) This thesis does not contain other persons' writing, unless expressly acknowledged as being sourced from other researchers. Where other written sources have been quoted, then:

a) Their words have been re-written but the general information attributed to them has been referenced;

b) Where their exact words have been used, their writing has been placed inside quotation mar, and referenced.

(v) This thesis does not contain text, graphics or tables copied and pasted from the Internet unless specifically acknowledged. The source is detailed in the theories and the references sections.

Candidate: Ms. N.L.G. Ndebele

Signature: Date: 13th May 2023

As supervisors of the candidate above, we agree to submit this dissertation.

Co-supervisor: Prof. B.F. Bakare

Signature: Date: 13th May 2023

Supervisor: Prof. P. Musonge

Signature: Date: 13th May 2023

LIST OF CONFERENCE PRESENTATIONS

- N.L.G Ndebele, P. Musonge and BF Bakare. Characterization of sugarcane bagasse for the removal of heavy metals from wastewater. Third International Conference on Composites, Biocomposites and Nanocomposites, Book of abstracts, Page 67 (2018); Nelson Mandela Bay Stadium, PE

- Ndebele N. and Musonge P. Biosorption of Fe (II) from wastewater using natural and modified sugarcane bagasse. Book of Abstracts. 4TH Interdisciplinary Research and Innovation Conference, Page 62 (2019)

- 6TH South African Young Water Professionals (YWP-ZA) Biennial Conference, 23-23 October 2019; Durban ICC

- N.L.G Ndebele, P. Musonge and B.F Bakare. Biosorption of Fe (II) from wastewater using natural and alkali-modified sugarcane bagasse. Green Technologies for Sustainable Development, Pages 119 -134 (2021).

ACKNOWLEDGEMENTS

I would firstly like to thank my Almighty for giving me the strength and courage throughout this work. I would also like to thank my supervisors, Prof. P. Musonge and Prof. B.F. Bakare for their continued support and guidance. I would like to thank my family for their support, not forgetting to give thanks to my friends and colleagues for their support.

I would like to thank NRF for their financial assistance.

ABSTRACT

Even though some metals are crucial for the health and development of human bodies, their presence in higher concentrations is worrisome because it has a detrimental effect on people's health. These heavy metals cause cancer and cannot be broken down by biological processes. The removal of heavy metals from water using traditional techniques; such as reverse osmosis, precipitation, ion exchange; has been the subject of extensive investigation. However, because these processes are so expensive to run, a lot of research is currently focusing on using agricultural biomasses to remove these heavy metals. Dumping of this agricultural waste (sugarcane bagasse) in landfills creates dangers of spontaneous combustion, because of microbial activities.

The functionality of circular economy depends on waste resources being utilized to their fullest potential, with almost no production of recoverable waste. In a circular economy, sugarcane bagasse is utilized as a fuel source for the boilers that generate process steam and electricity in the sugar mill facilities. Sugarcane bagasse is used in the manufacturing of paper and paper goods, as well as in the agricultural sector. Stakeholders across the value chain, from product design to waste management, This study fulfils the functionality of the circular economy where it looks at extracting the valuable components of the sugarcane bagasse, then further using the sugarcane bagasse to remove heavy metals from potable water.

In this study, the adsorption capacities of unmodified and modified sugarcane bagasse for removing Fe^{2+} from potable water were investigated in batch experiment studies. Sugarcane bagasse comprises cellulose, hemicellulose and lignin. In order to determine the effect of removing/ extracting each component from the sugarcane bagasse, sugarcane bagasse was pretreated with different concentrations of sodium hydroxide and sulphuric acid, ranging between 0.5 wt% and 2.5 wt%, predominantly used to extract lignin and hemicellulose.

A cellulosic structure was left behind after the simultaneous removal of both amorphous components (the lignin and the hemicellulose) using the combined pretreatments of sodium hydroxide and sulfuric acid. The advantages of extracting or eliminating these components came from their high value in many sectors. Lignin is used in the paper business and costs between R11 300 and R17 420 per ton, hemicellulose is used in the pharmaceutical sector and costs between R500 and R1000 per ton, and cellulose is utilized in the textile sector.

The concentrations of all chemical pretreatments used on the sugarcane bagasse ranged from 0.5 to 2.5%, with alkaline pretreatments intended to extract lignin, acid pretreatments intended to extract hemicellulose, and combination pretreatments intended to remove both lignin and hemicellulose. While cellulose content increased from 32.02 to 65.65% after sodium hydroxide pretreatment, lignin and hemicellulose content reduced from 22.30 and 24.30% to 7.56% and 13.63%, respectively. Lignin and hemicellulose concentration for the sulphuric acid pretreatment went from 22.30 and 24.30% to 14.90% and 13.63%, respectively, while cellulose content went from 35.02 to 65.65%.

After the sugarcane bagasse underwent chemical pretreatments, batch studies were conducted on both the natural and chemically pretreated sugarcane bagasse in order to determine how the removal of lignin, hemicellulose, and cellulose affected the performance of the biosorbents in the biosorption of Fe^{2+} from drinkable water. To assess the efficacy of natural and modified sugarcane bagasse on the Fe^{2+} removal, the operational parameters investigated in the batch experiments were initial concentration ranging from 1 to 30 mg/L; pH ranging from 2 to 7, contact time ranging from 5 -100 minutes, and adsorbent dose ranging from 0.2 to 1.4 g.

For every variation investigation, one variable was varied at a time while keeping the other variables constant. The experimental runs done were repeated thrice and average values are reported throughout the study. According to the biosorption results, 1% NaOH was the best performing biosorbent for the alkali-pretreatment. The most effective biosorbent for the acid-pretreatment variation was 2.5% H_2SO_4. The optimal combination for the pretreatment was (0.5% NaOH + 0.5% H_2SO_4).

Regarding initial concentration variations, all biosorbents were most effective at a concentration of 1 mg/L, where natural sugarcane bagasse was able to remove 50% of Fe^{2+}, 1% NaOH was able to remove 99.7% Fe^{2+}, 2.5% H_2SO_4 removed 75.93% Fe^{2+}, and the combined-pretreated biosorbent of (0.5% NaOH + 0.5% H_2SO_4) removed 87.17% Fe^{2+}.

The increase in biosorbent dose led to an increase efficiency of the natural and chemically pretreated biosorbents. The highest removal of Fe^{2+} was obtained at 1 g (both for the natural and for all the pretreated biosorbents), with 32.2% for the natural; 79.04% for the 1% NaOH; 58.79% for the 2.5% H_2SO_4 and 70.73% for (0.5% NaOH + 0.5% H_2SO_4).

Results of the study also showed that the highest removal of Fe^{2+} for the pH variation of 2-7 was at pH "6" for both the natural and pretreated biosorbents. For the variation of the agitation speed, the highest Fe^{2+} removal was at 160 rpm with 52% Fe^{2+} removal for the natural sugarcane bagasse.

The Langmuir and Freundlich adsorption isotherms were used to study the biosorption mechanisms. Good correlation coefficients (R^2) of > 0.95 were obtained for both the Langmuir and Freundlich isotherms for both the natural and modified sugarcane bagasse, indicating that the biosorption followed both homogeneous and heterogeneity interaction between Fe^{2+} ions and active functional groups of the surface and pores of the biosorbents. Biosorption results for the natural sugarcane bagasse best fitted with the Langmuir isotherm with q_{max} of 0.770 mg/g, R^2 of 0.987 and R_L of 0.938. The alkali and acid-pretreated biosorbents favoured both the Langmuir and Freundlich isotherms with $R^2 > 0.95$; $R_L < 1$ and $\frac{1}{n} < 1$. The highest q_{max} of 9.199 and 5.743 mg/g was obtained at 1% NaOH and 2.5% H_2SO_4, respectively. The combined pretreatment fitted best with only the Langmuir isotherm with R^2 of 0.987, the R^2 of the Freundlich isotherm was less than 0.9. The biosorption of Fe^{2+} followed both the pseudo-first-order and pseudo-second-order kinetic reactions with $q_{e_{(exp)}}$ in close proximity to $q_{e_{(calc)}}$ and $R^2 > 0.9$. These results showed that sugarcane bagasse had great adsorption capacity after removing the valued components, namely, lignin and hemicellulose.

Characterization studies, which included FTIR, XRD, BET and SEM, were also carried out on the natural and pretreated bagasse before and after adsorption experiments. FTIR confirmed the existence of carbonyl, hydroxyl and carboxyl functional groups as major groups responsible for the adsorption of Fe^{2+} onto the natural and pretreated sugarcane bagasse. XRD revealed that the natural structure of the sugarcane bagasse was of native cellulose consisting of both amorphous and crystalline regions; this structure became more crystalline after the chemical pretreatments as the crystallinity index increased from 39.04% to 66.85% at 1% NaOH; 57.47% at 2.5% H_2SO_4; and 57.92% at (0.5% NaOH + 0.5%H_2SO_4).

The natural sugarcane bagasse structure featured rough surfaces, according to SEM data, and the main constituents were silicon (Si), carbon (C), and oxygen (O). According to the BET data, employing 1% NaOH, 2.5% H_2SO_4, and (0.5% NaOH + 0.5% H_2SO_4), respectively, the initial surface area of 0.904 cm^3/g rose to 1.503, 1.233, and 1.376 cm^3/g and the pore size of 56.33˚A increased to 99.63, 93.680, and 99.10˚A. According to the EDS data, sodium hydroxide pretreatment performed better in terms of adsorption, followed by combined pretreatment and

sulphuric acid. The natural sugarcane bagasse, 1% NaOH, 2.5% H_2SO_4, and (0.5% NaOH + 0.5% H_2SO_4) were able to biosorb 0.77, 7.89, 1.63, and 3.8% Fe^{2+}, respectively.

***Keywords*: Sugarcane bagasse, heavy metals, cellulose, lignin, hemicellulose.**

TABLE OF CONTENT

LIST OF FIGURES

LIST OF TABLES

GLOSSARY

Symbol	Description
AAS	Atomic Absorption Spectroscope
˚A	Angstrom
˚C	Degree Celsius
BET	Brunauer Emmett Teller
C_e	Equilibrium metal ion concentration
C_o	Initial metal ion concentration
C_t	Concentration of metal ion at time *t*
CI	Crystallinity Index
EDX	Energy Dispersive X-ray Spectroscopy
I_{002}	Intensity diffraction (002) plane ($2\theta = 22.5^{o}$)
I_{am}	Intensity diffraction (002) plane ($2\theta = 18.4^{o}$)
k_1	pseudo-1st-order constant
k_2	pseudo-2nd-order constant
K_L	Langmuir adsorption constant
Q_e	Adsorption capacity at equilibrium
$Q_{e(exp)}$	Experimental adsorption capacity
$Q_{e(calc)}$	Calculated adsorption capacity
Q_m	Monolayer adsorption capacity
Q_{max}	Maximum metal ion update per unit mass of adsorbent
Q_t	Adsorption capacity at time *t*
R	Gas constant
R_L	Dimensionless constant of separation factor
rpm	revolution per minute
SEM	Scanning Electron Microscope
T	Temperature
t	time
V	Volume of the adsorbate solution

W	weight of the adsorbent
wt%	weight percentage
XRD	X-Ray Diffraction Spectroscope

N.B

Alkali-pretreated biosorbent - biosorbent that has been pretreated with sodium hydroxide

Acid -pretreated biosorbent - biosorbent that has been pretreated with sulphuric acid

Alkali-pretreated biosorbent - biosorbent that has been pretreated with sodium hydroxide followed by sulphuric acid

0.5%NaOH – biosorbent pretreated with sodium hydroxide concentration of 0.5%

0.5%H_2SO_4 – biosorbent pretreated with sulphuric acid concentration of 0.5%

0.5% NaOH + 0.5%H_2SO_4 – biosorbent firstly pretreated with 0.5% sodium hydroxide then followed by 0.5% sulphuric acid

PREFACE

This experimental project was carried out at the Mangosuthu University of Technology.

CHAPTER 1

1. Introduction

Significant health consequences from heavy metals in drinking water include stunted growth and development, organ and nervous system damage, and liver and organ damage. According to (Babel and Kurniawan 2003) exposure to heavy metals can have serious health consequences, such as stunted growth and damages to the organ and brain. The World Health Organization (WHO) has produced regulation laws that specify the permitted concentration of certain metals in potable water in order to reduce human and environmental exposure to these hazardous metals. The South African National Standard (SANS) states that Fe^{2+} levels in drinking water must not be more than 0.04 milligrams per litre. If Fe^{2+} levels rise over these permitted levels, it may cause diabetes as well as harm to the pancreas and cardiovascular system.

The World Health Organization (WHO) defines potable water as water that satisfies the national and state standards and is deemed safe for human consumption. However, to reduce wastewater to acceptable or specified concentrations, wastewater treatment plants adhere regulations established by the WHO. High concentrations of heavy metals have, nevertheless, been found in several drinkable water samples. According to (Lasheen *et al.* 2008), increasing Fe^{2+} concentration in potable water may have been caused by various water pipe types, pipe aging, stagnation of treated water in reservoirs, and other factors.

(Mebrahtu and Zerabruk 2011), conducted a study of the heavy metals present in potable water. They collected potable water from urban areas in Northern Ethiopia and found that the water's physico-chemical parameters were higher than those advised by the World Health Organization (WHO). In particular, Fe^{2+} concentrations were 37.3% higher than the WHO's allowable limit.

Their findings demonstrated that although wastewater treatment plants reduce wastewater to levels that are safe for drinking water, there are still additional factors that may increase the concentration of heavy metals in this water. High concentrations of heavy metals in drinking water may have physiological impacts on human health, including issues with the pancreas and the kidneys. As a result, it is necessary to put quality control tools like filters on drinking water faucets. There are currently wide varieties of established conventional technologies/methods for removing these heavy metals from wastewater, although some of them are limited by insufficient metal removal,

These conventional techniques include ion exchange, adsorption, solvent extraction, membrane filtering, chemical precipitation, lime coagulation, and reverse osmosis. According to numerous studies in the literature, the biosorption method has therefore become an effective, affordable, and environmentally friendly approach to eliminate heavy metals in potable water as a result of the drawbacks of the current technologies (Ngah and Hanafiah 2008; Sud, Mahajan and Kaur 2008). Due to its vast surface area, activated carbon has historically been the most popular adsorbent; nevertheless, due to its high maintenance requirements and significant waste production, it is also frequently associated with high disposal costs (Duranoğlu, Trochimczuk and Beker 2012).

Agricultural wastes have received a lot of attention as prospective biosorbents for the removal of heavy metals from contaminated water because of the limitations of activated carbon. A higher surplus of agricultural waste has also resulted from the rise in demand for food and agricultural wastes (Niu *et al.* 2014).

The biosorption technique used in this study to remove Fe^{2+} from potable water used sugarcane bagasse as a biosorbent. A tropical, perennial grass belonging to the tribe Andropogoneae, genus Saccharum, and family Poaceae is known as sugarcane. Sugarcane is mostly farmed in KwaZulu-Natal, Mpumalanga, and the Eastern Cape in South Africa, where it needs mean temperatures between 22 and 32℃. Little growth occurs at temps below 20 °C and above 34 °C. A common feedstock for the manufacturing of ethanol and sugar is sugarcane bagasse. The residue (sugarcane bagasse) left over after the sugarcane is milled to extract the sucrose has important components of 42% cellulose, 33.5% hemicellulose, and 20% lignin (Betancur and Pereira Jr 2010).

Due to microbial activity in the dumps, dumping of this agricultural waste in landfills creates dangers of spontaneous combustion (Devnarain, Arnold and Davis 2002). The functionality of circular economy depends on waste resources being utilized to their fullest potential, with almost no production of recoverable waste. Therefore, this study looks at removing the valuable components of the sugarcane bagasse and then using the sugarcane bagasse to remove heavy metals (Fe^{2+}) from potable water.

1.1 Problem statement

The presence of heavy metals in higher concentration in potable water is of great concern since these heavy metals have negative effect on human health. Although there are stipulated measures compiled by the World Health Organisation that strictly state the allowable lower and higher limits of heavy metals; there has been many case, backed up by previous researches, where heavy metals are detected in drinking water. Another motive behind this study was a visitation to one of the wastewater treatment plants in KwaZulu Natal where they had very high concentrations of Fe^{2+} and Mn^{2+} in their influent stream.

Given that heavy metals have harmful effects on human health, their presence in increased concentrations in drinking water is a major cause for concern. Although the World Health Organization has established precise guidelines that outline the acceptable lower and upper limits of heavy metals, there have been numerous instances of heavy metals being found in drinking water, which are supported by earlier studies. This work was also motivated by a visit to a wastewater treatment facility in KwaZulu Natal that showed extremely high levels of Fe^{2+} and Mn^{2+} in its influent stream.

Therefore, this study investigated the possibility of removing these two metals at the secondary stage of water treatment using a cheap and easily accessible sugarcane bagasse. If successful in getting rid of these metals, sugarcane bagasse can be utilized to create filters that can be put on household faucets of heavy metals prior to community use.

1.2 Aims and Objectives

The aim of this study was to evaluate the performance and biosorption mechanism of the natural and chemically modified forms of the sugarcane bagasse in removing Fe^{2+} and Mn^{2+} from potable water.

In order to achieve the aim of this study, the following steps were followed:

I. Preparation of the natural sugarcane bagasse
II. Chemical pretreatment of the modified sugarcane bagasse
III. Characterization of the natural and modified bagasse before adsorption experiments
IV. Batch adsorption experiments were conducted
V. Characterization of the natural and modified bagasse before adsorption experiments
VI. Batch experiments were conducted in order to establish the treatment kinetics and isotherms.

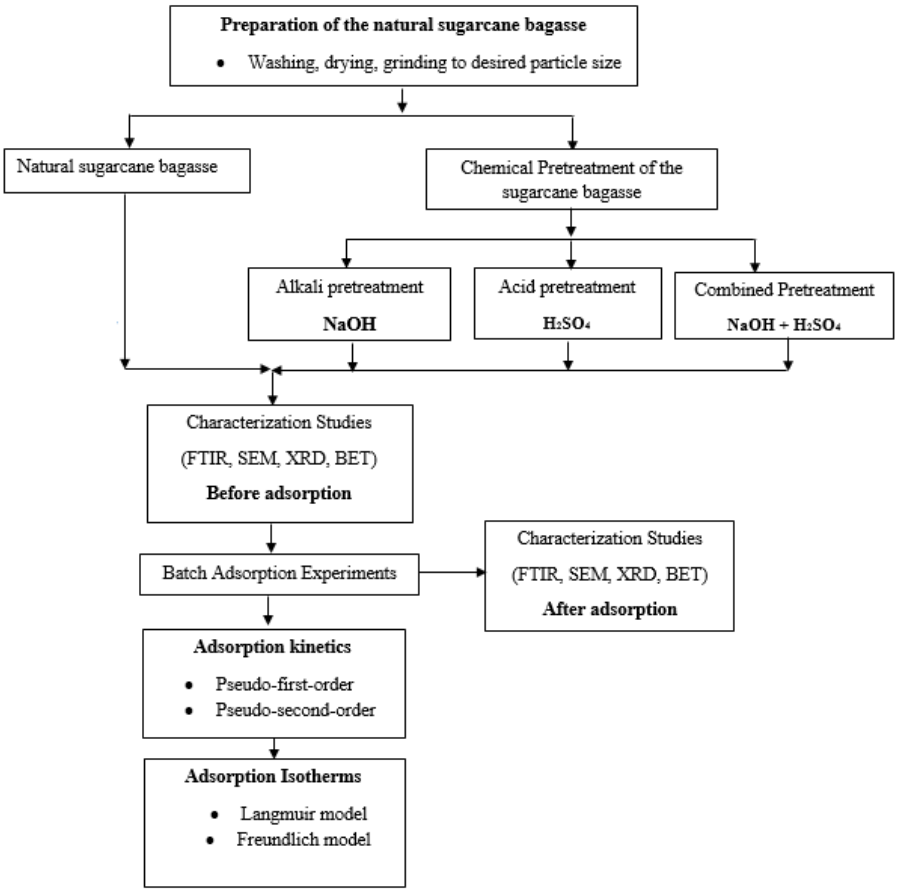

Figure 1.1: The graphical methodology of the study

1.3 Thesis outline

Chapter	Outline
1: Introduction	In this section, the project is introduced by stating the project statement. This chapter states the aims and objectives, forming the guideline and providing the structure for completing this work
2: Literature review	This section focuses on guidelines of heavy metals stipulated by WHO and the different conventional methods used to remove heavy metals potable water.
3: Materials and methods	This chapter discusses how the objectives were carried out in order to achieve the main aim of the project, listing all the equipments, reagents and procedure followed
4: Results and discussion	The data obtained from the experimental runs are explained and results clearly stated
5. Conclusion	Overall findings of the project are further discussed and conclusion stated

CHAPTER 2

2.1 Literature review

2.1.1 Potable water

The provision of safe potable water of sufficiently high quality should be regarded as an important health priority given the fact that fresh water is essentially a vital component for survival in human life. The presence of heavy metals in potable water can have a direct (drinking) or indirect (productivity of crops) negative impact on the human body. While most heavy metals are essential elements for the well-being of the human body, their presence at high levels can be associated with increased risks of heart and liver diseases, diabetes, endocrine problems, vomiting, vision problems, etc. In order to ensure that these heavy metals do not impose a danger to the community, the government has stipulated restrictions on allowable limit of heavy metal concentrations in potable water. For safe consumption of potable water, the allowable concentrations of heavy metals in potable water stipulated by the South African National Water standards (SANS 241) are ascribed in Table 2.1.

Table 2.1: Allowable concentration of heavy metals in potable water

Heavy metal	Recommended Operation limit (mg/L)	Heavy metal	Recommended Operation limit (mg/L)
Magnesium	0,007	Chromium	0,100
Potassium	0,005	Cobalt	0,500
Sodium	0,020	Copper	1.000
Zinc	0,005	Iron	0,030
Aluminum	0,030	Lead	0,020
Nickel	0,150	Manganese	0,010

2.1.2 Iron (Fe^{2+})

Fe^{2+} is essentially an abundant element in human nutrition. The requirement for Fe^{2+} depends on certain factors such as physiological status, sex, age and iron bioavailability ranging between 10 to 50 mg/day. In the human body, Fe^{2+} mainly exists in complex forms bound to proteins such as hemoglobin or myoglobin, heme-enzymes or nonheme compounds. Fe^{2+} is required by the body for the synthesis of its oxygen-transporting proteins, particularly hemoglobin, and myoglobin and

for the formation of heme enzyme and other iron-containing enzymes involved in electron transfer and oxidation-reaction processes. According to the WHO International Standard for drinking water, the allowable concentration of Fe^{2+} in drinking water ranges should be less than 0.03 mg/L. Excessive concentration of Fe^{2+} can have a negative impact on human health, which can lead to damage to tissues, vomiting and neurodegenerative diseases (Stephenson *et al.* 2014).

In order to mitigate the issue of heavy metals, many researchers have embarked on researches to remove these toxic metals using different types of conventional methods. These methods include ion exchange, reverse osmosis, precipitation, etc.

2.2 Conventional processes used to remove heavy metals

2.2.1 Ion exchange

This method is based on the capability of cations to exchange with metals present in the wastewater (Pagano *et al.* 2000). Different types of materials are used in this method; these materials may be natural (alumina, silicates, carbon) or synthetic (resins and zeolites). The ion exchange process takes place due to the exchange of cations and anions in the aqueous medium (Fernández *et al.* 2005) . The high sensitivity to pH of the solution and high operational costs are disadvantages of the ion exchange processes.

2.2.2 Reverse Osmosis

This particular process is used for the separation as well as the fractionation of organic, inorganic substances and heavy metals in both aqueous and the non-aqueous solution. This technique can be used to treat diverse industrial effluents such as the textile, petrochemical, paper and tannery industries (Mohsen-Nia, Montazeri and Modarress 2007). Though the efficiency of this technique increases when combined with the pilot membrane reactor, it however, has some drawbacks such as consuming high power for pressure pumping and restoration of the membrane (Dialynas and Diamadopoulos 2009).

2.2.3 Precipitation

Because different heavy metals precipitate at various pH levels, the pH of the solution and cellular metabolism may have both a dependent and independent effect on precipitation (Ahalya, Ramachandra and Kanamadi 2003). Due to its simplicity of use and affordability, this approach is

quite popular and widely used (Cannon 1997). Metal-containing wastewater is treated using chemical precipitation procedures, which create an insoluble precipitate as a result of chemical addition (Cannon 1997). The most common chemical precipitation processes include sodium precipitation, sulfide precipitation, and heavy metal chelating precipitation. Lime and limestone are the most commonly utilized precipitant agents because they are efficient in treating inorganic effluents at higher concentrations (Mirbagheri and Hosseini 2005). The precipitation method has the drawback of using excessive volume of chemicals and creating a lot of concentrated sludge, which is a disadvantage.

Even though these traditional technologies have been used extensively to remove heavy metals from contaminated water, they have disadvantages such as high costs, inefficiency at low metal concentrations, high energy consumption, operational challenges, and high levels of hazardous sludge generation (Chai *et al.* 2021). Even though these traditional technologies have been used extensively to remove heavy metals from contaminated water, they have disadvantages such as high costs, inefficiency at low metal concentrations, extreme energy consumption, operational challenges, and high levels of hazardous sludge generation. Nevertheless, it is drawn back by its high cost and poor rejuvenation behavior. Therefore, there are numerous ongoing research investigations for environmental friendly adsorbents where research is focused on using agricultural biomass. These agricultural biosorbents possess several advantages compared to conventional techniques, which include larger adsorption capacities, great efficiencies even at low metal concentrations and low-cost (Chai *et al.* 2021). Due to the disadvantages of these conventional technologies, the biosorption process has been deemed an alternative technology for the removal of heavy metals because of its low operational cost, high efficiency, ease of operation, regeneration of biosorbents and heavy metal recovery.

2.2.4. Biosorption Process

Heavy metal ions from aqueous solutions attach quickly and irreversibly to functional groups on the surface of biomass during the biosorption process (Davis, Volesky and Mucci 2003). The biosorption process, which comprises a solid phase (sorbent) and a liquid phase (solvent) containing a dissolved species of sorbate/metal, is dependent on a number of factors, including the mass of adsorbate, temperature, pH, and starting concentration (Ahalya, Ramachandra and

Kanamadi 2003). In the biosorption process, there are three main mechanisms at play: (1) the transfer of heavy metals from polluted water onto the surface of the biosorbent; (2) the adsorption of heavy metals onto solid surfaces; and (3) the transport of heavy metals into the pores of the biosorbent.

The composition of the cell wall of the biomass is of great importance to the biosorption process. The cell wall of biomasses is composed mainly of polysaccharides, proteins and lipids, and functional groups such as hydroxyl, carboxyl, amino, ester. These functional groups play a key role in the biosorption of cations from aqueous solutions, where heavy metals are attracted and bound to the biosorbents by different mechanisms. These biosorbents usually have higher affinity to heavy metals in waste/ potable water.

The biosorption process continues until equilibrium is established between the mass of solid-bound adsorbate species and its portion remaining in the solution and the degree of adsorption affinity for the adsorbate determines its distribution between the solid and the liquid phase (Ahalya, Ramachandra and Kanamadi 2003). The performance of an adsorbent is generally defined in terms of the adsorption capacity, which is determined using batch adsorption experiments. Batch adsorption studies are important to calculate the design parameters for a given adsorption system.

2.3 Factors Affecting Biosorption

2.3.1 Characteristics of biosorbent

The nature of the biosorbent may be considered one of the most important factors as it possesses functional groups that play an important role in the biosorption process. Physical treatment such as boiling, drying and mechanical disruption may affect the binding properties of the biosorbents while biosorption capacity may be improved by chemical treatments such as alkali and acidic treatments (Wang and Chen 2006)**.**

2.3.2 Initial Concentration

The specific uptake of ions may be affected by the concentration of the sorbate in the solution since more ions can be adsorbed by the biomass (Gourdon *et al.* 1990). Electrostatic interactions between cells can affect the metal uptake since the specific uptake of metals is increased at lower biomass concentrations. Therefore, an increase in biosorbent concentration leads to interference between the binding sites (Malkoc and Nuhoglu 2005)**.**

2.3.3 The surface area

When an adsorbent is used to remove heavy metals in potable water, the adsorption rate is a function of the available surface area and therefore the greater the surface area available to the metals, the greater the adsorption. The pore structure of an adsorbent is another characteristic that determines the extent of adsorption as it contributes to the surface area.

2.3.4 Acidity

The pH of the metal solution's acidity, according to (Puranik, Modak and Paknikar 1999), is a crucial factor in the adsorption process because it affects the solubility of metal ions and the concentration of counter ions on the functional groups of the biosorbent. The pH affects the electrostatic binding of the ions to the appropriate functional groups during the biosorption process. The chemistry of the solution as well as the activity of the functional groups of the adsorbent and their competitiveness are both impacted by this acidity (Crist, Martin and Crist 1999). The solubility of metals declines as the pH of the solution rises, allowing precipitation to take place and altering the adsorption process. The activity of the binding sites can be changed by changing the pH using alkaline or acid compounds.

2.4 Components of sugarcane bagasse

The sugarcane bagasse is a fibrous lignocellulosic material that comprises of ash, lipids, starch, hydrocarbons, proteins, and a variety of other substances, including 20 to 25% lignin, 18 to 24% hemicellulose, and 45 to 55% cellulose (Sud, Mahajan and Kaur 2008).

2.4.1 Cellulose

The semi-crystalline hydrophilic polymer cellulose ($C_6H_{10}O_5$) is made up of hydroxyl groups that give it strong hydrogen bonds and -1, 4-linked anhydro-D-glucose units. Wool, cotton, sugarcane bagasse, banana rachis, corncob, and sugarcane cob are significant sources of lignocellulosic biomass (Fortunati *et al.* 2013). Cellulose is mostly used to make cellophane, textiles, medicines, and paper goods. Figure 2.1 depicts the structural makeup of the cellulose.

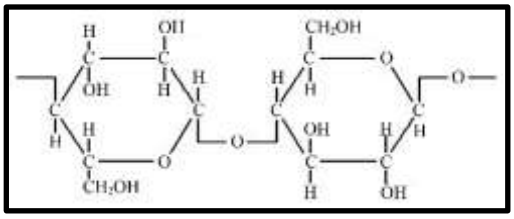

Figure 2.1: The structure of the cellulose

2.4.2 Lignin

An ester-type bond that is sensitive to alkali solutions and an ester-type bond that is insensitive to alkali solutions make up the cementing matrix for cellulose and hemicellulose known as lignin. The phenol components (trans-coniferyl, trans-sinapyl, and trans-p-coumaryl) that make up lignin are also thought of as a highly branched amorphous polymer that is resistant to degradation. Additionally, it is insoluble in water and possesses both dietary and practical fiber properties. The mass of lignin in the cell wall is regarded as the primary determinant of how resistant the cell wall is to hydrolysis (Zhang and Lynd 2004)**.** Lignin is employed as stabilizing agents, coating and emulsifying agents, polymers, adhesives, and polymers. Figure 2.2 depicts the structural breakdown of the lignin.

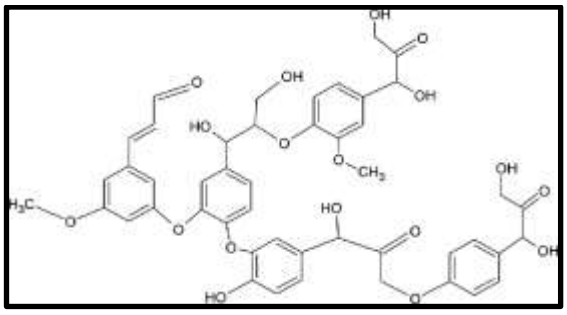

Figure 2.2: The structure of the lignin

2.4.3 Hemicellulose

Hemicellulose, which ranks next to cellulose in the plant cell wall structure, is an amorphous polymer comprising xylose, mannose, and arabinose that is securely bonded to lignin. It is challenging to separate hemicellulose from cellulose and lignin without significantly altering the structure because hemicellulose is not chemically homogeneous and is rather securely bonded in the network of plant cell walls (Ansari and Gaikar 2014)**.**

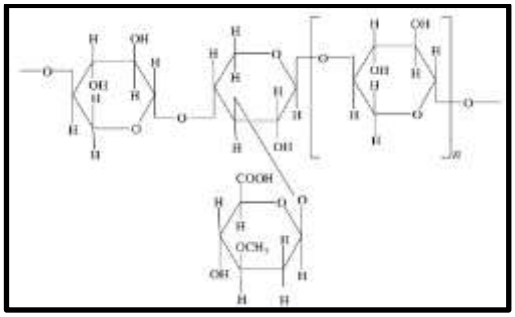

Figure 2.3: The structure of the hemicellulose

2.5 Pretreatment of Lignocellulosic Materials

The rate of adsorption when a biosorbent is employed to remove heavy metals depends on the available surface area; hence, the more surface area that is accessible to the metal, the larger the adsorption capacity. According to (Brígida *et al.* 2010), the biosorbent can be physically or chemically altered to increase the lignocellulosic material's adsorption ability. To lessen the recalcitrance of the components, lignocellulosic materials must be subjected to pretreatment procedures (Zhang and Lynd 2004). The processing of lignocellulosic materials has undergone a variety of processes. These pretreatments consist of physical operations like grinding (Chang and Holtzapple 2000)**,** physical-chemical treatments (Swatloski *et al.* 2002), treatments with dilute acids and alkalis, and biological pretreatments using bacteria and fungi (Srilatha *et al.* 1995)**.** One of the potential outcomes of pretreatments is the breakdown of the biomass's amorphous-crystalline structure, which separates lignin and hemicellulose (Siqueira *et al.* 2011)**.** Deconstruction of the lignocellulosic material is depicted in Figure 2.4.

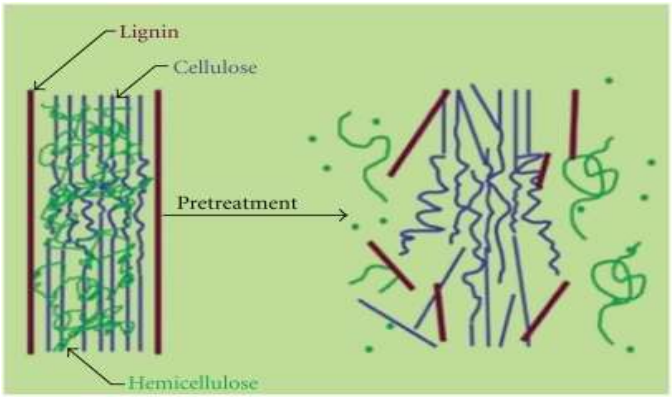

Figure 2.4: The schematic presentation showing the effect of chemical pretreatment on the lignocellulosic material

According to (Pandey *et al.* 2000) the use of chemical pretreatment using acids and bases is considered effective and economical because acid hydrolyzes hemicellulose and produces a liquid that is rich in xylose, with traces of lignin. This then makes acid pretreatments an outstanding method for hemicellulose recovery. In a study done by Geddes and collaborators where sulfuric and phosphoric acid efficiencies, in dissolving hemicellulose from sugarcane bagasse, were compared where the maximum yields of 257g sugar/ kg bagasse and 246g sugar/ kg bagasse were obtained for sulphuric and phosphoric acids, respectively. Diluted alkali treatments lead to the disruption of lignocellulosic cell walls by hydrolyzing uronic and acetic esters of the lignin and swelling of cellulose (Zhang and Lynd 2004) . The decomposition of lignin is due to the cleavage of the α-aryl ether bonds from its polyphenolic monomers and the weakening of hydrogen bonds leads to the dissolution of hemicellulose and swelling of cellulose (Jackson 1977)**.**

2.5.1 Pretreatment Methods

2.5.1.1 Steam Explosion

Although explosive decomposition can lead to the separation of fibers, chemical changes have the biggest influence on this separation (Brownell and Saddler 1987)**.** Steam explosion pretreatment solubilizes hemicellulose by auto hydrolysis through the conversion of acetyl groups to acetic acid when no acid catalysis is added. Following this pretreatment, lignin is hydrolyzed and degraded, crystallinity is increased, and cellulose polymerization is reduced. The partial breakdown of xylan and lignin as well as the incomplete disruption of the lignin-carbohydrate matrix are drawbacks of this method (Brownell and Saddler 1987)**.**

2.5.1.2 Liquid Hot Water (LHW)

In this method, water is used to pre-treat the biomass under high pressure and temperature (Mosier et al. 2005). At temperatures between 200 and 300 °C and pressures above 5 MPa, the process can take up to 15 minutes. Most of the lignin and hemicellulose are solubilized by LHW, which improves cellulose accessibility (Mosier *et al.* 2005). Because water breaks the hemiacetal linkages, which in turn causes the ether linkages of the biomass to break, acids are released from the lignocellulosic components. 40–60% of the total biomass was dissolved in the LHW process in a study by **(**Mosier *et al.* 2005**)**, and it was found that 4–22% of the cellulose, 35–60% of the lignin, and all of the hemicellulose were eliminated. Although this method has advantages in terms of cost and corrosion, its main drawback is the increased water and energy requirements.

2.5.1.3 Microwave Irradiation

One of the pretreatments used for lignocelluloses is microwave irradiation, which affects the lignocellulosic material by electromagnetic radiation with wavelengths of 1 m to 3 mm and frequencies of 300 MHz to 300 GHz. The chemistry of the biomass matrix can be deconstructed at specific wavelengths and frequencies, causing the lignocellulose to change physically and chemically and boosting cellulose exposure (Wang *et al.* 2002)**.** The high cost and energy demands of this procedure, however, are a disadvantage.

2.5.1.4 Weak Acid Hydrolysis

One of the most efficient pretreatment techniques for lignocellulosic biomass is diluted acid pretreatment. This procedure involves spraying diluted acid onto raw lignocellulosic material, which is subsequently heated for a brief period, between 160 and 220 °C. Hemicellulose subsequently undergoes hydrolysis, releasing monomeric sugars and soluble oligomers into the hydrolysate from the cell wall matrix. The lignocellulosic material's porosity increases when hemicellulose is removed (Chen *et al.* 2007)**.** Strong acid hydrolysis techniques are also favored because to their versatility in feedstock selection, high yield of monomeric sugar, and minimal temperature requirements. However, due to its corrosive nature and high price, it is disadvantageous (Sun and Chen 2007)**.**

2.5.1.5 Alkaline Hydrolysis

The lignin in the lignocellulosic biomass is primarily removed by alkaline pretreatment, which boosts the reactivity of the residual polysaccharides. Since acetyl and uronic acid substitutions on lignin reduce the enzyme's accessibility to the surface of hemicellulose and cellulose, alkali pretreatment works by eliminating these changes (Chang and Holtzapple 2000)**.** Alkaline hydrolysis, according to (Chang and Holtzapple 2000), is based on the saponification of intermolecular ester linkages that crosslink lignin and other component hemicelluloses. Ammonia, calcium hydroxide, and sodium hydroxide are the three most often utilized alkaline pretreatments.

.

2.6 Batch adsorption experiments

By adding a sorbent to a specified volume of liquid sorbate (metal ions to be removed) under predetermined circumstances, such as contact time, pH, biomass-metal concentration, temperature, and ionic strength, creates a batch system for metal sorption (Kumar *et al.* 2014b)**.** After a predetermined contact period, the sorbent is extracted from the solution using sedimentation, filtration, or other techniques, either for disposal or regeneration (reuse). It has been discovered that when equilibrium is attained, the quantity of pollutants (metal ions/sorbate) adsorbed by a sorbent in contact with polluted water remains constant. The equilibrium isotherm is therefore utilized to connect the loading of the adsorbate on the adsorbent to the final concentration of the adsorbate (El-Naas and Alhaija 2011)**.**

The main advantages of a batch adsorption system (Sankhla *et al.* 2016).

• Batch adsorption systems help define the kinetic order of the sorption process, which improves understanding of the kinetics of the sorption reaction.

• To increase an adsorbent's capacity to bind metal ions, various pre-treating substances and other variations might be investigated.

• Batch systems are valuable for gathering information on the behavior of metal ions as they bind to biomass or other adsorbents in single- and multi-metal systems.

The mass balance equation used to determine adsorption capacity at equilibrium or at any time *t* for a batch adsorption procedure used to adsorb solutes from liquid solution is:

$$\mathrm{q_o m + C_o V = q_e m + C_e V} \qquad (2.1)$$

Where q_o and *qe* (mg/g) are adsorption capacities or initial and final adsorbate concentration in solid phase at equilibrium, respectively, and C_o and C_e (mg/L) are initial and final adsorbate concentration in liquid phase at equilibrium, respectively. *V* and *m*, respectively denote the volume

of the solution (L) and the mass of the adsorbent (g). Given that there is no solute adsorbed onto the adsorbent's surface at first, thus $q_o = 0$

Equation 2.1 then reduces to:

$$C_oV = q_em + C_eV \tag{2.2}$$

Hence, solving for q_e as follows:

$$q_e = \frac{(C_o - C_e)V}{m} \tag{2.3}$$

Various researchers have used Equation 2.3 to calculate the adsorption capacity or removal efficiency of an adsorbent, which is defined as the mass of heavy metal(s)/adsorbate(s) adsorbed at equilibrium qe (Muhamad, Doan and Lohi 2010)**.** The equation for % removal efficiency of metal ion is given by:

$$\%\text{Removal} = \frac{C_o - C_e}{C_o} \times 100 \tag{2.4}$$

2.7 Adsorption Kinetics

The time it takes for the concentration of adsorbate on the adsorbent surface and the concentration of adsorbate in the surrounding liquid phase to equalize is referred to as adsorption kinetics. The chemical and physical characteristics of the adsorbent material affect the adsorption kinetics, which in turn affects the adsorption process. The results from the batch experiments were fitted into the two most popular kinetic models—pseudo-first-order and pseudo-second-order kinetic models—in order to study the adsorption kinetics of Fe^{2+}.

2.7.1. Pseudo-first-order Lagergern model

(Lagergren 1898) used the first-order ordinary differential equation to describe the adsorption kinetics of a solute (adsorbate) in an adsorbent particle.

$$\frac{dq_t}{dt} = k_1(q_e - q_t) \tag{2.5}$$

Equation 2.5 can be linearized to:

$$\log(q_e - q_t) = \log q_e - \frac{k_1}{2.303} t \quad (2.6)$$

Where q_e and q_t (mg/g) are the adsorbate adsorbed (adsorption capacities) at equilibrium at time *t*, respectively; k_1 (min^{-1}) is the adsorption process's pseudo-first order rate constant. The parameters of the pseudo- first order (k_1 and q_e) can be determined using the linear plot of $\log(q_e - q_t)$ versus *t.*

2.7.2 Pseudo-second-order model

In this model, the rate-limiting step is surface adsorption, which incorporates chemisorption adsorption (Ho and McKay 1999; El-Naas and Alhaija 2011). The driving force (q_e - q_t) is proportional to the fraction of active sites available for adsorption (Ho and McKay 1999). The kinetic rate equation is given by equation 2.7

$$\frac{dq_t}{dt} = k_2(q_e - q_t)^2 \quad (2.7)$$

Where; k_2 is the pseudo-second order equation's rate constant (g/mg. min), q_e (mg/g) are the adsorbates adsorbed (adsorption capacity) at equilibrium, q_t (mg/g) is the quantity of adsorbates on the adsorbent's surface (adsorption capacity) at any moment, and *t* is the time (min). Equation 2.8 is obtained by separating the variables in equation 2.7 (Ho and McKay 1999)**.**

$$\frac{dq_t}{(q_e - q_t)^2} = k_2 dt \quad (2.8)$$

The linear form of equation 2.8 is:

$$\frac{t}{q_t} = \frac{1}{k_2 q_e^2} + \frac{t}{q_e} \quad (2.9)$$

The values of k_2 and q_e can be determined from the linear plot of $\frac{t}{q_t}$ vs *t*

2.8 Adsorption Isotherms

(Foo and Hameed 2010) reported that when an adsorbate-containing phase has been in contact with the adsorbent for a significant period, and a dynamic balance exists between adsorbate concentration in the bulk solution and interface concentration, adsorption equilibrium, which is the ratio between the adsorbed mass and that remaining in the solution, develops.

According to (Bhattacharya, Mandal and Das 2006), adsorption isotherms are the correlation between the solute concentration in the solution at equilibrium (C_e) and the mass of the solute adsorbed per unit mass of adsorbent (q_e). The ability to approximate the impact of feed concentration on adsorption capacity using the isotherm data is useful for process design, allowing the opportunity, for instance, to concentrate the feed before applying it to the system. An isotherm is created by plotting the concentration of adsorbed solute per unit mass of adsorbent (dependent variable) against the equilibrium solute concentration in the liquid phase (independent variable) (Bhattacharya, Mandal and Das 2006).

Each data point should indicate an equilibrium between the mass of adsorbate adsorbed on the adsorbent's surface and the mass of adsorbate in the solution in a dynamic, thermodynamically partitioned system (Latour 2015). Information on the thermodynamics of the adsorption process can then be supplied by fitting an appropriate adsorption isotherm model to the corresponding shape of the adsorption isotherm (Latour 2015). An isotherm might be advantageous or detrimental depending on the thermodynamics of the system.

An in-depth mathematical description of equilibrium adsorption capacity is required for the accurate estimation of adsorption parameters and quantitative comparison of adsorption behavior for diverse adsorbent systems. Although there are other models that can be used to explain the dynamics of a solid-liquid sorption system, the Langmuir and Freundlich adsorption isotherms were selected for this study since they are the most often used isotherms.

2.8.1 Langmuir Isotherm

The Langmuir isotherm was initially created to describe a gas-solid phase adsorption system that used activated carbon as a sorbent (Langmuir 1916), but it has subsequently been applied to explain the performance of a number of bio-sorbents (Foo and Hameed 2010)**.** According to (Xu, Cai and Pan 2013)**,** monolayer sorption, in which a free adsorbate molecule collides with a vacant adsorption site, removes sorbate from the aqueous phase on homogenous active sites on the adsorbent that are equal and identical. In the Langmuir isotherm, molecules are only adsorbed in a single layer at a fixed number of well-defined places (Xu, Cai and Pan 2013)**.**

The Langmuir isotherm is expressed by the non-linear equation:

$$q_e = \frac{q_{max} k_L C_e}{(1 + k_L C_e)} \tag{2.10}$$

Where q_e (mg/g) is the equilibrium solute mass adsorbed per unit adsorbent mass, and C_e (mg/L) is the equilibrium adsorbate concentration in the solution. K_L (L/ mg) is the Langmuir isotherm constant, or affinity relation between the sorbent and the sorbate, while q_{max} (mg/g) the maximal adsorption capacity. The reformed form of equation 2.10 is given by following linearized form:

$$\frac{C_e}{q_e} = \left(\frac{1}{k_L q_{max}}\right) + \frac{C_e}{q_{max}} \tag{2.11}$$

Where C_e (mg/L) is the concentration at equilibrium; q_e (mg/g) is the adsorption capacity of the adsorbent, q_{max} (mg/g) is the maximum adsorption capacity of the adsorbent and K_L (L/mg) is the Langmuir adsorption constant. The slope $\left(\frac{1}{q_L}\right)$ and intercept $\left(\frac{1}{q_L k_L}\right)$ was determined from the plot of $\left(\frac{C_e}{q_e}\right)$ versus C_e.

According to (Mckay, Blair and Gardner 1982), the dimensionless separation factor (R_L) can also be used to evaluate the favorability of the adsorption process.

$$R_L = \frac{1}{(1 + k_L\, C_o)} \tag{2.12}$$

Where C_o (mg/L) is the initial metal concentration of the adsorbate. The adsorption is regarded favorable when the value of R_L is less than 1.0; linear when R_L equals 1.0 and unfavorable when R_L is greater than 1.0.

2.8.2 Freundlich isotherm

The Freundlich isotherm in the description of the equilibrium of heterogeneous surfaces and is not limited to monolayer adsorption (Freundlich 1906).

$$log\ log\ Q_{eq} = logK_f + \frac{1}{n\ logC_{eq}} \tag{2.13}$$

Where K_f (mg/g) is an adsorption capacity, n indicates the strength of adsorption and Q_{eq} (mg/g) is the concentration of ions adsorbed at equilibrium.

2.9 Characterization of Biosorbent

The biosorption process heavily depends on the composition of the cell wall of the biosorbent. Functional groups including hydroxyl, amino, esters, carboxyl, and carbonyl are present in the cell walls of the biosorbents and are important in the biosorption of cations from aqueous solutions.

2.9.1 Fourier- Transform Infrared (FTIR) Spectroscopy

Fourier- Transform Infrared (FTIR) is a vibrational spectroscopy that records the absorption of Infra-Red (IR) light by means of chemical bonds in all molecules. It is crucial to recognize the functional groups that are present on the adsorbent's surface in order to comprehend the biosorption mechanism. These functional groups can either promote or impede the biosorption process. As demonstrated in Table 2.2, FTIR spectroscopy offers crucial details about the nature of the bonds that enable the identification of various functional groups on the cell wall of the adsorbent.

Table 2.2: Functional groups of lignocellulosic material

Wavenumber (cm^{-1})	Functional groups
3600-3000	OH stretching
2860-2970	C-H_2
1700-1730	C=O stretching
1632 - 1450	C=C
1470-1430	O-CH_3
1440-1400	OH bending
1402	CH bending
1232	C-O-C stretching
1215	C-O stretching
1170 - 1060	C-O-C stretching vibration
1108	OH association
1060	C-O stretching and C-O deformation
700- 400	C-C; C-H stretching

2.9.2 Scanning Electron Microscopy with an Energy Dispersing X-ray Analytical System (SEM-EDX)

The surface morphology of the adsorbent is examined using scanning electron microscopy (SEM) both before and after metal ion biosorption. This is accomplished by assessing the biomass surface's qualitative morphological alterations (Reategui *et al.* 2010). When Scanning Electron Microscopy (SEM) and an Energy Dispersing X-ray Analytical System are combined, it is possible to determine the distribution of different elemental components. According to its definition, EDX is an X-ray method that quantitatively determines the elemental composition of the biomass**.**

2.9.3 Brunauer Emmet Teller (BET)

Brunauer Stephen, Emmet Paul Hugh and Teller Edward developed the BET method in 1913. This method directly measures the specific surface area, pore size distribution and pore volume of an adsorbent. The concept of this method is an extension of the Langmuir models that follows a hypothesis that although the gas molecules are physically adsorbed on the solid surface in layers, there is no literal interaction between these layers. Therefore, the Langmuir theory is applicable to each layer. The BET equation is expressed as follows:

$$\frac{1}{W\left(\left(\frac{P}{P_o}\right)-1\right)} = \frac{1}{cW_m} + \frac{(c-1)}{W_m.C}\left(\frac{P}{P_o}\right) \quad (2.14)$$

Where; $P\ and\ P_o$ (bar) are the equilibrium and saturation pressure ($\frac{P}{P_0}$ is the relative pressure), W is the weight of gas adsorbed (g), W_m is the weight of adsorbent as monolayer (g), C is the BET constant.

2.9.4 X-ray Diffraction (XRD)

Diffraction occurs when monochromatic X-rays interact with a crystalline sample. The XRD technique provides detailed information regarding the chemical composition and crystallographic structure of the adsorbent. This method, described by Bragg's Law, is given by equation 2.15:

$$n\lambda = 2d\ sin\theta \quad (2.15)$$

Where, λ (m) is the wavelength of the X-rays; d (m) is the distance between different plans of atoms in the crystal lattice, Θ (°) is the angle of diffraction and n is an integer determined by the order.

2.9.5 Atomic Absorption Spectroscopy (AAS)

The concentration of a specific metallic element in a sample can be quantified using an Atomic Absorption Spectroscopy (AAS), an analytical technique. It is necessary to use standard solutions with known elemental concentrations to establish a link between the measured absorbance and the elemental concentration. This method depends on the Beer-Lambert equation, which explains the connection between an absorbing sample's concentration and its absorption. Eq. 2.16 yields the Beer-Lambert Law:

$$A = \lambda bc \quad (2.16)$$

Where; A (nm) is the absorbance, λ (m) is the wavenumber of the absorption of the element interested in; b (cm) is the path length and c is the molar concentration of the sample.

CHAPTER 3

3.1. Materials and apparatus

The objective of this study was to valorize biomass while removing heavy metals from potable water. Waste sugarcane bagasse was the biomass that was taken into consideration for this investigation. Three primary pretreatments—alkali, acid, and combined pretreatments of (acid + alkali)—were used in the valorization of sugarcane bagasse. The Illovo sugar mill at Umkomaas near Durban was where the sugarcane bagasse was obtained (South Africa). The pretreatment processes of sugarcane bagasse were carried out at Mangosuthu University of Technology (Chemical Engineering Laboratory).

Sulfuric acid (H_2SO_4) and pure sodium hydroxide (NaOH) pellets, bought from Sigma Aldrich Chemical Company, were the acid and base employed for the pretreatment processes. Analytical methods such Fourier Transform Infrared Spectroscopy (FTIR), Scanning Electron Microscope (SEM), X-ray Diffraction (XRD), and Brunauer Emmett Teller (BET) were used to characterize the natural and modified sugarcane bagasse.

3.1.1 Preparation of Adsorbents

3.1.1.1 Preparation of Natural Material

Figure 3.1: The image of the raw/ natural sugarcane bagasse

Sugarcane bagasse was collected from Illovo sugar mill in Umkomaas Area in Durban, South Africa. The sugarcane bagasse was first washed with de-ionized water to remove any impurities before being dried in a Gunt Hamburg CE 130 air-convention dryer at 30 °C with an air velocity of 1.0 m/s until the mass of the sugarcane bagasse remained constant. Using a household blender, the dried sugarcane bagasse was subsequently broken down until it reached the appropriate 200-micron particle size.

Figure 3.2: Gunt Hamburg air-convention drier (CE 1300 model)

3.1.1.2 Modification of Sugarcane Bagasse through Chemical Pretreatments

In order to evaluate sugarcane bagasse's efficacy in removing heavy metals, components like cellulose, hemicellulose, and lignin were removed as part of the modification/pretreatment process. The pretreatments attempted to change the characteristics of sugarcane bagasse by removing lignin and hemicellulose with sodium hydroxide and sulfuric acid, respectively. The combined pretreatment's objectives were to separate the lignin and hemicellulose, respectively.

3.1.1.2.1 Modification of Sugarcane Bagasse using Sodium Hydroxide Pretreatment

By adding the proper quantity of pure sodium hydroxide pellets to 1000ml of deionized water, a stock solution of sodium hydroxide was prepared. Additionally, the stock solution was thoroughly mixed while being agitated in an orbital shaker at a speed of 160 rpm before being diluted with deionized water to create various alkali pretreatment solutions of 0.5%, 1%, 1.5%, 2%, and 2.5%.

All pretreatment solutions were held at a consistent volume. Each beaker containing 100 ml of alkali solution received 60 g of raw sugarcane bagasse (shown by Figure 3.3). To allow for a

prolonged extraction of lignin, the combination was allowed to come into contact with one another for a period of 24 hours. After 24 hours, the mixture of alkali solution and bagasse was filtered through a screen. The mesh size was chosen to prevent cellulose-hemicellulose particles from penetrating. Each of the solid particles (0.5% NaOH, 1% NaOH, 1.5% NaOH, 2% NaOH, and 2.5% NaOH) was carefully washed with deionized water until neutral pH was reached, and then dried using a Gunt Hamburg air-convention dryer CE 130 model.

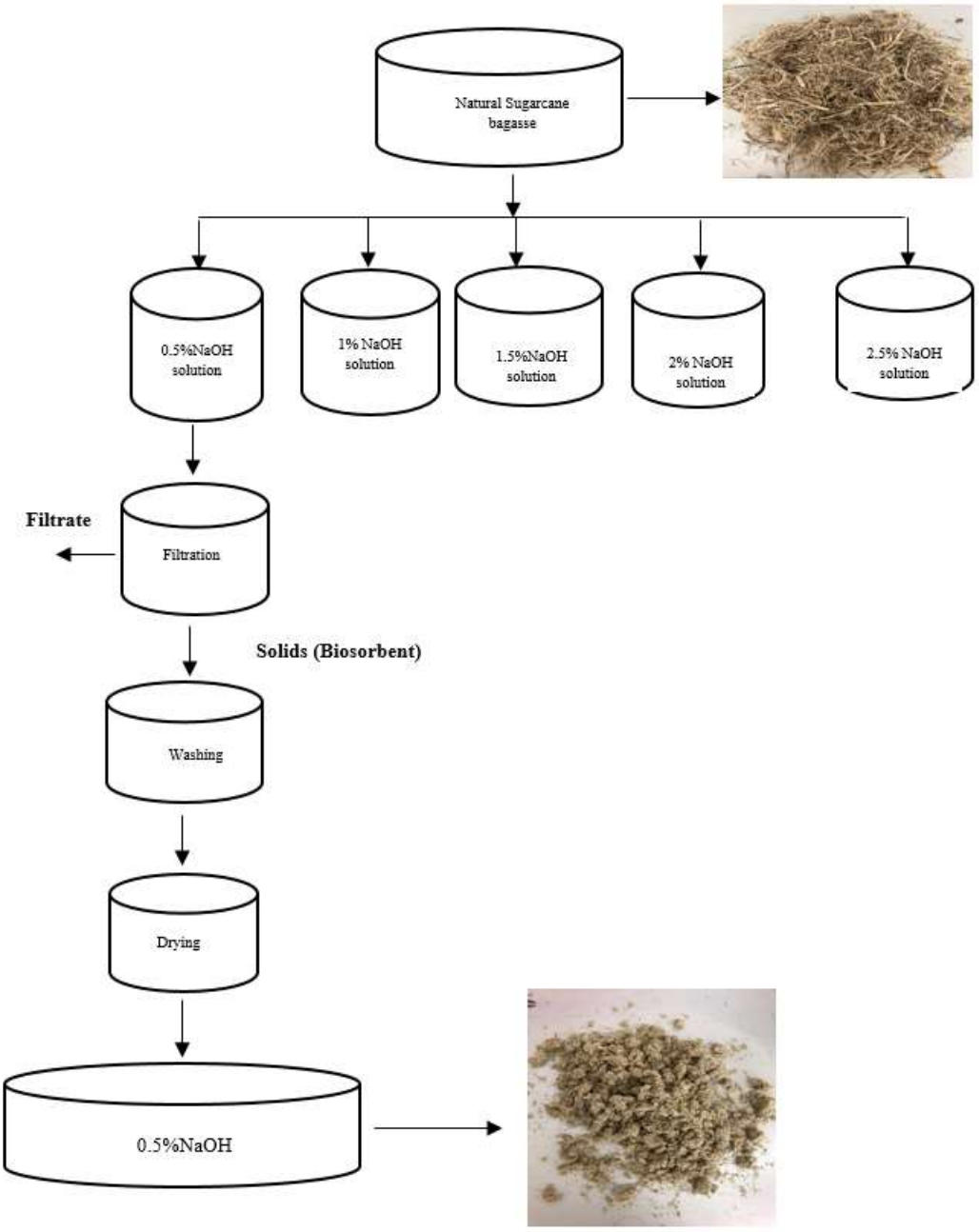

Figure 3.3: Alkali-pretreatment of the sugarcane bagasse

3.1.1.1.2 Modification of adsorbent using acid pretreatment

A stock solution of sulphuric acid was prepared by adding an appropriate volume of 98% concentrated sulphuric acid in 1000ml deionized water (as shown by Figure 3.4). The stock solution was, firstly, agitated in an orbital shaker at a speed of 160 rpm for thorough mixing before it was diluted with deionized water to obtain different acid pretreatment solutions of 0.5%; 1%; 1.5%; 2%; 2.5%. The volume of all pretreating solutions were kept constant. Sixty grams (60 g) of raw sugarcane bagasse was added into each beaker containing 1000 ml of pretreatment solution. The acid solutions and sugarcane bagasse were left in contact for a duration of 24 hours.

After the pretreatment duration of 24 hours, the contents (acid solution + sugarcane bagasse) were filtered using a sieve, filtrates shown in Figure 3.6. The selected size of the mesh was to avoid penetration of cellulose-lignin particles. The cellulose-lignin solid particles were, first, thoroughly washed with deionized until neutral pH was obtained then followed by drying using the Gunt Hamburg air-conventional drier CE 130 model. The content of cellulose, lignin and hemicellulose present on the bagasse after all pretreatments was determined using a direct estimation method proposed by (Moubasher *et al.* 1982)**.**

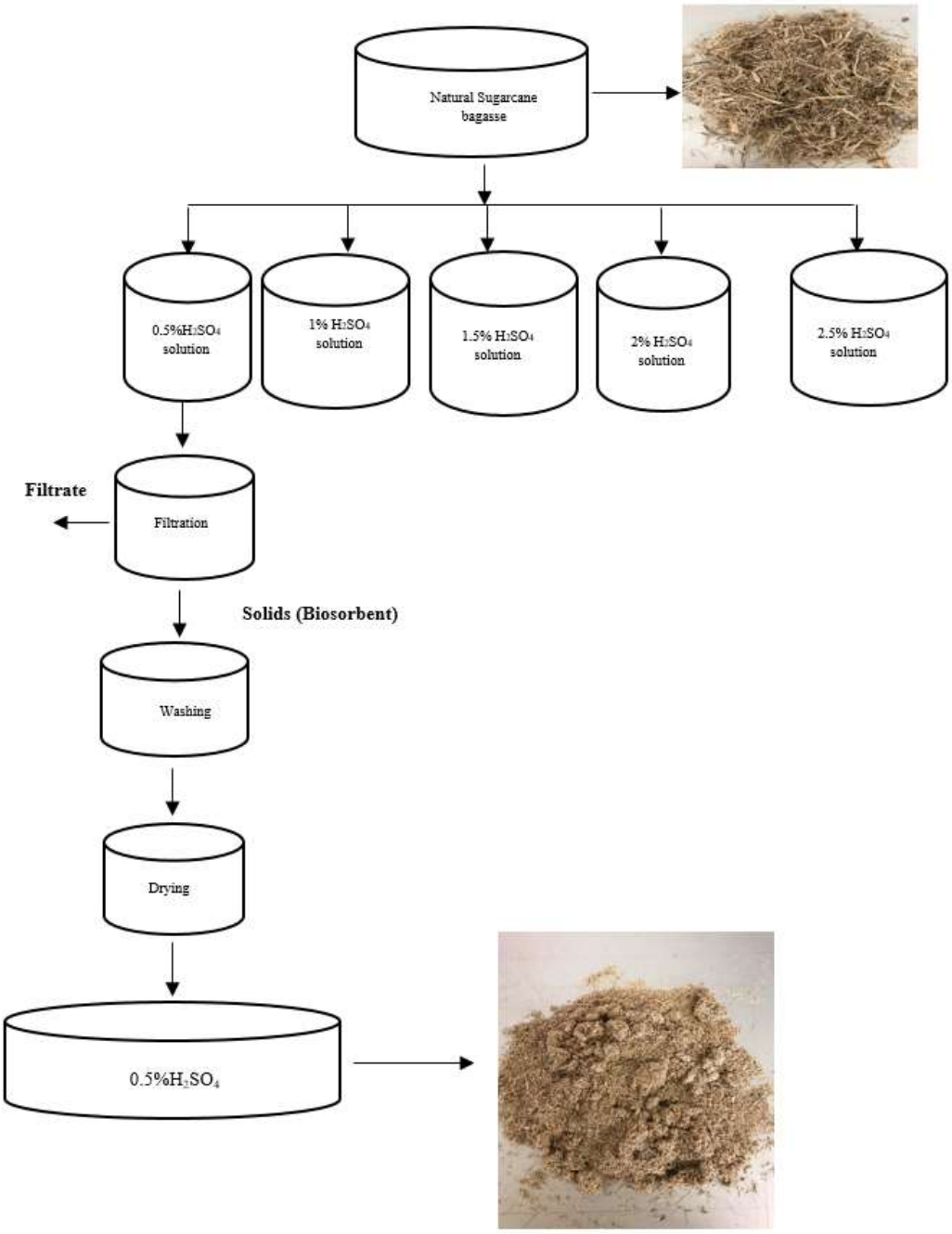

Figure 3.4: Acid-pretreatment of the sugarcane bagasse

3.1.1.2.3. Combined Pretreatment of Acid and Alkali Pretreatment

Step 1: A stock solution of sodium hydroxide was prepared by adding an appropriate mass of pure sodium hydroxide pellets in 1000 ml deionized water. The stock solution was also, firstly, agitated in an orbital shaker at a speed of 160 rpm for thorough mixing before it was diluted with deionized water to obtain different alkali pretreatment solutions of 0.5%; 1%; 1.5%; 2%; 2.5%. The volume of all pretreating solutions were kept constant. Sixty grams (60 g) of raw sugarcane bagasse was

added into each beaker containing 1000 ml of alkali- pretreatment solution. The alkali solution and sugarcane bagasse were left in contact for a duration of 24 hours (shown by Figure 3.5). The contents (alkali solution + sugarcane bagasse) were filtered using a sieve with designated mesh size of 100, after 24 hours, filtrates shown in Figure 3.6. The selected size of the mesh was to avoid penetration of cellulose-hemicellulose particles. The solid particles (0.5% NaOH; 1.0% NaOH; 1.5% NaOH; 2% NaOH 2.5% NaOH) were each thoroughly washed with de-ionised water until neutral pH was attained, then dried in an air conventional drier at 30 ^{o}C and air velocity of 1.0 m/s.

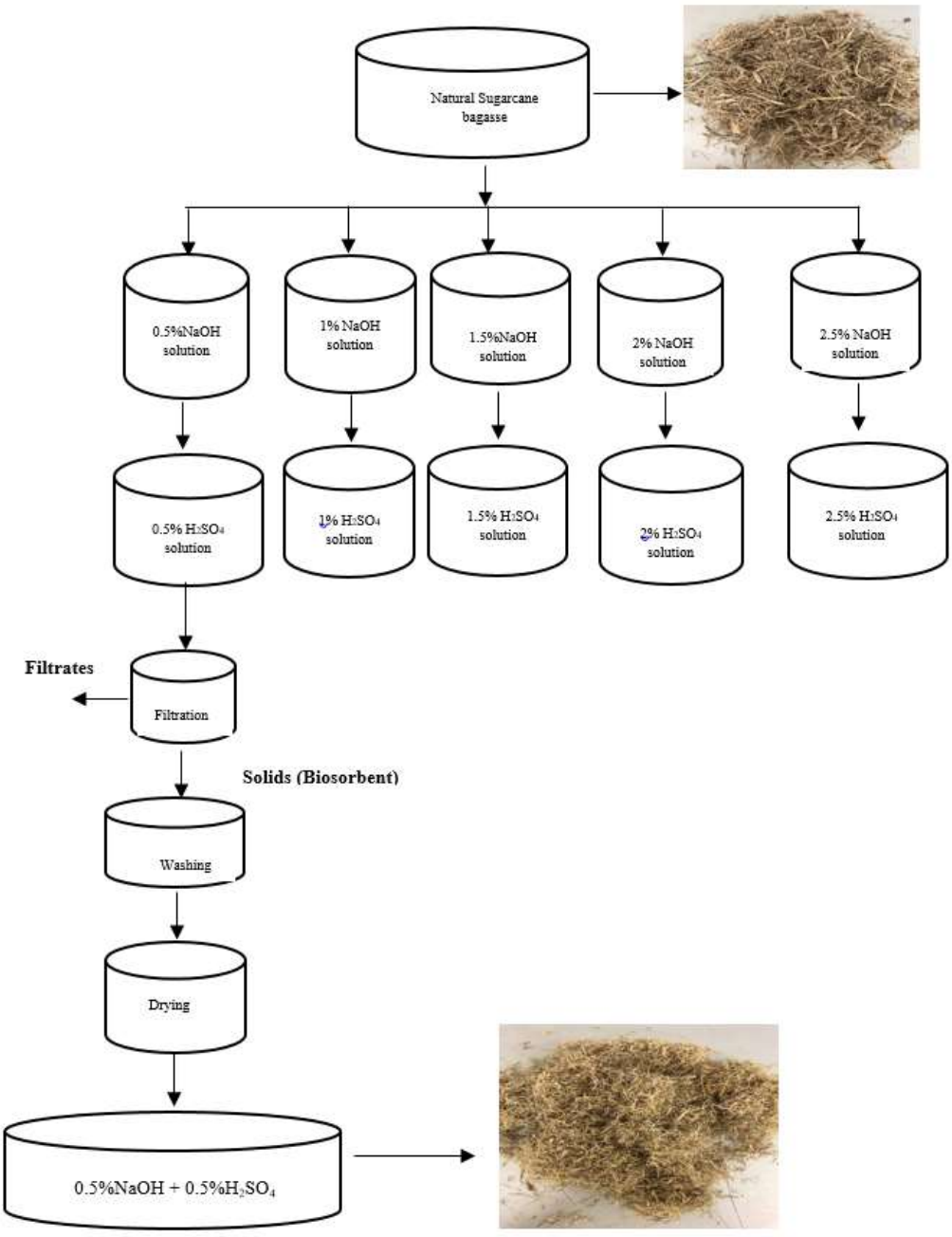

Figure 3.5: Combined-pretreatment of the sugarcane bagasse

Step 2: Different concentrations of sulphuric acid solutions were prepared, each in a volume of 1000ml. The dried solids (cellulose-lignin) from (Step 1) were then added to each beaker, i.e. 0.5% NaOH- pretreated biosorbent was added into 0.5% H_2SO_4 solution; 1% NaOH added into 1% H_2SO_4 solution and so forth. This current step was done to remove hemicellulose present in the alkali-treated adsorbent. The alkali-treated adsorbent and acidic solution were left in contact for a duration of 24 hours. The contents (acid solution + alkali treated adsorbent) were filtered using a sieve with a designated mesh size after 24 hours, filtrates shown in Figure 3.6. The selected size of the mesh was to avoid penetration of cellulose particles. The solid particles were each thoroughly washed with de-ionised water until neutral pH was attained, then dried in an air conventional drier at 40 degrees Celsius and air velocity of 1 m/s. The final adsorbent obtained from this step was celluloses with small traces of lignin and hemicellulose denoted as (0.5% NaOH + 0.5% H_2SO_4); (1% NaOH + 1% H_2SO_4), etc.

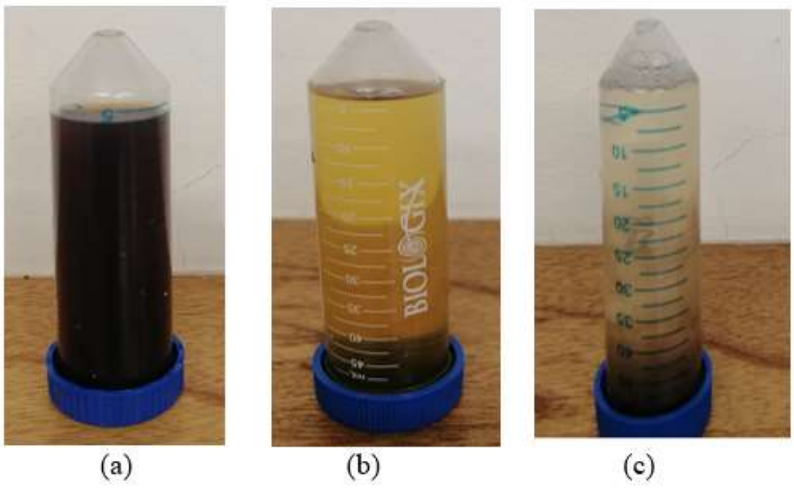

Figure 3.6: Filtrates obtained after pretreatment of (a) alkali, (b) acid, (c) combined pretreatments

3.2 Batch biosorption studies

The batch adsorption studies were used to examine the impact of operational parameters such as starting concentration, adsorbent dosage, pH, contact time, and agitation speed. These operational tweaks were made in an effort to assess the effectiveness of sugarcane bagasse, both natural and modified, in removing heavy metals, particularly Fe^{2+} ions from drinkable water.

By adding the proper mass of ferrous sulphate heptahydrate salt ($FeSO_4.7H_2O$) to 1000 mL of deionized water, synthetic solutions of Fe^{2+} were created. The synthetic solutions were thoroughly mixed by agitating them at 160 rpm for 30 minutes in a Cole-Parmer Stuart Orbital Shaker SSL1 type (Figure 3.7a). By diluting the stock solutions to replicate the concentration of heavy metals in potable water, different quantities of Fe^{2+} were obtained for the biosorption experiments. Using the Pelkin Elmer AAnalyst 400 Absorption Atomic Spectrometry (Figure 3.6b) with an Iron Lamp of 10 Amperes, Wavenumber of 248.3nm, and an Air/Acetylene flame, the final concentrations after each biosorption experiments were determined. For all data to be reported as averages, all adsorption experiments were triple duplicated.

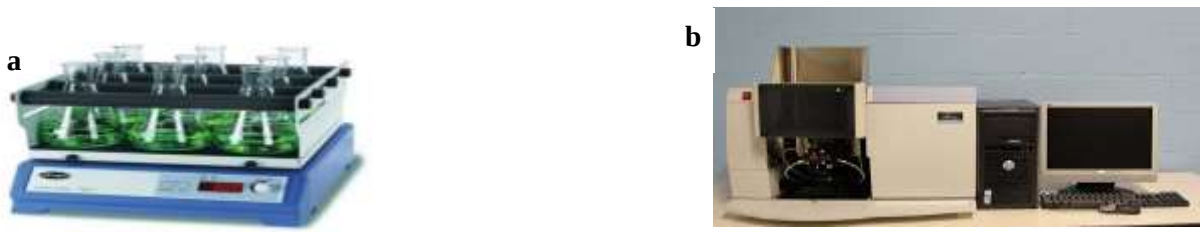

Figure 3.7: (a) Cole-Parmer orbital shaker SSL model, (b) Perkin Elmer Absorption Atomic Spectrometry (AAnalyst 400)

3.2.1 Effect of Adsorbent Dosage

Different biomass dosages between 0.2 and 1.4 g were applied to a fixed volume of 100ml of Fe^{2+} solution to evaluate the impact of adsorbent dosage on the removal of metal ions. By diluted the stock solution with water, the necessary working solution concentration of 1mg/L was created. The pH was maintained at 6 to replicate the characteristic of drinkable water. To maintain the pH, 1M sulphuric acid and sodium hydroxide were utilized. The solutions and biosorbents were then allowed to agitate at 25°C for 100 minutes at a constant speed of 160 rpm. Atomic Absorption Spectroscopy was used to determine the concentration after the biosorption experiments.

3.2.2 Effects of Initial Concentration

From the stock solutions, solutions of 100ml with Fe^{2+} concentrations varying between 1 and 30 mg/L were prepared. Each solution received one gram of sugarcane bagasse while maintaining a pH of 6 and an agitation speed of 160 rpm, respectively. For 100 minutes, the solutions were left to agitate. The contents were then filtered after 100 minutes, and the concentration of the filtrates was assessed using AAS.

3.2.3 Effect of pH

Both the natural and modified forms of sugarcane bagasse were exposed to Fe^{2+} solutions of various pHs ranging from 2 to 7, at constant adsorbent dosages of 1 gram, agitation contact times of 100 minutes, and agitation speeds of 160 rpm, in order to determine the impact of pH on the biosorption of Fe^{2+}. Utilizing an atomic absorption spectrometer, concentration analysis was performed following the adsorption procedure (Perkin Elmer, AAnalyst 400 model). An Orion Star A215pH/ conductivity meter (electrode: Orion 8157 BNUMD Ross Ultra pH/ATC Triode) was used to measure the pH. It was calibrated using three standard buffer solutions, namely 4, 7, and 10. To correct pH readings, 1.0 M NaOH and 1.0 M H_2SO_4 solutions were utilized.

3.2.4 Effect of Contact Time Variation

By altering the time in contact between the adsorbent and the metal concentration—from 5 to 100 minutes—it was possible to examine the impact of contact time on the removal of Fe^{2+}. The starting concentration of the adsorbent was kept at 1 mg/L, pH was kept at 6, and the agitation speed was kept at 160 rpm. After 100 minutes, the mixture was filtered using Whatman No. 5 filter paper, and the final concentrations were determined using an AAS.

After the adsorption period has lapsed, the percentage removal of Fe^{2+} was calculated using the following equation:

$$\% \, Removal = \left(\frac{C_o - C_e}{C_o}\right) * 100\% \qquad (3.1)$$

Where, C_o and C_e are the initial concentration and concentration at equilibrium, respectively measured in mg/L.

3.3 Batch adsorption isotherms and kinetics

To get equilibrium data, batch experiments were utilized to investigate the removal of Fe^{2+} from potable water. The kinetic tests entailed filling 100ml sample bottles with various Fe^{2+} concentrations while maintaining the ideal pH of 6. Each sample bottle contained Fe^{2+} in concentrations ranging from 1 to 30 mg/L, and one gram of the recommended adsorbent dose was added to each container (natural and modified). Then, the samples were stirred using an orbital shaker that was set to 160 rpm. The residual metal concentration of the solutions was analyzed by atomic absorption spectroscopy (AAS) at different time intervals of 5, 10, 20, 40, 60, 80, and 100 minutes.

3.4 Characterization of Adsorbents

3.4.1 Fourier Transform Infrared Spectroscopy (FTIR)

A vibrational spectroscopy known as Fourier-Transform Infrared (FTIR) measures the absorption of Infra-Red (IR) light by all molecules' chemical bonds. It is crucial to recognize the functional groups that are present on the surface of the adsorbent in order to comprehend the biosorption mechanism because their presence can either enhance or inhibit the biosorption process.

Figure 3.8: Perkin Elmer Fourier Transform Infra Spectroscopy (FTIR)

The nature of the bonds and various functional groups present on the adsorbent's cell wall were crucially revealed by FTIR spectroscopy. The level of band shifting in naturally occurring and metal-loaded biomass served as a sign of the interaction between functional groups and metal cations (Murphy, Hughes and McLoughlin 2007). This study employed Perkin Elmer's Spectrum2 FTIR and Spectrum 10 software to generate the results. The device has a MIR (Lithium tantalite)

detector and an ATR attachment with a diamond prism for analysis. The wavenumber ranged from 400 – 4000cm^{-1}.

3.4.2 Scanning Electron Microscope (SEM)

Scanning Electron Microscopy is a tool used to investigate the surface morphology of the adsorbent before and after metal ion adsorption by evaluating qualitative morphological changes of the biomass surface (Reategui *et al.* 2010).

Figure 3.9: Scanning Electron Microscope (SEM)

The surface morphology of both the original and the modified sugarcane bagasse was investigated using SEM. When scanning electron microscopy (SEM) and an energy dispersing X-ray analytical system are combined, information about the distribution of different elemental components on the biomass surface may be obtained. The operational SEM-EDS specification employed in this investigation included a beam intensity of 0.19NA, a beam height of 20Kv, magnifications of 300x and 1200x, view fields of 995um and 249um, and an image size of 850Kb.

3.4.3 X-Ray Diffraction (XRD)

XRD is a method used to identify if a substance is crystalline, amorphous, or both. This methodology provides a full output of the chemical composition and crystalline structure of the materials using an X-ray source of Cu- K radiation (K_1=1.5406A) and the Brag Brentano method. This suggests that the XRD technique could be used to monitor structural changes in a material brought on by chemical treatments. The XRD employed in this investigation was a BRUKER AXS (Germany) diffractomer of D8 Advanced with a 0.5 sec/step, 0.034℃, 2 and 5-60 scan range, respectively.

Figure 3.10: X-Ray Diffractograms (XRD)

3.4.4 Brunauer Emmett Teller (BET)

The BET method, created in 1913 by Stephen Brunauer, Emmet PH., and Edward Teller, is used to calculate the specific surface area and pore volume of sugarcane bagasse in its natural and modified forms. This method's idea is similar to that of the Langmuir theory, which is that molecular adsorption, occurs in monolayers to multilayers. At -196℃, nitrogen sorption measurements were made using a Micrometrics ASAP 2460 surface area porosity analyzer. Prior to characterization, the samples were degassed using N_2 gas at 90 °C for 8 hours. The Brunauer Emmett Teller (BET) method was used to determine the surface areas.

Figure 3.11: Micrometric ASAP 2460 Brunauer Emmett Teller (BET)

CHAPTER 4

4.1 Preliminary studies for the biosorption of Fe^{2+} and Mn^{2+}

The effectiveness of the natural sugarcane bagasse in removing Fe^{2+} and Mn^{2+} from potable water, as well as the impact of these factors on the removal of Fe^{2+}, were assessed through preliminary tests for the agitation speed, pH, and dose. According to preliminary research on agitation speed, the greatest removal for the 1 mg/L Fe^{2+} was found to be 160 rpm, as shown in Figure 4.1. Preliminary research was also conducted on the pH range of 2- 7, as shown in Figure 4.2, and it was discovered that for all concentration ranges of Fe^{2+} and $Mn^{2+,}$ the best removal of Fe^{2+} and Mn^{2+} occurred at the pH of 6 and 7. To assess the impact of the dosage of the biosorbent against the concentration range of 1,5,30 mg/L Fe^{2+} and Mn^{2+}, biosorbent dosage was varies from 0.2 to 1.4g.

The maximum clearance for these metals is found at 1 gram of natural sugarcane bagasse, as shown in Figure 4.3. According to the preliminary study findings, sugarcane bagasse was more effective at eliminating Fe^{2+} ions than $Mn^{2+.}$ As a result, the batch experiment's metal of choice was the metal ion Fe^{2+}.

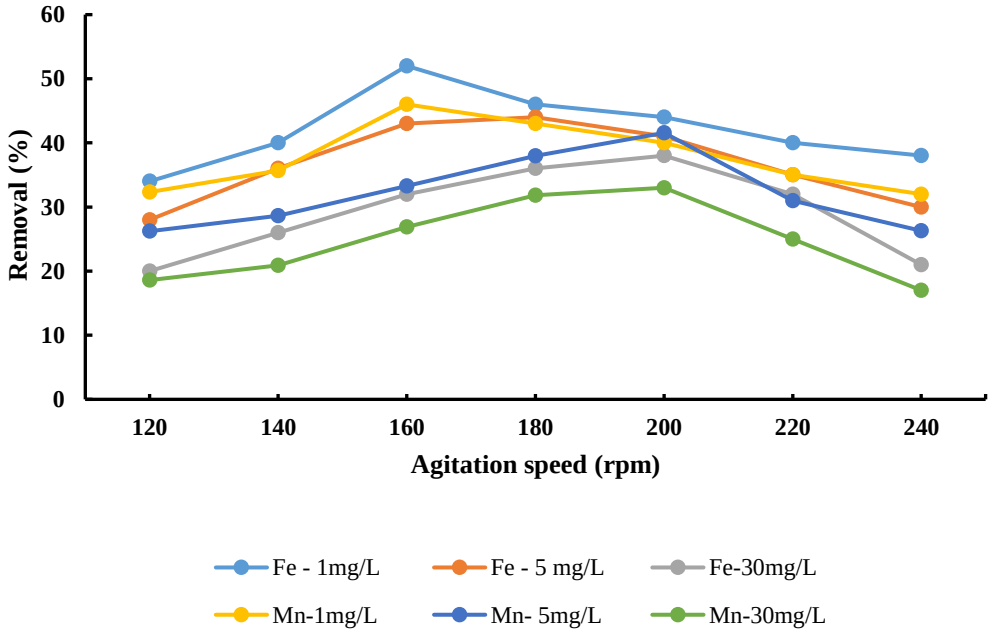

Figure 4.1: Preliminary results of the effect of agitation speed on the biosorption of Fe^{2+}

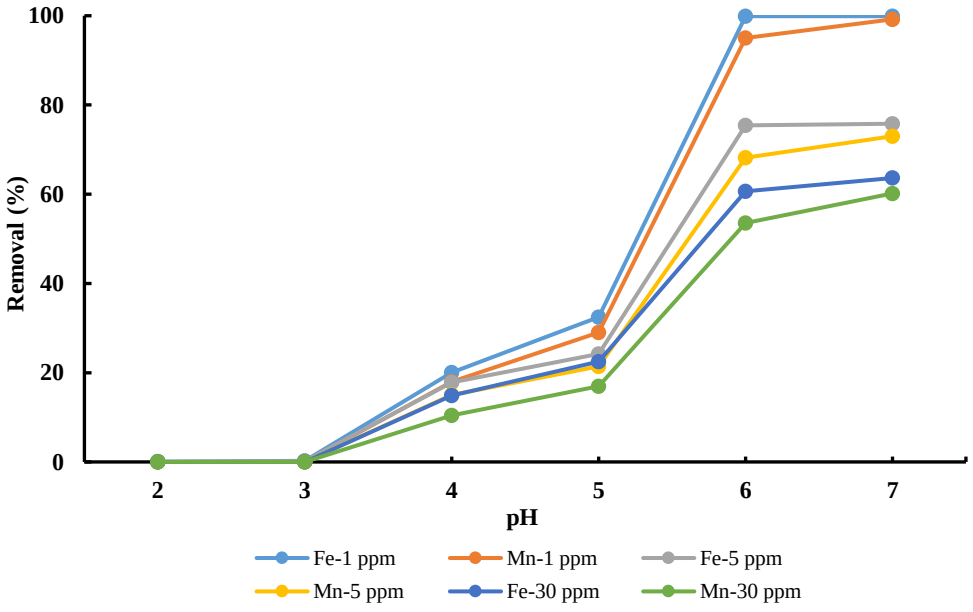

Figure 4.2: Preliminary results for the effect of pH of the biosorption of Fe^{2+}

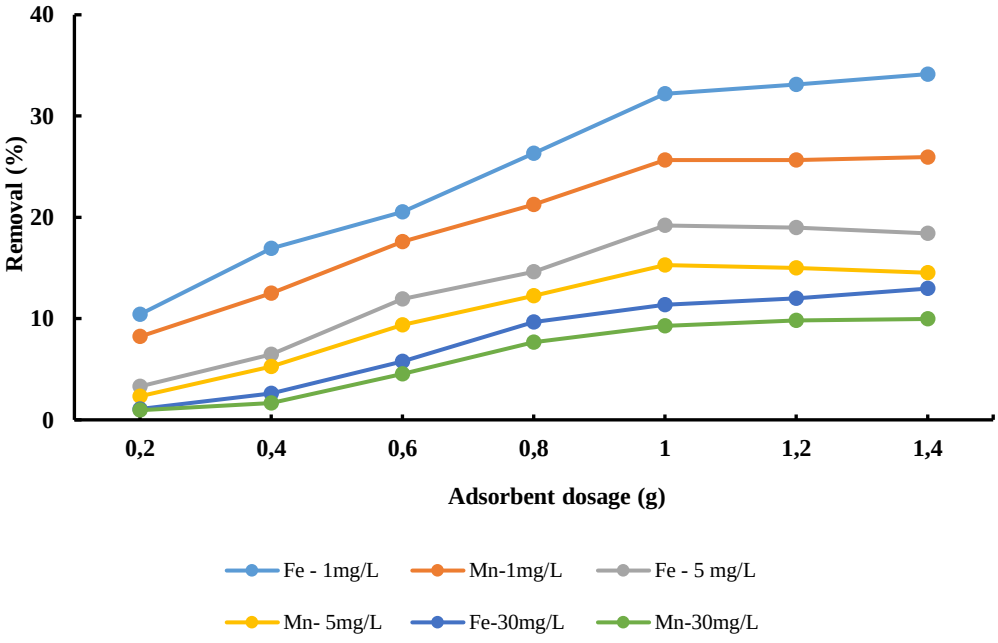

Figure 4.3: Preliminary results of the effect of biosorption dosage on the biosorption of Fe^{2+} and Mn^{2+}

The effect of biosorbent dose variations ranging from 0.2 to 1.4 g on the adsorption of Fe^{2+} and Mn^{2+} is depicted in Figure 4.3. Figure 4.3 shows that when the sugarcane bagasse dosage increased from 0.2 to 1.4 g, the percentage elimination increased for Mn^{2+} and Fe^{2+}, respectively, from 0.66 to 13.03% and 3.3 to 19.31%. Using 1.4 g of natural sugarcane bagasse resulted in the maximum removal of 19.31% for Fe^{2+} and 13.03% for Mn^{2+}; nevertheless, it was found that increasing the mass of biosorbents from 1.0 to 1.4 g had little impact on the removal of Fe^{2+} and Mn^{2+}. This might be due to the fact that there are more particles/ active sites of the adsorbents (as the adsorbent dose increases) than the number of heavy metal particles (constant concentration of the metal) (Tao *et al.* 2015).

Following biosorption process of Fe^{2+} and Mn^{2+} (of 1 mg/L), the aliquots were filtered and dried in an air convention dryer set to 25°C and 1.1 m/s. The mass of Fe^{2+} and Mn^{2+} absorbed by sugarcane bagasse was then measured using SEM-EDX on the corresponding dried sugarcane bagasse that was heavy with Fe^{2+} and Mn^{2+} ions. Sugarcane bagasse was able to biosorb 0.12% of Mn^{2+} and 0.77% of Fe^{2+}, according to the findings of the SEM-EDX investigation, as shown in Table 4.1.

Table 4.1: Preliminary results for SEM analysis of natural sugarcane bagasse after the biosorption of Fe^{2+} and Mn^{2+}

	C (wt %)	O (wt %)	Si (wt %)	Fe (wt %)	Total
SB	56,45	43,32	0,23	0	100
SB- Fe	52.81	45.22	1.59	0.77	100
SB-Mn	53.73	45.38	0.78	0.12	100

The findings in Figures 4.1 to 4.3 demonstrate that sugarcane bagasse was more effective at eliminating Fe^{2+} than Mn^{2+}. These heavy metals' atomic radii, which are 161 pm for Mn^{2+} and 156 pm for Fe^{2+}, may have been crucial to the biosorption process. This indicates that some Fe^{2+} ions were able to pass through the pores of the sugarcane bagasse during the biosorption process. According to the data, sugarcane bagasse was more effective at eliminating Fe^{2+} than Mn^{2+}. Fe^{2+} was then selected as the heavy metal to concentrate on throughout the studies for this investigation.

4.2 Chemical pretreatment results

Tables 4.2 and Table 4.3 display the compositional analysis of natural, alkaline (0.5% - 2.5% NaOH) and acid (0.5% - 2.5% H_2SO_4) samples. The weight percentages (wt%) of cellulose, lignin, and hemicellulose were estimated using a direct approach by (Moubasher *et al.* 1982) after the pretreatment of sugarcane bagasse with different concentrations of alkali, acid, and combination pretreatment of alkali and acid. The wt (%) of cellulose, lignin, hemicellulose, and ash were calculated on a dry weight basis. The cellulose was made up of glucose, cellobiose, and hydromethylfurfural; hemicellulose was made up of arabinose, xylose, glucuronic, and acetic acids; lignin was made up of both insoluble and soluble lignin; and ash was made up of the inorganic fractions left over after the carbonization of the bagasse sample.

Table 4.2: Chemical composition of natural and alkali-pretreated biosorbents

	Cellulose (wt %)	**Hemicellulose (wt %)**	**Lignin (wt %)**	**Ash (wt %)**
Natural	35.20	24.50	22.30	18.00
0.5% NaOH	50.29	20.84	15.86	13.00
1% NaOH	68.54	17.35	8.42	5.69
1.5% NaOH	69.73	16.71	8.36	5.20
2% NaOH	70.71	16.59	7.70	5.00
2.5% NaOH	72.27	15.17	7.56	5.00

According to Table 4.2, the natural sugarcane bagasse contains 35.20 wt% cellulose, 24.5 wt% hemicellulose, 22.30 wt% lignin, and 18.00 wt% ash. Table 4.2 shows that after alkaline pretreatment, the content of the crystalline component, cellulose, grew from 35.20% to 72.27% while the content of the amorphous component, hemicellulose, gradually reduced from 24.50% and 22.30% to 15.17% and 7.56%, respectively. Small masses of hemicellulose were also removed throughout the pretreatment even though alkaline pretreatments removed the majority of the lignin. As can be seen from the compositional analysis, increasing the sodium hydroxide concentration above 1% had little effect on lignin removal, as 1%, 1.5%, and 2% NaOH had 8.42%, 8.36%, and 7.70%, respectively.

According to the observation given above, the mass of lignin eliminated overall for 1%, 1.5%, and 2% NaOH were 13,88%, 13.94%, and 14,6%, respectively. These findings are in line with study conducted by (Rezende *et al.* 2011), who submitted sugarcane bagasse to various sodium hydroxide concentrations in order to delignified it. Their findings revealed that concentrations beyond 1% NaOH did not further remove lignin. The quantity of lignin in the bagasse in their investigation was 11%, 9.5%, and 9.5% for 1% NaOH, 2% NaOH, and 3% NaOH, respectively, after alkali pretreatment.

Table 4.3: Chemical pretreatment of the natural and acid-pretreated biosorbents

	Cellulose (wt %)	**Hemicellulose (wt %)**	**Lignin (wt %)**	**Ash (wt %)**
Natural	35.20	24.50	22.30	18.00
0.5% H_2SO_4	40.97	22.06	20.75	16.22
1% H_2SO_4	47.88	22.84	19.28	10.00
1.5% H_2SO_4	53.20	19.92	18.82	8.06
2% H_2SO_4	63.30	14.09	15.58	6.22
2.5% H_2SO_4	65.65	13.63	14.90	5.82

Table 4.3 shows a contrasting pattern for acid pretreatment, where the ratio of hemicellulose removed to sulphuric acid concentration was inversely. Hemicellulose content dropped from 24.50% to 13.63 % and lignin content from 22.30% to 14.90 % when sulphuric acid concentration was increased from 0.5% to 2.5% H_2SO_4. When an alkali and acid combination pretreatment, ranging from (0.5% NaOH + 0.5% H_2SO_4) to (2.5% NaOH + 2.5% H_2SO_4), was utilized, the % of cellulose rose with an increase in the combined pretreatment's concentration. This resulted from the elimination of the lignin and hemicellulose, two amorphous components of the sugarcane bagasse. It is important to note that combined pretreatment did not involve combining sodium hydroxide and sulfuric acid; rather, it began with an alkali pretreatment and ended with an acid pretreatment.

4.3 Experimental results and discussion

4.3.1 Batch Adsorption Results

Operating factors, such as agitation speed, pH, starting concentration, and dosage, were taken into consideration in order to study the impact of Fe^{2+} biosorption onto the natural and modified bagasse. Following is a discussion of the influence of the aforementioned parameters as well as adsorption kinetics and isotherms.

4.3.1.1 Effect of Agitation Speed

The interaction between the Fe^{2+} ions and the active sites on the surface of the adsorbent is affected by the agitation speed, which is a crucial factor in the phenomenon of adsorption (sugarcane bagasse).

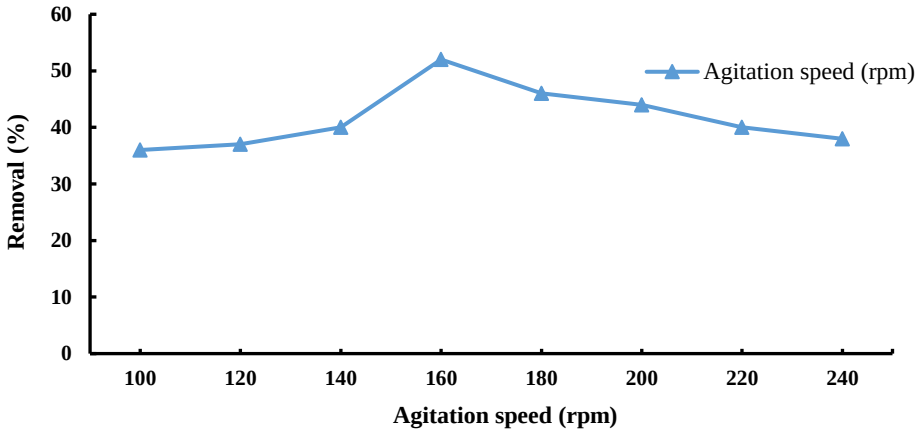

Figure 4.4: The effect of the agitation on the biosorption of Fe^{2+}

In this investigation, the adsorption speed was varied from 100 to 240 rpm while the starting concentration and contact time were held constant at 1 mg/L and 100 minutes, respectively. As can be seen in Figure 4.4, the maximum removal of Fe^{2+} (52%) was discovered to occur at a speed of 160 rpm. Furthermore, it was shown that the percentage elimination decreased as agitation speed rose above 160 rpm. This could be explained by the potential fluctuation in the physicochemical environmental circumstances, which could have changed how long it took the equilibrium to be reached. Furthermore, surface diffusion rather than pore diffusion may be the cause for the observed desorption of Fe^{2+}. Due to increased energy that overcomes the binding energy between

the adsorbate and the adsorbent molecule, the adsorbate can therefore readily become separated from the surface of the adsorbent molecules at high agitation speeds.

4.3.1.2 Effect of pH

Sugarcane bagasse in its native, acidic, and alkali-modified forms were exposed to a single metal ion of Fe^{2+} solution at a concentration of 1 mg/L in order to study how pH affects the biosorption of Fe^{2+} ions. Over a range of pH values between 2 and 7, the absorption of Fe^{2+} was examined while the adsorbent dosage and contact time were held constant at 1g and 100 minutes, respectively. The solutions were filtered after the predetermined contact time had passed, and final concentrations of each solution were determined using an AAS. The presence of hydrogen ions in the solution was found to have a significant impact on the removal efficiency.

Figure 4.5 displays the percentage of Fe^{2+} removed using natural buffers at various pH levels. The results shown in Figure 4.5 demonstrate that the removal of Fe^{2+} ions increased with a rise in pH based on the data gathered from the pH fluctuation. As shown in Figure 4.5, when the pH of the solution was elevated from 2 to 6, the removal percentage of Fe^{2+} when using natural sugarcane bagasse to remove Fe^{2+} from potable water increased from 0.07% to 99.2%.

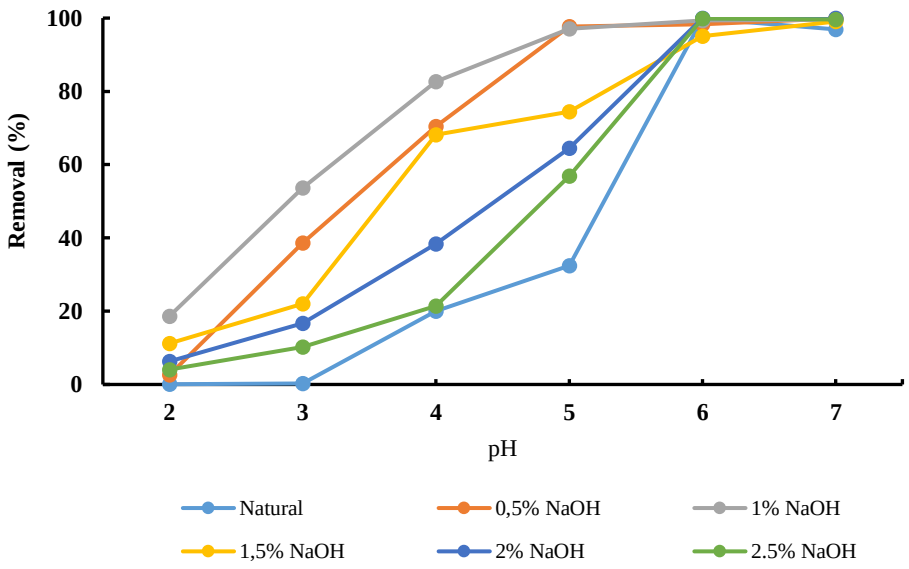

Figure 4.5: The effect of pH on the biosorption of Fe^{2+} by the alkali-pretreated biosorption

Alkali-pretreatment of the sugarcane bagasse enhanced the sorption capacity of the alkali-pretreated biosorbent from 2.6% and 18.66% to 99.06% and 99.60% using 0.5% NaOH and 2.5% NaOH, respectively.

When utilizing acid pretreatment concentrations of 0.5 and 2.5% H_2SO_4, respectively, for the acid pretreatment (Figure 4.6), the percentage removal of Fe^{2+} rose with a rising pH, from the range of 0.4% -25.04% to the range of 98.07% - 99.18%.

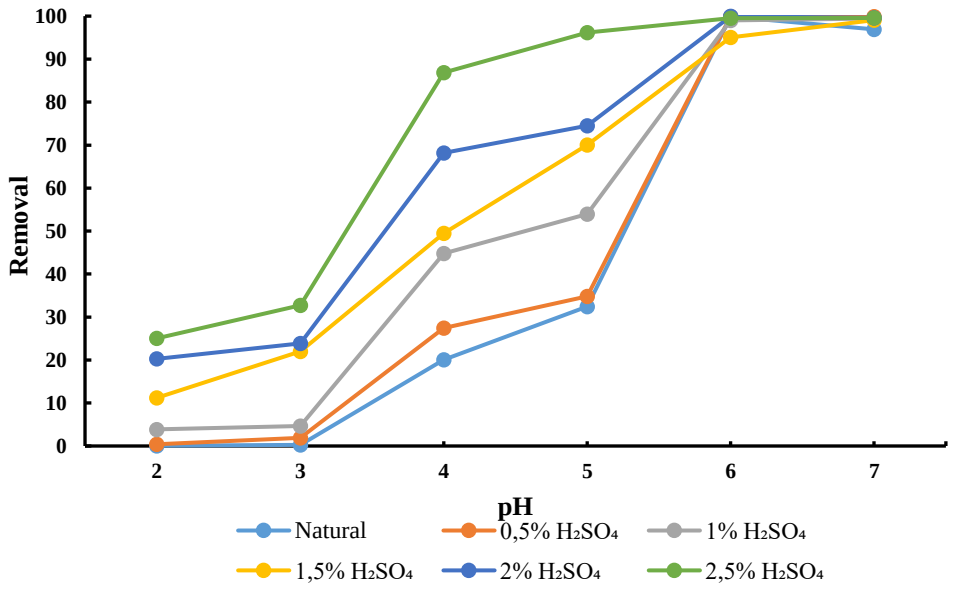

Figure 4.6: The effect of pH on the biosorption of Fe^{2+} by the acid-pretreated biosorbent

The outcome of the combined pretreatment data further demonstrated that pH has a significant impact on the adsorption of Fe^{2+}. Figure 4.7 illustrates how the percentage of Fe^{2+} removal increased as pH rose. At pH values of 2 and 6, respectively, the percentage of Fe^{2+} removed was 0.03% and 99.06% when employing (0.5%NaOH + 0.5%H_2SO_4). At pH values of 2 and 7, respectively, the percentage of Fe^{2+} removed was 0.03 and 97.53% when employing (2.5% NaOH + 2.5% H_2SO_4).

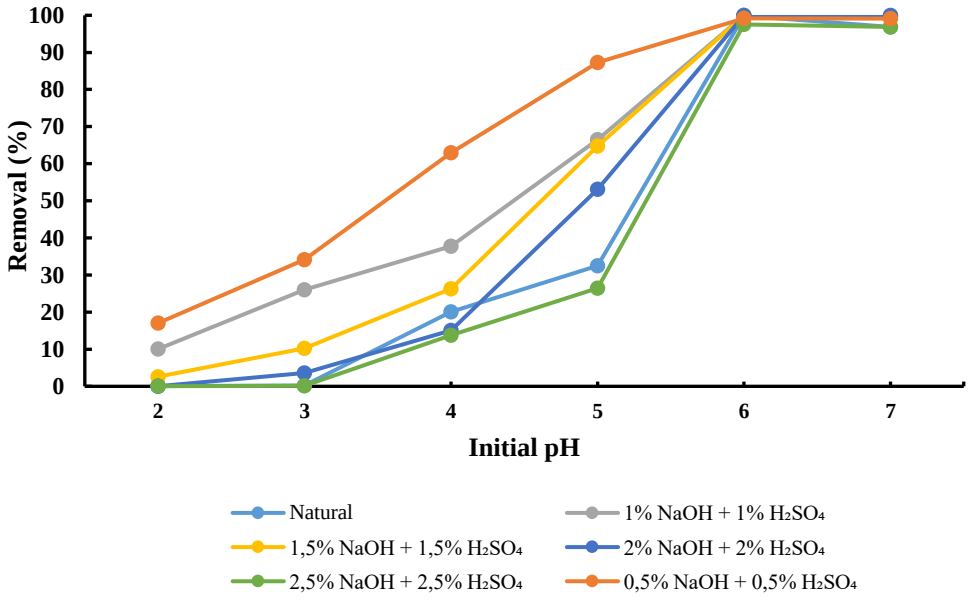

Figure 4.7: The effect of pH on the biosorption of Fe^{2+} by the combined-pretreated biosorbent

The highest percentage removal of the Fe^{2+} was attained at pH 6, according to the results of the pH variation utilizing both natural and modified biosorbents. As a result, pH 6 was chosen as the ideal pH for all research experiments of this study. When attempting to understand how pH affects the removal of metal ions by biosorbent material, the surface charge might be taken into account. Due to protonation of the active sites at higher H^+ ion concentrations and increased electrostatic repulsion during the biosorption of metal ions, at low pH levels (4), the active sites are less accessible for metal ions, which reduces Fe^{2+} adsorption. The electrostatic repulsion diminishes due to the lowering of H^+ on the sorption sites at moderate pH levels (4–6), allowing for the release of H^+ ions from the active sites and an increase in the mass of Fe^{2+} ions adsorbed.

Ion exchange and complex formation processes, according to (Üçer *et al.* 2005),), are the predominant adsorption mechanisms for the removal of metal ions from the solution in this pH range. The hydroxyl ions compete with the metal ions on the biosorbent's active sites at higher pH levels (Kalyani *et al.* 2003). These pH measurements are consistent with those produced by (Aklil, Mouflih and Sebti 2004; Kandah 2004).

4.3.1.3 Effect of initial Fe^{2+} concentration

While adsorbent dosage of the natural and modified sugarcane bagasse, pH, and contact duration were held constant at 1 g, 6, and 100 minutes, the initial sorbate content was varied from 1 to 30 mg/L in order to study its effect. As the starting concentration of the Fe^{2+} increased from 1-30 mg/L while using the natural sugarcane bagasse, the findings given in Figure 4.8 showed the drop in percentage of Fe^{2+} from 50.03 to 4.58%.

However, after chemical pretreatments utilizing alkali, acid, and combined pretreatments of alkali and acid pretreatments, an improvement in the performance of the sugarcane bagasse was noted. The performance of the alkali-pretreated adsorbent increased from 0.5% NaOH to 1%NaOH and then gradually deteriorated, as shown in Figure 4.8, as the concentration of sodium hydroxide pretreatment increased from 0.5% to 2.5% NaOH. For the initial concentration of 1-30 mg/L, the percentage removal of Fe^{2+} dropped from 74.03 to 57.04% for 0.5% NaOH, 99.7 to 69.37% for 1% NaOH, 98.11 to 66.91% for 1.5% NaOH, 91.45 to 65.19% for 2% NaOH, and 88.34 to 55.35% for 2.5% NaOH.

The 1% NaOH pretreated biosorbent produced the highest Fe^{2+} percentage removal of 99.7% at 1 mg/L for the alkali pretreatment, whereas 2.5% NaOH produced the lowest performance at 1 mg/L with 88.34%.

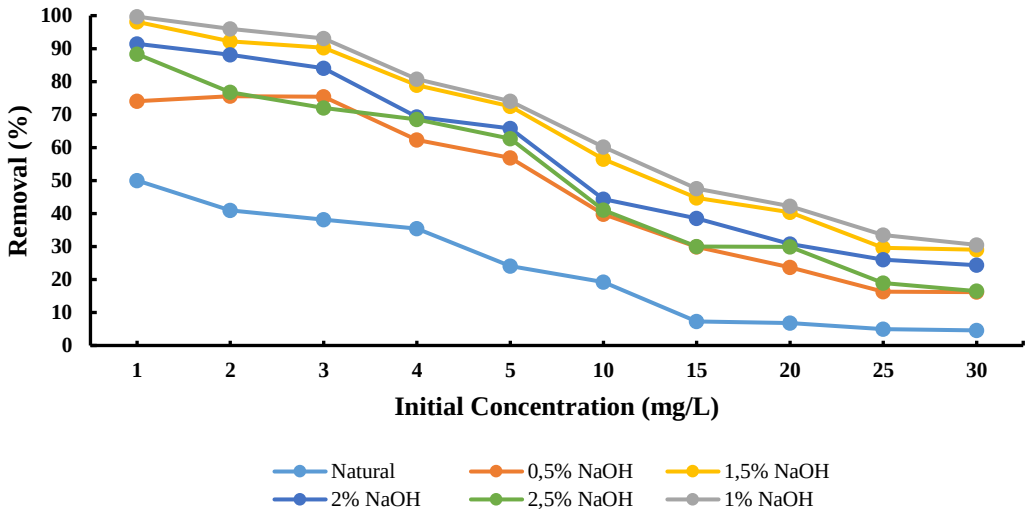

Figure 4.8: The effect of initial concentration on the biosorption of Fe^{2+} by alkali-pretreated biosorbents

As demonstrated in Figure 4.9, the proportion of Fe^{2+} removed during acid pretreatment rose as the concentration of sulphuric acid pretreatment increased from 0.5 to 2.5% H_2SO_4. The efficiency of the acid treatment dropped when the initial Fe^{2+} content was between 1 and 30 mg/L. The initial percentage removal of Fe^{2+} for the 0.5% H_2SO_4 acid-pretreated solution was 57.25% at 1 mg/L and fell to 11.53% at 30 mg/L. The mostly performed acid-pretreated biosorbent was that of 2.5% H_2SO_4, where the percentage removal of Fe^{2+} was 75.93% at 1mg/L and 17.73% mg/L at 30 mg/L.

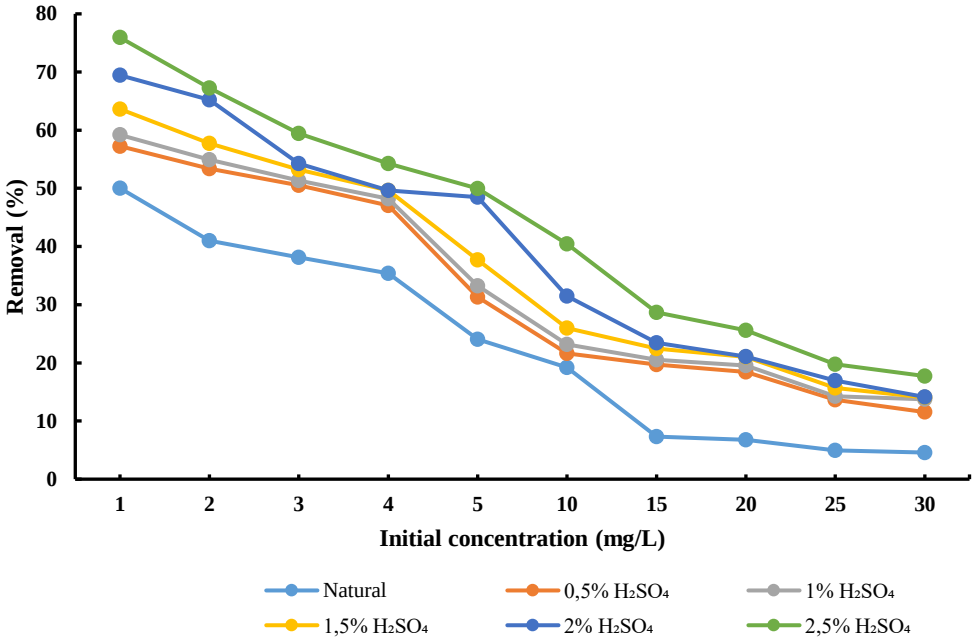

Figure 4.9: The effect on initial concentration on the biosorption of Fe^{2+} by the acid-pretreated biosorbents

The performance of the cellulose after the extraction of hemicellulose and lignin is shown in Figure 4.10; which is a depiction of the combined pretreatment of sugarcane bagasse (alkali and acid). Figure 4.10 illustrates the relationship between the performance of the adsorbent post-pretreatment and the concentration of the combined pretreatment, which ranged between (0.5% NaOH + 0.5% H_2SO_4) and (2.5% NaOH + 2.5% H_2SO_4). At an initial Fe^{2+} concentration of 1 mg/L, the combination of (0.5% NaOH + 0.5% H_2SO_4) showed the highest percentage removal of Fe^{2+} (87.17%) for the combined pretreatment. For the initial Fe^{2+} concentration of 1 mg/L, the lowest removal percentage (63.72 of Fe^{2+} for the combined pretreatment) was noted at (2.5 NaOH + 2.5 H_2SO_4).

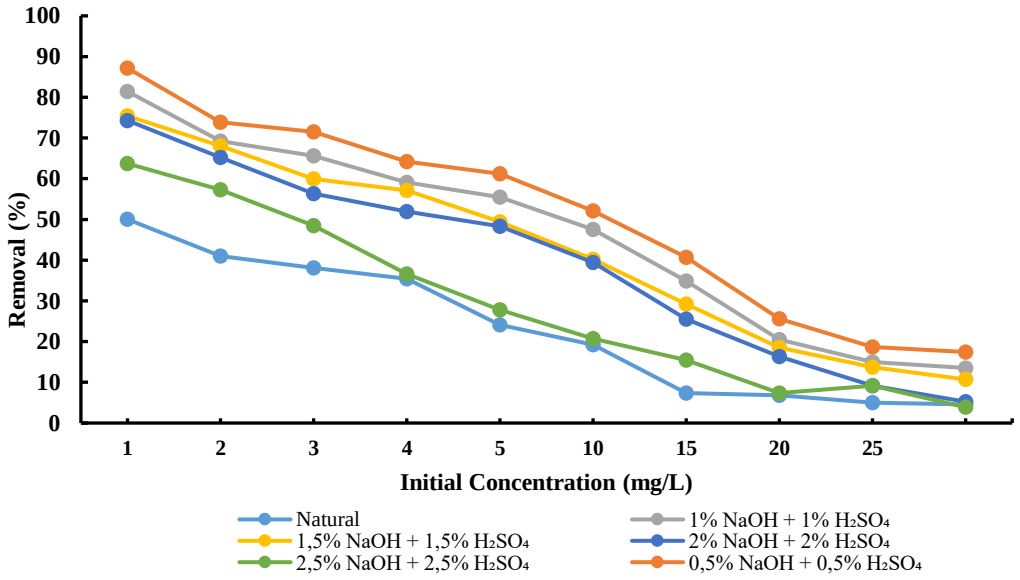

Figure 4.10: The effect of initial concentration on the biosorption of Fe^{2+} by the combined-pretreated biosorbents

In summary, the maximum percentage of Fe^{2+} removal, 99.7% (1 mg/L), was found at 1% NaOH. The combined pretreatment at (0.5% NaOH + 0.5% H_2SO_4) had the second-best performance in removing $Fe^{2+,}$ with a value of 87.17% (1 mg/L), while the acid pretreatment had the third-best performance in removing Fe^{2+}, with a percentage removal of 75.93% (1 mg/L). The overall finding from Figures 4.8 to 4.10 was that as the initial concentration was raised from 1 to 30 mg/L, the metal biosorption decreased. In both natural and modified adsorbents, the drop in metal was caused by a reduction in the active sites on the surface as a result of an increase in the number of ions vying for accessible binding sites at a higher concentration.

The effect of initial concentration can, therefore, be explained as follows: the metal ions adsorption involves higher energy binding sites at low metal ion/adsorption ratio, therefore an increase in metal ion/adsorbent ratio at higher concentrations lead to the saturation of active binding sites and thus decrease adsorption efficiency. Higher concentrations of both sodium hydroxide and combined pretreatment proved insignificant as it resulted in lowest percentage removal for Fe^{2+}. Hence, the pretreatments proved to be cost effective as lower concentration of sodium hydroxide is required in order to obtain highest percentage removal for Fe^{2+}.

4.3.1.4 Effect of biosorbent dosage

The active sites that are present on the surface of an adsorbent relies on a variety of variables, including particle size, adsorbent type, nature, mass used, etc. In order to achieve a biosorption system that can produce larger biosorption uptakes, it was crucial to verify an appropriate adsorbent dosage. Agglomerates may occur, reducing overall surface area and the number of accessible active sites, which may lead to a decrease in the Fe^{2+} ions adsorbed.

By varying the masses of natural and modified sugarcane bagasse in a 100 mL solution from 0.2 to 1.4 g while maintaining constant values for the Fe^{2+} concentration, pH, and contact time of 1 mg/L, 6, and 100 minutes, respectively; the effect of adsorbent dosage on the removal of Fe^{2+} was studied. The proportion of Fe^{2+} removed from sugarcane bagasse after NaOH pretreatment is shown in Figure 4.11. Figure 4.12 shows the percentage of Fe^{2+} removed from sugarcane bagasse that has been prepared with H_2SO_4, while Figure 4.13 shows the percentage of Fe^{2+} removed from sugarcane bagasse that has been pretreated with ($NaOH + H_2SO_4$).

Figures 4.11 to 4.13 show that for both treated and untreated biosorbent, the % of Fe^{2+} biosorbed increased with an increase in adsorbent dosage. As a result, increasing the mass of adsorbent results in more active adsorption sites. The subsequent reduction in the adsorbent's active sites was attributable to the development of clusters of Fe^{2+} on its surface, which reduced the available surface area for adsorption. As a result, adsorbent dosages above 1.0 g did not exhibit any discernible adsorption. Using 0.2 and 1.0 g of natural sugarcane bagasse, a percentage increases of 10.42% and 32.20% for Fe^{2+} were attained.

An increase in metal uptake was seen upon chemical pretreatment with alkali as illustrated in Figure 4.8, where the highest removal of Fe^{2+} was achieved at 1% NaOH with 45.42% and 79.04% was obtained at 0.2 and 1 g, respectively. The percentage removal of 0.5% NaOH was 42.02% and 71.03 % at 0.2 and 1.0 g, respectively. Furthermore, it was observed in Figure 4.11 that as the concentration of alkaline solution increased above 1.5% NaOH, the metal uptake decreased. The respective percentage removal of Fe^{2+} obtained after using 1.5% NaOH was 30.22and 56.57% for 0.2 and 1g. The alkali-pretreated adsorbent with the lowest removal rates of Fe^{2+} was 2.5% NaOH, which had removal rates of 10.42 and 37.70% when using 0.2 and 1.0g, respectively.

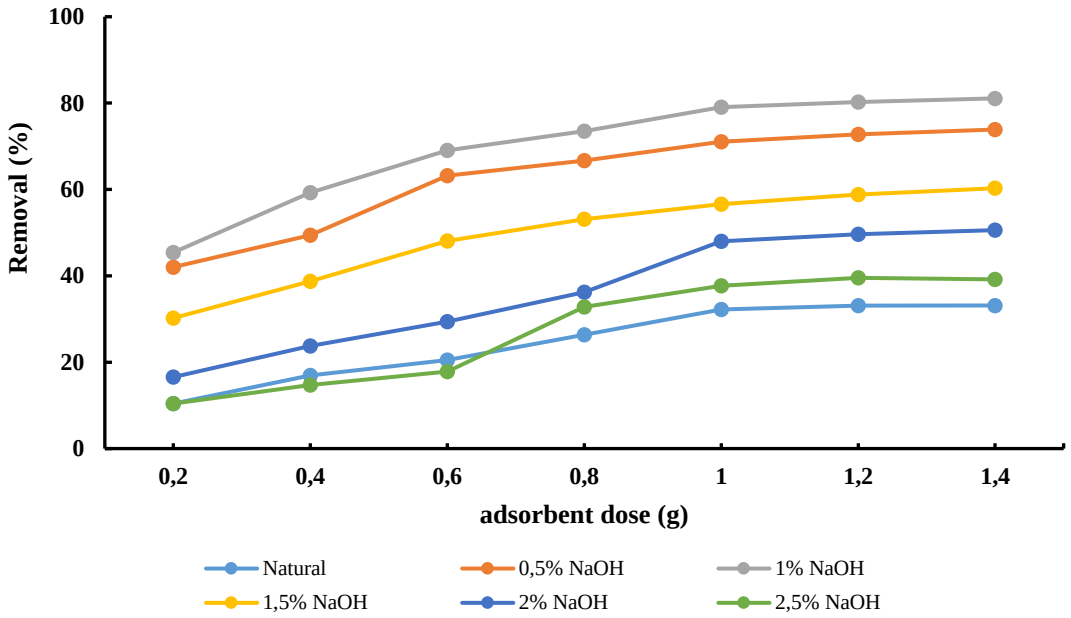

Figure 4.11: The effect of the biosorbent dosage on the biosorption of Fe^{2+} by the alkali-pretreated biosorbents

A different trend (presented in Figure 4.13) was observed for acid pretreatment of sugarcane bagasse, the concentration of sulphuric acid increased with the percentage removal of Fe^{2+}.

For the acid pretreatment of sugarcane bagasse, a distinct pattern was seen; the concentration of sulphuric acid increased with the % removal of Fe^{2+} (shown in Figure 4.13). After pretreatment with 0.5% H_2SO_4 to 2.5% H_2SO_4, the percentage of Fe^{2+} removed rose from 12.82 to 34.51% for 0.5% H_2SO_4 and from 20.87 to 58.79% for 2.5% H_2SO_4, respectively (at 0.2 and 1.0g). When adsorbent dosage was varied from 0.2 to 1.4 g, it was shown that an acid pretreatment of 2.5% H_2SO_4 pretreatment was the best performing acid-pretreated biosorbent in removing Fe^{2+}.

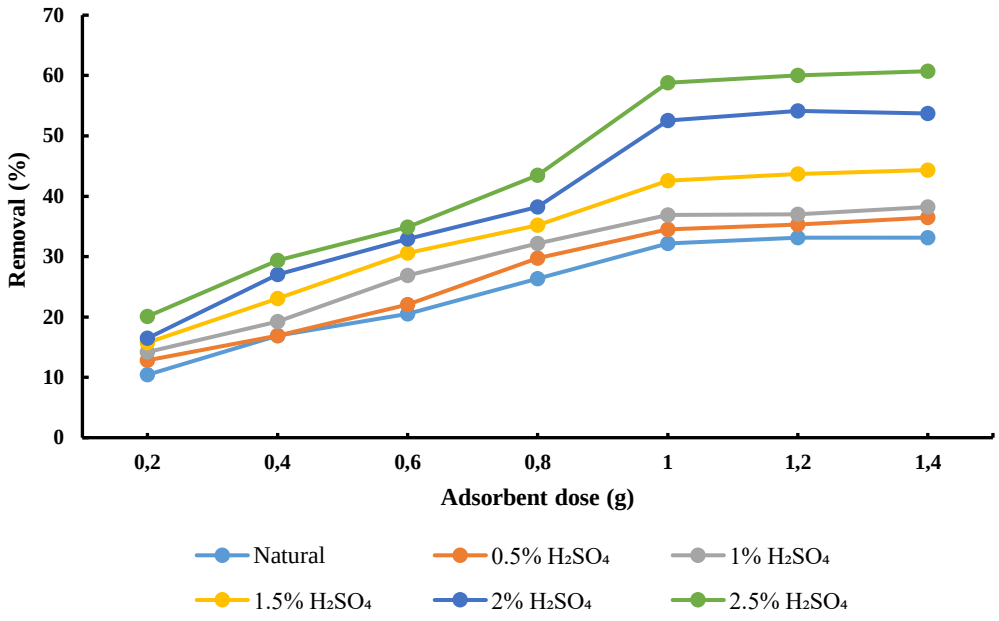

Figure 4.12: The effect of the biosorbent dosage on the biosorption of Fe^{2+} by the acid-pretreated biosorbents

When the adsorbent dose was increased from 0.2 to 1.4 g per 100 ml Fe^{2+} solution, the observed overall trend was that an increase in the concentration of sulphuric acid and sodium hydroxide resulted in an increased % removal of Fe^{2+}.

At (0.5% NaOH + 0.5% H_2SO_4), the observed percentages for the elimination of Fe^{2+} were 19.53% (0.2 g), 16.93% (0.4 g), 26.03% (0.6 g), 32.77% (0.8 g), 62.39% (1 g), 62.73% (1.2 g), and 62.75%. (1.4 g). The elimination of Fe^{2+} at (2.5% NaOH + 2.5% H_2SO_4) was seen to occur at the following rates: 6.07% (0.2 g), 27.4% (0.4 g), 38.62% (0.6 g), 53.4% (0.8 g), 70.73% (1 g), 70.73% (1.2 g), and 73.61%. (1.4 g).

For the combined pretreatment (Figure 4.13), the concentration of (0.5% NaOH + 0.5% H_2SO_4) for 1.0 g of biosorbent resulted in the best percentage Fe^{2+} removal of 70.73%, with the lowest percentage removal of Fe^{2+} seen at (2.5% NaOH + 2.5% H_2SO_4)- pretreated biosorbents. That there was no change in the percentage of metal uptake, increasing the adsorbent dosage from 1.0g to 1.4g for (0.5% NaOH + 0.5% H_2SO_4) pretreatment showed to be irrelevant. Therefore, when scaling up, an optimal adsorbent dosage of 1 g rather than 1.4 g can be employed to save costs.

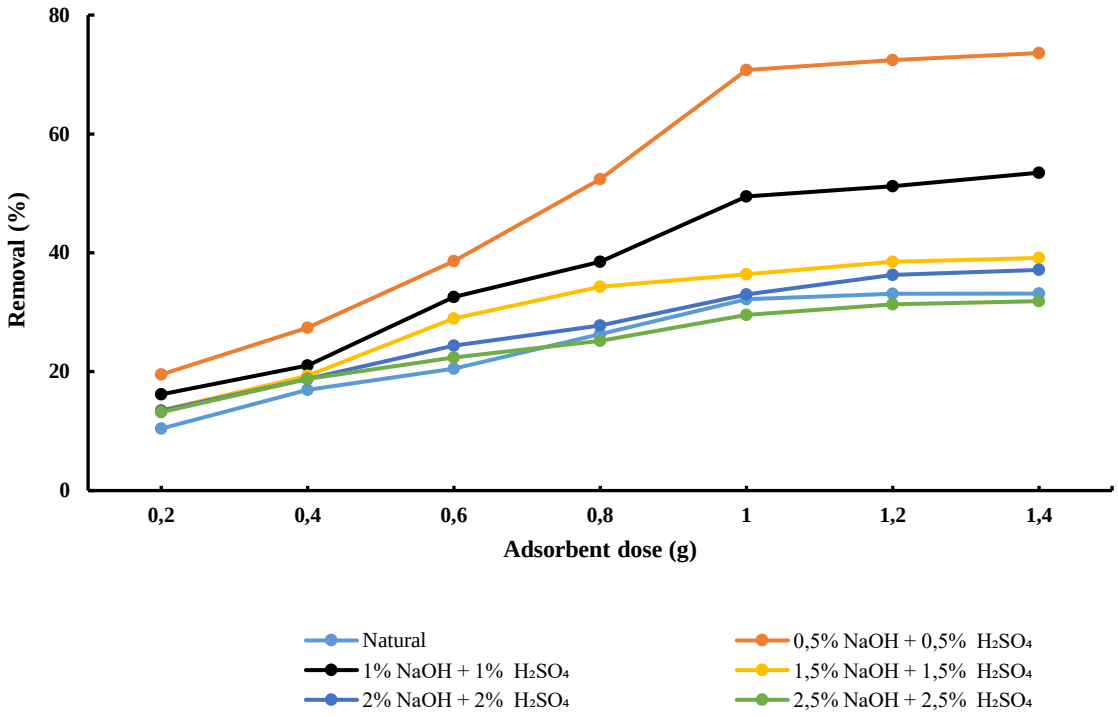

Figure 4.13: The effect of biosorbent dose of the biosorption of Fe^{2+} by the combined-pretreated biosorbent

4.3.1.5 Effect of contact time

The effect of contact time on adsorption of Fe^{2+} onto the active sites of natural and pretreated sugarcane bagasse was investigated by varying the contact time range of 5 to 100minutes, while all the other parameters were kept constant at pH 6; initial concentration at 1 mg/L and adsorbent dose at 1gram. Figures 4.14 to 4.16 illustrate the effect of contact time for natural and pretreated sugarcane bagasse during alkali, acid and alkali and acid pretreatments, respectively.

By varying the contact time range of 5 to 100 minutes, the effect of contact time on the biosorption of Fe^{2+} onto the active sites of natural and pretreated sugarcane bagasse was investigated. All other parameters, including initial concentration at 1 mg/L and adsorbent dose at 1 gram, were kept constant at pH 6. The impact of contact duration during alkali, acid, and alkali and acid pretreatments on natural and pretreated sugarcane bagasse is shown in Figures 4.14 – 4.16, respectively.

It was noted that as contact duration increased, the percentage elimination rose until equilibrium was established after 60 minutes. According to Figure 4.16, for natural sugarcane bagasse, the clearance rate increased from 2.36% to 50.22%. Following chemical pretreatment with a combination pretreatment of sodium hydroxide and sulphuric acid, as illustrated in Figure 4.16, an improvement in the structure of the bagasse was observed.

The performance of alkali-pretreated adsorbent decreased with an increase in pretreatment concentration from 0.5% NaOH to 1% NaOH thereafter decreased from 1.5% to 2.5% NaOH as shown in Figure 4.14. The percentage removal of Fe^{2+} increased from 39.13 to 74.03% for 0.5% NaOH; 55.22 to 99.62% for 1% NaOH; 48.77 to 98.2% for 1.5% NaOH; 45,6 to 92,5% for 2% NaOH and 43,2 to 88,67% for 2,5% NaOH.

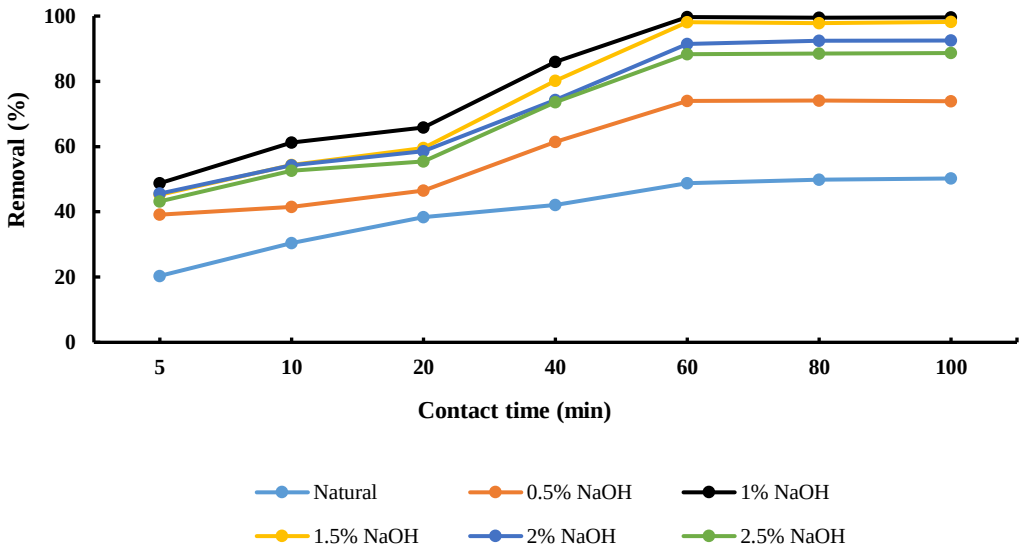

Figure 4.14: The effect of contact time on the biosorption of Fe^{2+} by the alkali-pretreated biosorbents

With an increase in acid pretreated adsorbent, the percentage of Fe^{2+} removal increased. Fe^{2+} removal was increased in a percentage ranging from 24.33 to 57.12% for 0.5% H_2SO_4, 26.41 to 58.66% for 1% H_2SO_4, 28.74 to 63.32% for 1.5% H_2SO_4, 31.48 to 69.51% for 2% H_2SO_4, and 38.63 to 57.61% for 2.5% H_2SO_4. According to Figure 4.15, the pretreated adsorbent with 2.5% H_2SO_4 produced the best percentage removal of Fe^{2+}.

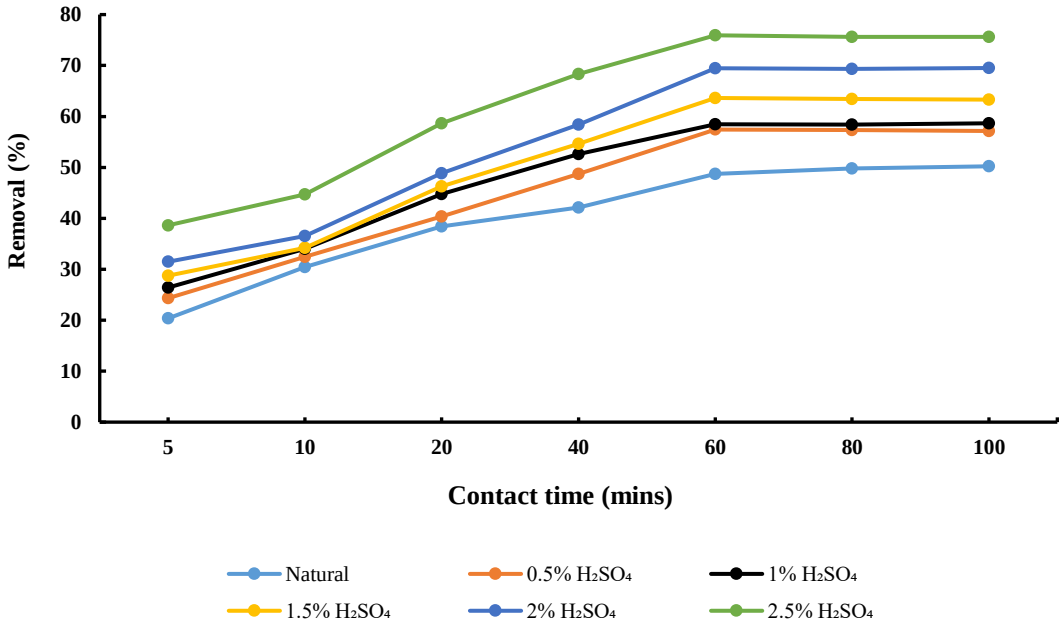

Figure 4.15: The effect of contact time on the biosorption of Fe^{2+} by the acid-pretreated biosorbents

According to the outcomes of the combined pretreatment of acid and alkali reported in Figure 4.16, the % removal of Fe^{2+} was inversely related to the concentration of the pretreated adsorbent. While the percentage of the metal ion removed increased when the pretreated adsorbent was exposed to the Fe^{2+} solution for 100 minutes and the pretreatment concentration increased from 0.5 to 2.5% (NaOH + H_2SO_4), the percentage of the metal ion removed decreased when comparing (0.5% NaOH + 0.5% H_2SO_4) to (2.5% NaOH + 2.5% H_2SO_4).

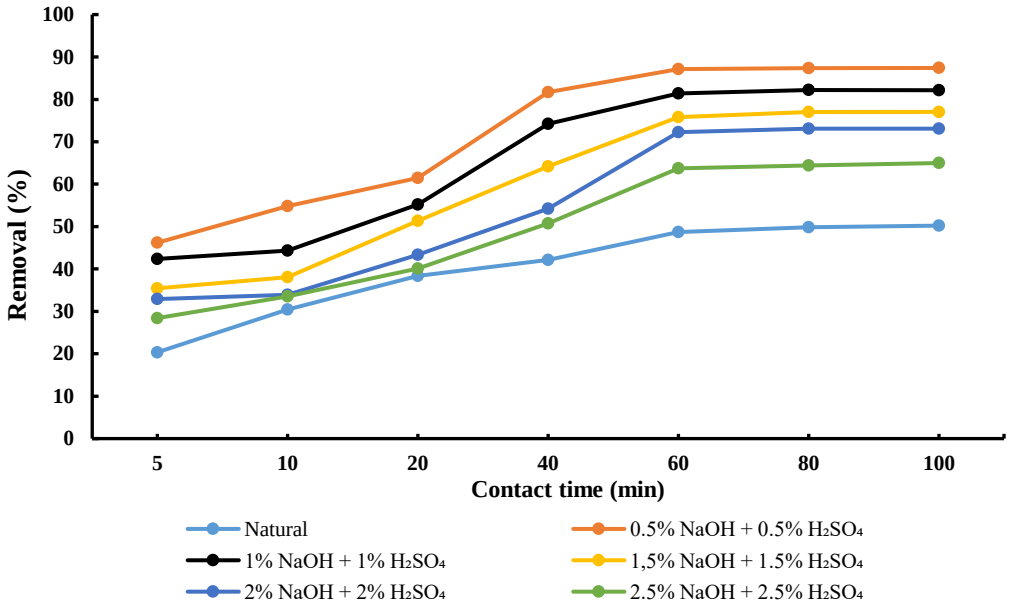

Figure 4.16: The effect of contact time on the biosorption of Fe^{2+} by the combined-pretreated biosorbents

4.4 Adsorption Isotherms

To comprehend the dynamics of the adsorption of Fe^{2+} onto the natural and modified sugarcane bagasse, the investigation on adsorption kinetics was carried out. Chemical and physical adsorption are two different types of the adsorption process. Chemical adsorption occurs when chemical bonds are formed, whereas physical adsorption happens when electrostatic forces interact with the adsorbent and adsorbate. The simplest adsorption isotherm is based on the idea that every adsorption site, regardless of whether or not adjacent sites are occupied, is identical in terms of a particle's ability to bond there.

The findings of the batch adsorption tests were examined using the generally employed isotherms, namely the Langmuir and Freundlich models, in order to ascertain the chemical mechanistic parameters related to Fe^{2+} sorption. The removal of Fe^{2+} by biosorption isotherm models was investigated at various initial concentrations ranging from 1- 30 mg/L at a dosage of 1 g adsorbent. Adsorption isotherms, which correspond to the relationship between the mass of the solute adsorbed per unit mass of the adsorbent qe and the solute concentration of the solution at equilibrium C_e, are a suitable representation for the adsorption equilibrium data.

The value of the maximal uptake adsorption capacity (q_{max} (mg/g)) and the energy of the biosorption (K_L (L/mg)) were calculated using linear plots of C_e/q_e *vs* C_e. The linear plots of the natural sugarcane bagasse are shown in Figures 4.17 (a,b); the linear plots of the modified biosorbents are shown in Appendices A to F. Table 4.4 contains the information gathered for the Langmuir and Freundlich constants.

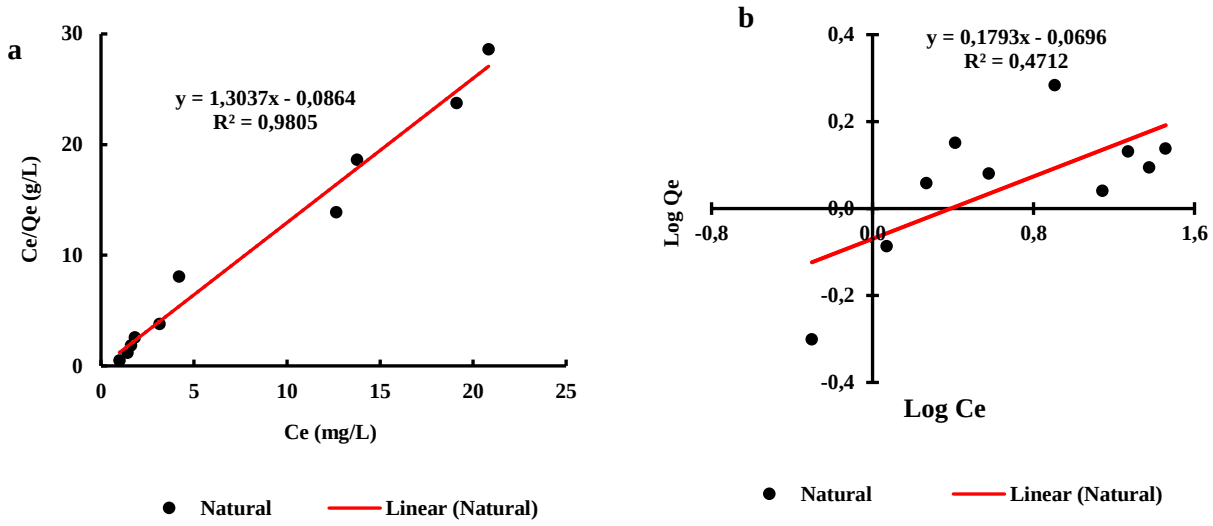

Figure 4.17: Adsorption isotherms of the biosorption of Fe^{2+} using natural sugarcane bagasse (a) Langmuir, (b) Freundlich

Table 4.4: Parameters for the Freundlich and Langmuir isotherms

	FREUNDLICH MODEL				**LANGMUIR MODEL**			
	$\log Q_e = \frac{1}{n}\log C_e + \log K_f$				$\frac{C_e}{q_e} = \frac{1}{q_{max}} C_e + \left(\frac{1}{K_L q_{max}}\right)$			
	K_f (mg/g)	***n***	$\frac{1}{n}$	***R^2***	***K_L (L/mg)***	***q_{max} (mg/g)***	***R^2***	***R_L***
Natural	0.852	5.577	0.179	0.471	0.066	0.770	0.981	0.938
0.5% NaOH	1.875	2.967	0.337	0.858	1.204	4.810	0.987	0.454
1% NaOH	4.019	3.851	0.260	0.983	1.432	9.199	0.988	0.469
1.5% NaOH	3.439	3.251	0.308	0.989	1.218	8.547	0.983	0.451
2% NaOH	2.615	2.982	0.335	0.971	1.121	7.310	0.983	0.366
2.5% NaOH	0.323	3.101	0.322	0.948	0.991	5.200	0.986	0.502
0.5% H_2SO_4	1.058	2.496	0.401	0.921	3.700	4.435	0.974	0.213
1% H_2SO_4	1.100	2.398	0.417	0.941	3.805	4.433	0.965	0.208
1.5% H_2SO_4	1.206	2.413	0.414	0.959	3.330	4.647	0.981	0.231
2% H_2SO_4	1.396	2.581	0.387	0.958	2.409	4.645	0.995	0.293
2.5% H_2SO_4	0.323	3.101	0.322	0.975	2.587	5.743	0.994	0.279
0.5% NaOH + 0.5% H_2SO_4	0.852	5.577	0.179	0.892	0.869	5.297	0.987	0.535
1% NaOH + 1% H_2SO_4	1.827	3.047	0.328	0.831	0.574	4.144	0.985	0.635
1.5% NaOH + 1.5% H_2SO_4	1.618	3.189	0.314	0.816	0.368	3.486	0.982	0.731
2% NaOH + 2% H_2SO_4	1.537	4.577	0.18	0.449	-1.220	1.646	0.884	-4.545
2.5% NaOH + 2.5% H_2SO_4	1.105	3.140	0.318	0.458	-0.875	1.435	0.872	8.000

The maximal adsorption capacity q_{max} and adsorption energy K_L for the natural sugarcane bagasse were determined to be 0.770 mg/g and 0.066 L/mg, respectively, using the Langmuir model study presented in Table 4.4. After applying all of the chemical pretreatments to the sugarcane bagasse, these metrics increased. However, it should be noted that the maximal adsorption capacities for 0.5% NaOH and 1% NaOH were 4.81 mg/g and 9.199 mg/g, respectively, whereas the K_L values for these concentrations were 1.204 and 1.432 L/mg.

The adsorption capacity and adsorption energy dropped to 8.547 mg/g and 1.218 L/mg for 1.5% NaOH and 5.2 mg/g and 0.99 L/mg for 2.5% NaOH when the sodium hydroxide pretreatment

concentration increased from 1.5% NaOH to 2.5% NaOH. The greatest q_{max} (9.199 mg/g) and K_L (1.432) for the alkali pretreatment are for 1% NaOH. The natural sugarcane bagasse's correlation factor (R^2) was 0.988.

The maximal adsorption for the acid pretreatment Langmuir isotherm was inversely related to the acid pretreatment's concentration. The q_{max} increased from 4.435 mg/g at 0.5% H_2SO_4 to 5.743% at 2.5% H_2SO_4, whereas the adsorption energy (K_L) increased from 3.7 to 4.59 L/mg as the pretreatment concentration increased from 0.5% H_2SO_4 to 2.5% H_2SO_4. Among the range of acid pretreatment concentrations, 2.5% H_2SO_4 had the maximum adsorption capacity of 5.743 mg/g and K_L of 2.587.

The maximum adsorption capacity declined from 5.297 mg/g to 1.435 mg/g and from 0.869 L/mg to -0.875 L/mg when the concentration of the combined pretreatment rose from (0.5% NaOH + 0.5% H_2SO_4) to (2.5% NaOH + 2.5% H_2SO_4). Natural sugarcane bagasse, alkali-pretreated material and acid-pretreated material all had correlation coefficients (R^2) above 0.95; however, for the combined pretreatment, the correlation factor for (0.5% NaOH + 0.5% H_2SO_4) was 0.987 and decreased to 0.872 for (2.5% NaOH + 2.5% H_2SO_4). For 0.5% H_2SO_4 and 2.5% H_2SO_4, the correlation coefficient (R^2) increased from 0.921 to 0.975, respectively.

The Langmuir equation provides an excellent fit to the adsorption isotherm, as shown by the parameters of the Langmuir isotherm and the correlation coefficient for all adsorbents. The values of the dimensionless constant separation factor (R_L) for the natural and modified biosorbents are shown in Table 4.1 at initial concentrations of 1 mg/L and 30 mg/L (highest concentration studied). According to (Mckay, Blair and Gardner 1982), these results, which were all in the ranges of 0 and 1, show that the adsorption of Fe^{2+} onto the natural and modified sugarcane bagasse was successful.

The sorption capacity and correlation factor for the natural sugarcane bagasse under the Freundlich model were 5.57 and 0.471, respectively. For 1% NaOH, the greatest sorption capacity of 3.581 and K_f of 4.019 were attained. With an increase in acid pretreatment concentration, the sorption

capacity similarly increased, rising from 2.496 at 0.5% H_2SO_4 to 3.101 at 2.5% H_2SO_4. The concentration of (0.5% NOH + 0.5% H_2SO_4) had the maximum sorption capacity (*n*) of 5.577 for the combined pretreatment. When (0.5% NaOH + 0.5% H_2SO_4) and (2.5% NaOH + 2.5% H_2SO_4) were used as a combined pretreatment, the correlation coefficient (R_L) dropped from 0.892 to 0.318. All pretreatments have values for the sorption intensity (*n*) that range from 0 to 10, indicating that the adsorption is favorable (Calace *et al.* 2002; Kadirvelu and Namasivayam 2003).

4.5 Adsorption kinetics

Adsorption kinetics is the study of how long it takes to attain equilibrium for the adsorption of heavy metals onto an adsorbent's surface and to pinpoint an appropriate model that accounts for the adsorption. According to the findings of the contact variation investigation, equilibrium was attained for all of the investigated biosorbents in less than 60 minutes. In Figures 4.18 to Figure 4.23, the kinetic results for the pseudo-first and pseudo-second orders are represented graphically. Beyond 60 minutes, there was no appreciable rise in the removal percentage. The data from the batch trials was fitted into two widely used kinetic models, namely pseudo-first-order and pseudo-second-order kinetic models, in order to explore the adsorption kinetics of Fe^{2+}.

The parameters of the pseudo-first-order model (k_1 and q_e) were determined using linear plots of log (qe-qt) versus t. For pseudo-second-order, the slope and intercept of the linearized plot of *t/q* vs *t* were used to calculate the rate constant (k_2) and equilibrium adsorption capacity (q_e) (refer to appendices H_1 to H_3 for full results). Tables 4.5 to 4.10 display the findings from the pseudo-first and pseudo-second-order kinetic models.

4.5.1 Pseudo-First-Order kinetic model

Figure 4.18, where $ln\ (q_e - q_t)$ was plotted against time *t*, display pseudo-first-order graphically. Both the natural and alkali-modified sugarcane bagasse are represented by the data in Figure 4.18 and Table 4.5. The natural bagasse had an R^2 of 0.84, indicating that the model did not fit well between 5 and 60 minutes. However, Table 4.5 also shows that when the biosorbent that had been prepared with 1% NaOH was utilized to remove Fe^{2+} ions, R^2 was found to have increased to 0.941, demonstrating an excellent fit for the model.

After that, the R^2 dropped to 0.850, 0.893, and 0.821 for 1.5%, 2%, and 2.5% NaOH, respectively, indicating that the alkali-modified sugarcane bagasse's active sites had been saturated and inhibited the biosorption of Fe^{2+}.

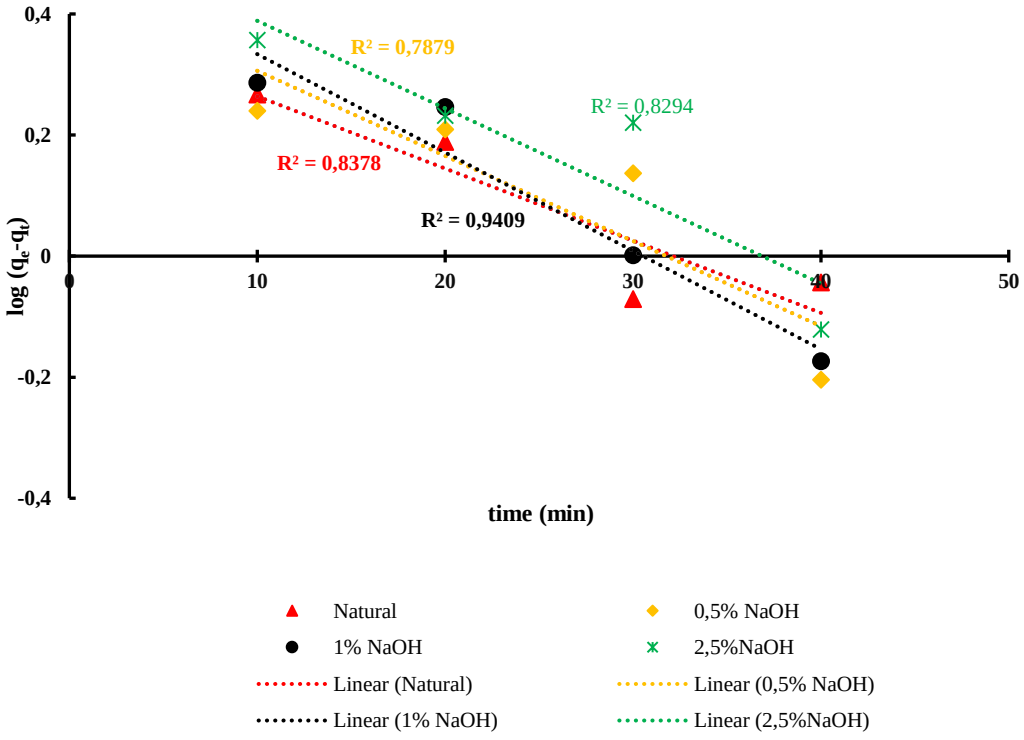

Figure 4.18: Linearized pseudo-first-order kinetic model for the alkali-pretreated biosorbents

Table 4.5: Parameters for the pseudo-first-order of the alkali-pretreated biosorbents

	qe_{exp} (mg/g)	$qe_{(calc)}$ (mg/g)	$K_1(min^{-1})$	R^2
Natural	2,437	3,805	0,055	0,838
0,5% NaOH	3,702	2,798	0,032	0,788
1% NaOH	4,975	3,599	0,041	0,941
1,5% NaOH	4,906	4,288	0,043	0,850
2% NaOH	4,573	5,076	0,057	0,893
2,5% NaOH	4,426	3,415	0,033	0,829

The graphical representation of the pseudo-first order for the acid-pretreated biosorbents ranging from 0.5% H_2SO_4 to 2.5% H_2SO_4 is shown in Figure 4.19 and Table 4.6. Log (q_e- q_t) was plotted against time *t* in order to determine the parameters of the pseudo-first-order. The findings in Table 4.6 demonstrate a strong connection with an R^2 above 0.95. For all variable concentrations of the acid pretreatment, the experimental results $q_{e(exp)}$ were very near to the theoretical results ($q_{e(calc)}$), indicating that the biosorption of Fe^{2+} onto the acid-pretreated biosorbent was a good fit for the pseudo-first-order. The graph's complete data set is available in Appendix G_1 to G_3.

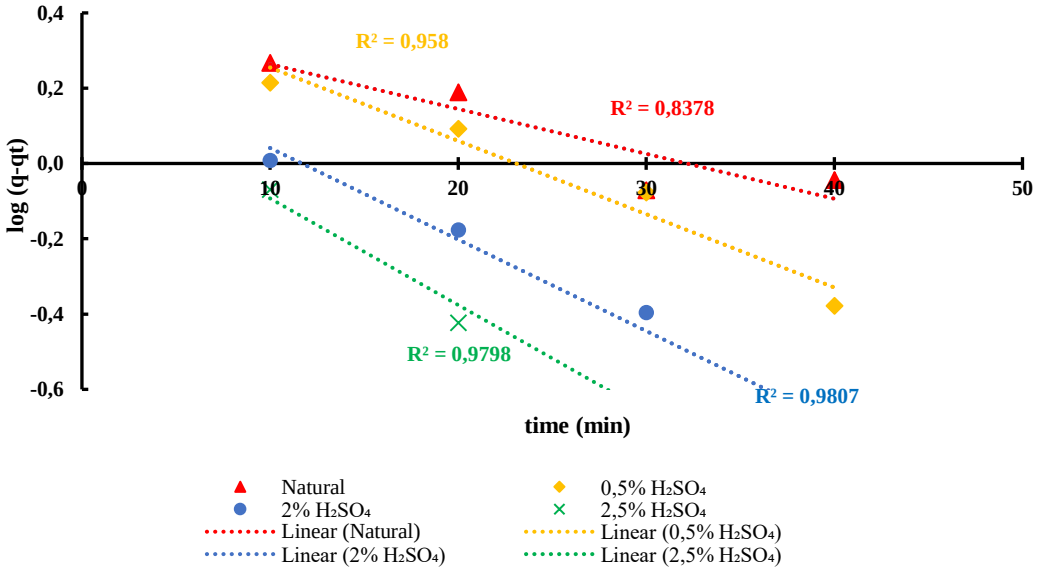

Figure 4.19: Linearized pseudo-first order for the biosorption of Fe^{2+} using acid-pretreated biosorption

Table 4.6: Parameters of the pseudo-first-order for the acid-pretreated biosorbent

	$q_{e(exp)}$ (mg/g)	$q_{e\ (calc)}$ (mg/g)	$K_1(min^{-1})$	R^2
Natural	2,437	3,805	0,055	0,838
0,5% H_2SO_4	2,867	2,816	0,044	0,958
1% H_2SO_4	2,922	3,267	0,056	0,951
1,5% H_2SO_4	3,182	3,164	0,047	0,944
2% H_2SO_4	2,451	1,924	0,056	0,981
2,5% H_2SO_4	2,766	1,55	0,065	0,98

The graphical and tabulated results for the combined pretreatment's pseudo-first-order are shown in Figure 4.20 and Table 4.7. The R^2 for the variable concentration of the combined pretreatments was quite low, indicating poor correlation of the model to the biosorption process of the Fe^{2+} ions, even if the calculated $q_{e\ (calc)}$ and the experimental $q_{e\ (exp)}$ were close to each other.

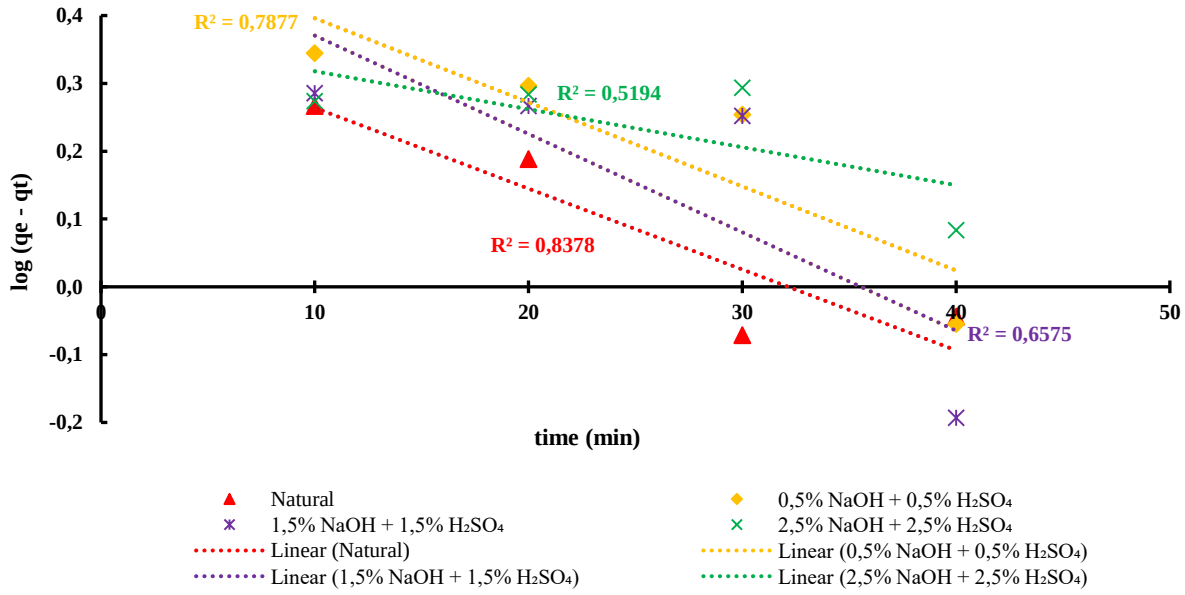

Figure 4.20: Linearized pseudo-first-order for the biosorption of Fe^{2+} using combined pretreated biosorption

Table 4.7: Kinetic parameters of the pseudo-first-order for the combined pretreatment

	$q_{e\ (exp)}$ (mg/g)	$q_{e\ (calc)}$ (mg/g)	K_1(min^{-1})	R^2
Natural	2,437	3,805	0,055	0,838
0,5% NaOH + 0,5% H_2SO_4	4,367	5,836	0,063	0,788
1% NaOH + 1% H_2SO_4	4,111	4,337	0,049	0,677
1,5% NaOH + 1,5% H_2SO_4	3,791	3,277	0,033	0,658
2% NaOH + 2% H_2SO_4	3,715	2,441	0,02	0,671
2,5% NaOH + 2,5% H_2SO_4	3,223	2,365	0,014	0,519

4.5.2 Pseudo-Second-Order kinetic model

For the biosorption of Fe^{2+} onto the alkali, acid and combined-pretreated biosorbent, the pseudo-second order parameters are shown in Figures 4.21 to 4.23 and Tables 4.8 to 4.10. The natural sugarcane bagasse had corresponding $q_{e\ (exp)}$ and $q_{e\ (calc)}$ values of 2.44 mg/g and 3.46 mg/g. With an increase in alkali-pretreatment concentration, these values rose. The estimated $q_{e\ (calc)}$ for the changed biosorbents were all in line with the individual biosorbents' experimental $q_{e\ (exp)}$. $Q_{e\ (exp)}$ values for 0.5% and 1% NaOH were 3.702 and 4.975 mg/g, respectively, and $q_{e\ (calc)}$ values were 6.031 and 6.506 mg/g.

However, Table 4.8 also shows that for 1.5% - 2.5% NaOH, these values ($q_{e\ (exp)}$ and $q_{e\ (calc)}$) declined. The natural bagasse's R^2 was discovered to be 0.89. After alkali pretreatment, this R^2 rose to 0.93 for 0.5% NaOH, 0.97 for 1% NaOH, 0.96 for 1.5% NaOH, and 0.93 for 2.5% NaOH. These findings demonstrate that the biosorption of Fe^{2+} suited the pseudo-second-order model quite well.

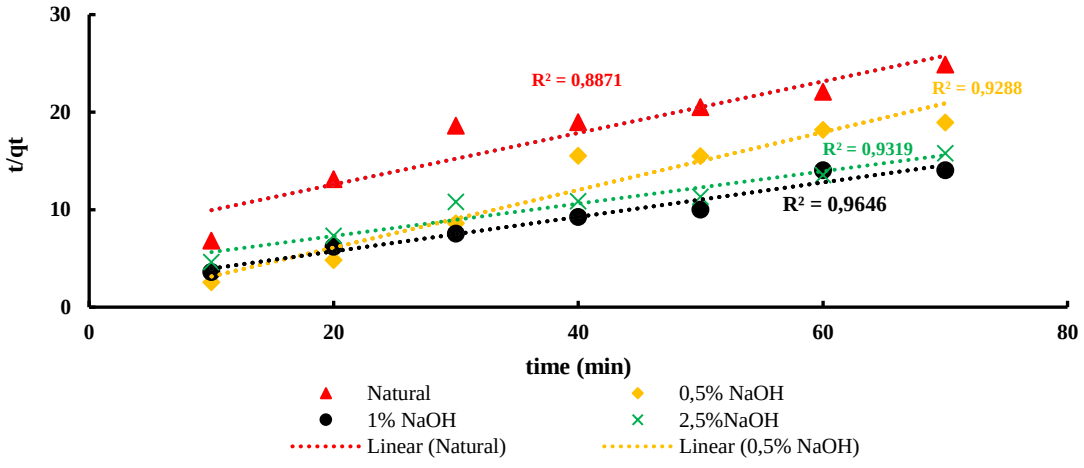

Figure 4.21: Linearized pseudo-second-order for the biosorption of Fe^{2+} using the alkali-pretreated biosorbents

Table 4.8: Pseudo-second-order for the alkali-pretreated biosorbents

	$q_{e(exp)}$ (mg/g)	$q_{e(calc)}$(mg/g)	K_2(min^{-1})	R^2
Natural	2,437	3,458	0,012	0,887
0,5% NaOH	3,702	6,031	0,007	0,929
1% NaOH	4,975	6,506	0,007	0,965
1,5% NaOH	4,906	6,158	0,011	0,960
2% NaOH	4,573	6,131	0,008	0,955
2,5% NaOH	4,426	3,644	0,072	0,932

The data for the pseudo-second-order Fe^{2+} adsorption by the acid-pretreated biosorbent is shown in Figure 4.22 and Table 4.9. As the concentration of the acid pretreatment was raised, the R^2 value climbed from 0.905 to 0.981, and the values of the $q_{e\ (exp)}$ from the pseudo-second order were closer to those of the computed $q_{e\ (calc)}$.

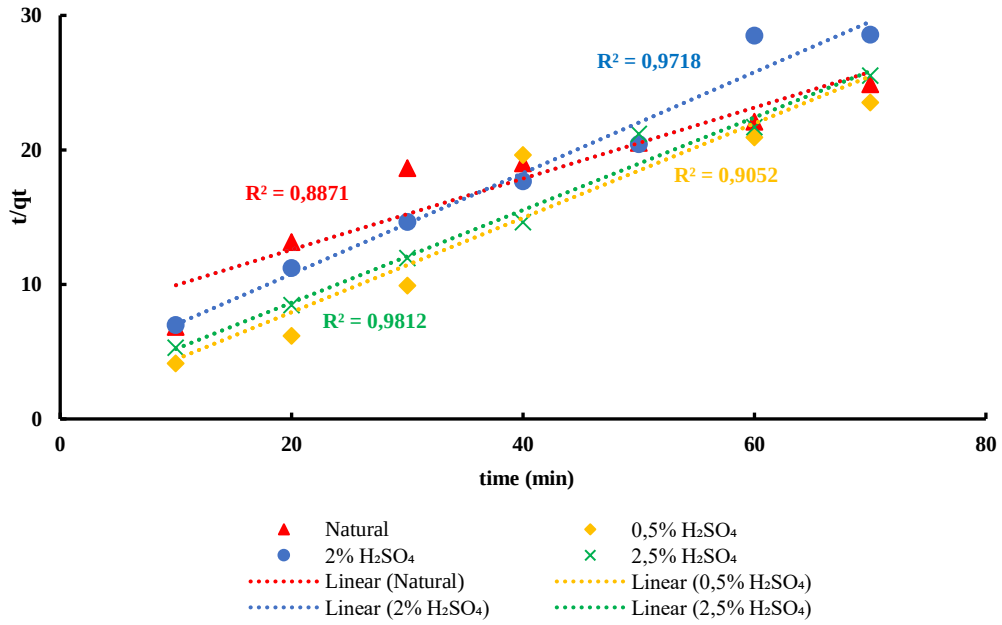

Figure 4.22: Linearized pseudo-second-order for the biosorption of Fe^{2+} using acid-pretreated biosorbents

Table 4.9: Pseudo-second-order for the acid-pretreated biosorbents

	$q_{e(exp)}$ (mg/g)	$q_{e(calc)}$(mg/g)	K_2(min^{-1})	R^2
Natural	2,437	3,458	0,012	0,887
0,5% H_2SO_4	3,702	2,851	0,091	0,905
1% H_2SO_4	4,975	3,992	0,011	0,926
1,5% H_2SO_4	4,906	4,762	0,007	0,943
2% H_2SO_4	4,573	2,885	0,031	0,972
2,5% H_2SO_4	4,426	2,998	0,063	0,981

The pseudo-second-order of the combined pretreatment is shown by the results in Figure 4.23. The (0.5% NaOH + 0.5% H_2SO_4) combination pretreatment in Table 4.10 had an R^2 of 0.95, indicating that the model had an excellent fit for the experiments between 5 and 60 minutes. The estimated and experimental *qe* values coincided very closely.

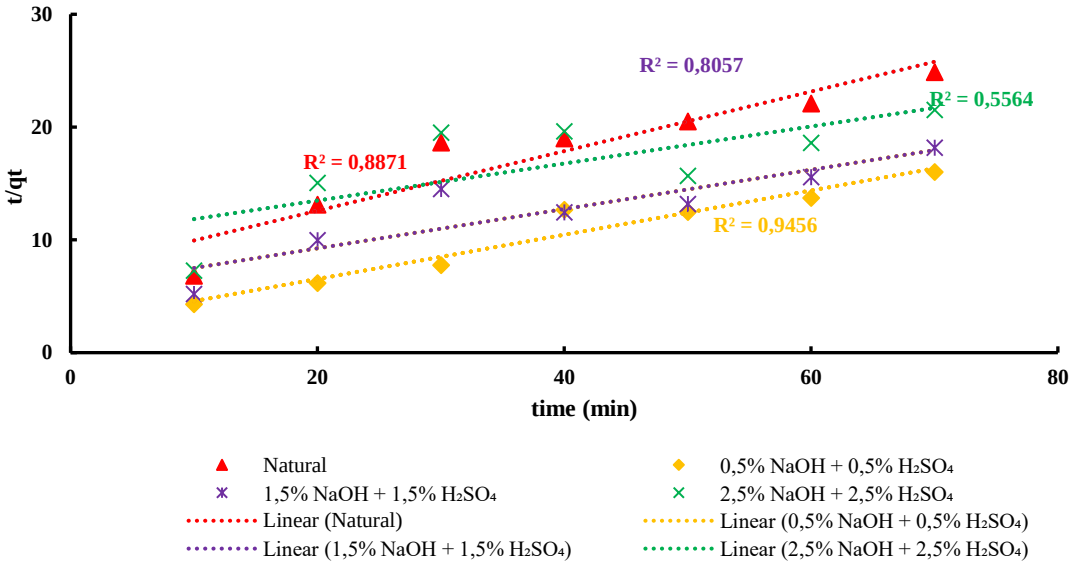

Figure 4.23: Linearized pseudo-second-order for the combined-pretreated biosorbents

Table 4.10: Pseudo-second-order for the combined pretreatment

	qe_{exp} (mg/g)	$q_{e(calc)}$ (mg/g)	K_2 (min^{-1})	R^2
Natural	2,437	3,458	0,012	0,8871
0,5% NaOH + 0,5% H_2SO_4	3,702	4,38	0,058	0,9456
1% NaOH + 1% H_2SO_4	4,975	5,945	0,006	0,8218
1,5% NaOH + 1,5% H_2SO_4	4,906	5,741	0,005	0,8057
2% NaOH + 2% H_2SO_4	4,573	5,376	0,006	0,8016
2,5% NaOH + 2,5% H_2SO_4	4,426	6,086	0,003	0,5564

In summary, the findings indicate that the biosorption of Fe^{2+} onto the natural and combined pretreatments occurred through pseudo-second-order, and that the adsorption for the natural sugarcane bagasse as well as the combined pretreatments occurred by chemisorption adsorption through the ion exchange between the adsorbate and the adsorbent. The pseudo-first and pseudo-second orders were favored by the biosorption of the acid pretreatment and the alkali pretreatment, respectively. This indicates that physical (pores) and chemical adsorption processes were used to biosorb Fe^{2+} onto the alkali-pretreated and acid-pretreated biosorbents (ion exchange).

4.6 Characterization studies

4.6.1 Fourier-Transform Infrared spectroscopy (FTIR)

In cellulosic materials, the FTIR has been extensively employed to get direct knowledge of the chemical changes that take place during chemical pretreatments (Ristolainen *et al.* 2002). The FTIR analysis was carried out on both natural and modified sugarcane bagasse in order to identify the functional groups involved in adsorption that are present on their surfaces. The majority of agricultural biomass, according to the literature, contains functional groups such hydroxyl, carbonyl, ketones, ether, and carboxylic groups. Figures 4.24 to 4.26 show the FTIR spectra of alkali, acid, and combination pretreatments.

The appearance of an intense and broad absorption band at 3450–3343 cm^{-1} in the spectra of natural bagasse indicated the presence of intermolecularly bonded hydroxyl (O–H) groups, while peaks at 2945–2920 cm^{-1} represented the C–H stretching vibration of the methylene units found in cellulose, hemicellulose, and lignin. The ester carbonyl (C=O) stretching vibration of the acetyl and uronic groups in hemicellulose or the ester linkage of the carboxylic groups of the ferulic and p-coumaric acids in lignin and/or hemicellulose were attributed to the occurrence of the broad peak at 1739 cm^{-1} (Sain and Panthapulakkal 2006).

The bands at 1600 and 1500 cm^{-1} are due to the existence of the C=C aromatic vibration present in lignin and are features of the aromatic compounds, phenolic hydroxyl groups (Garside and Wyeth 2003; Wang *et al.* 2009). Bands at 1426 cm^{-1} were related to the degree of cellulose's crystalline structure. The aryl group in lignin's C-O out of plane stretching vibrations is believed to be responsible for the peak at 1241 cm^{-1} in the natural sugarcane bagasse (Le Troedec *et al.* 2008). The stretch vibrations of the C=C and C-O bonds of the acetyl ester groups found in the

hemicellulose were identified as the source of the peak at 1243 cm^{-1} on the spectra of natural sugarcane bagasse.

The graphs of the FTIR spectra following chemical pretreatment with alkali, acid, or combined pretreatment of acid and alkali are shown in Figures 4.24 to 4.27. Following the same pattern, some functional groups' intensities in the adsorbents' spectra after the chemical pretreatments. The peaks that indicated that the chemical pretreatments had a significant impact were at 832, 1206, 1240, 1348, 1522, 1743, 2848, and 3330 cm^{-1}. Due to the elimination of lignin and hemicellulose, both the acid and alkali pretreatments generated several variations in the structure of the sugarcane bagasse, as seen by these shifts in intensity.

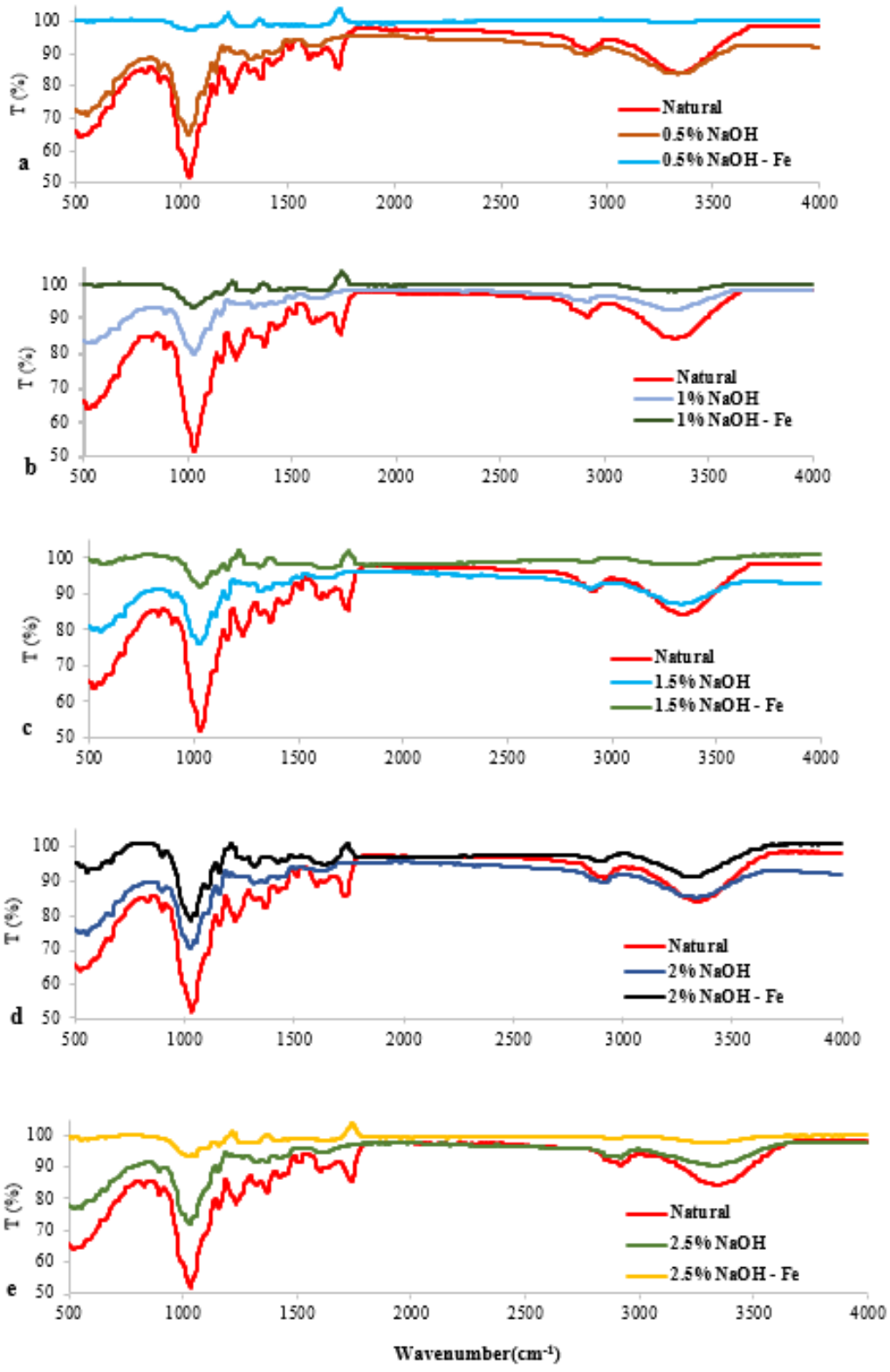

Figure 4.24: The FTIR spectra for the alkali-pretreated biosorbents

It is important to note that small mass of lignin were partially released into the filtrate following processing, as seen by the peaks at 3372 and 3332 cm^{-1}, which showed a drop in the intensity of hydroxyl groups due to alcoholic and phenolic hydrogen bonds in lignin. Peaks at 1756 cm^{-1} in every pretreatment eliminated as a result of the lignin removal. These alterations were anticipated given that lignin is mostly associated to this region, and the decrease was brought on by sodium hydroxide's breakdown of lignin into smaller units by cleaving the links between phenylpropane units, which produced phenolic hydroxyl groups. As the sulphuric acid concentration rose, it was seen in Figure 4.25 that the intensity of these bands diminished.

This demonstrated that sulphuric acid had a greater impact on the removal of arabinoxylan contained in hemicellulose, which led to a proportionally higher lignin content in the acid-pretreated sugarcane bagasse and produced the sharp band at 1515 cm^{-1} that denotes a higher lignin content. The hydrolysis of ester bonds between hemicellulose and lignin caused the peaks to vanish. The lowering of the signal at 1032 cm^{-1} provided evidence that the hemicellulose component had been dissolved.

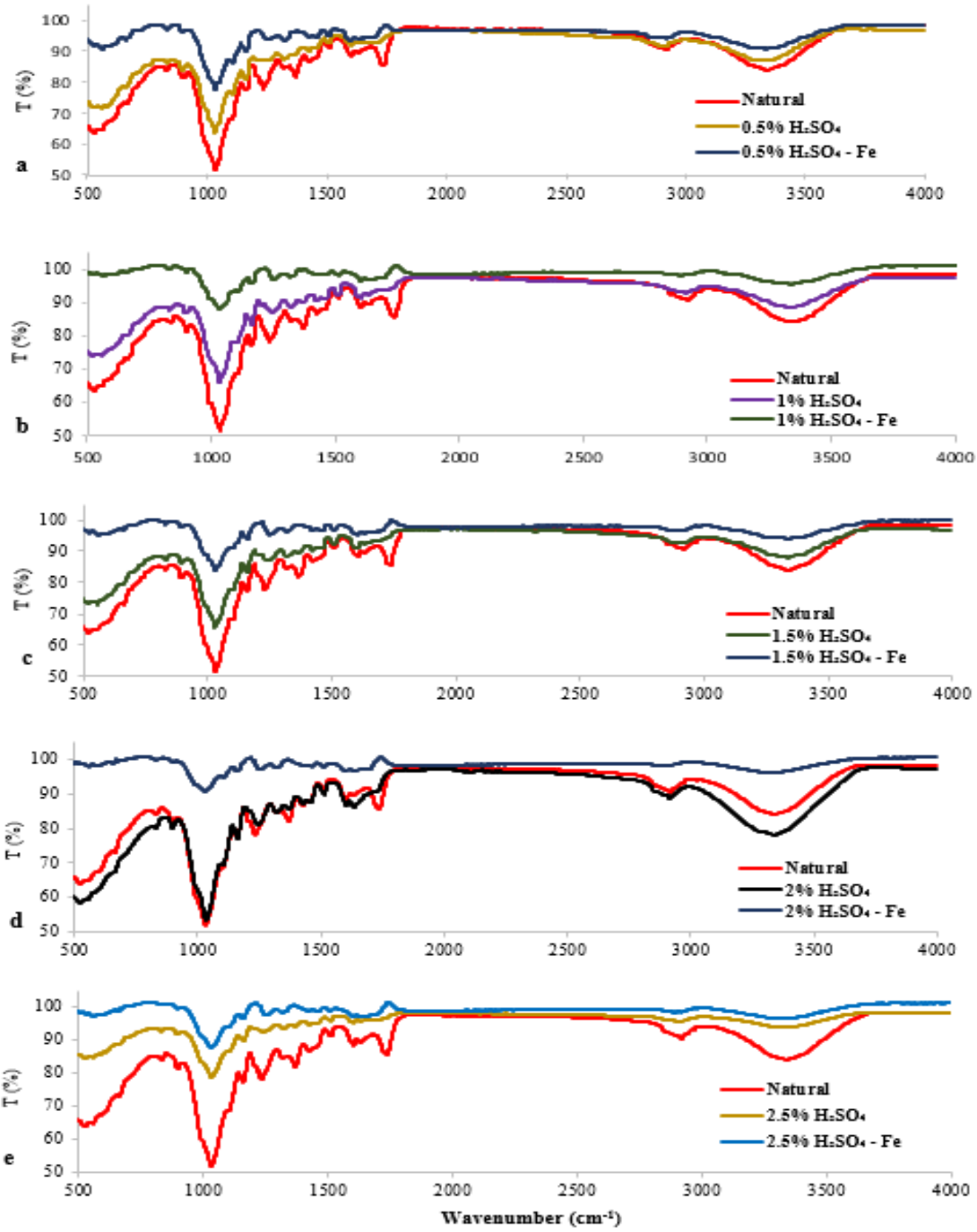

Figure 4.25: The FTIR spectra for the acid-pretreated biosorbents

An effective breakdown of the cross-linkages between the acetyl group of the lignin and hemicellulose components was suggested by a decrease and complete disappearance of peaks at 1756 cm^{-1} from the spectra of alkali and acid-modified structure. This likely resulted in the separation of the lignin components from the cellulose-hemicellulose linkages complex matrix from all types of modified bagasse. On the NaOH-modified spectrum, it should be noted that the peaks at 1756, 1510, 1030, and 833 cm^{-1} have vanished. Peaks at 1630, 1602, 1510, 1325, 1270, 1060, and 833 cm^{-1} in the H_2SO_4 spectra were reduced after pretreatment with acid. This implied that both lignin and hemicellulose have been removed. After H_2SO_4 pretreatments, the hemicellulose-related peaks at 1043 and 997 cm^{-1} reduced.

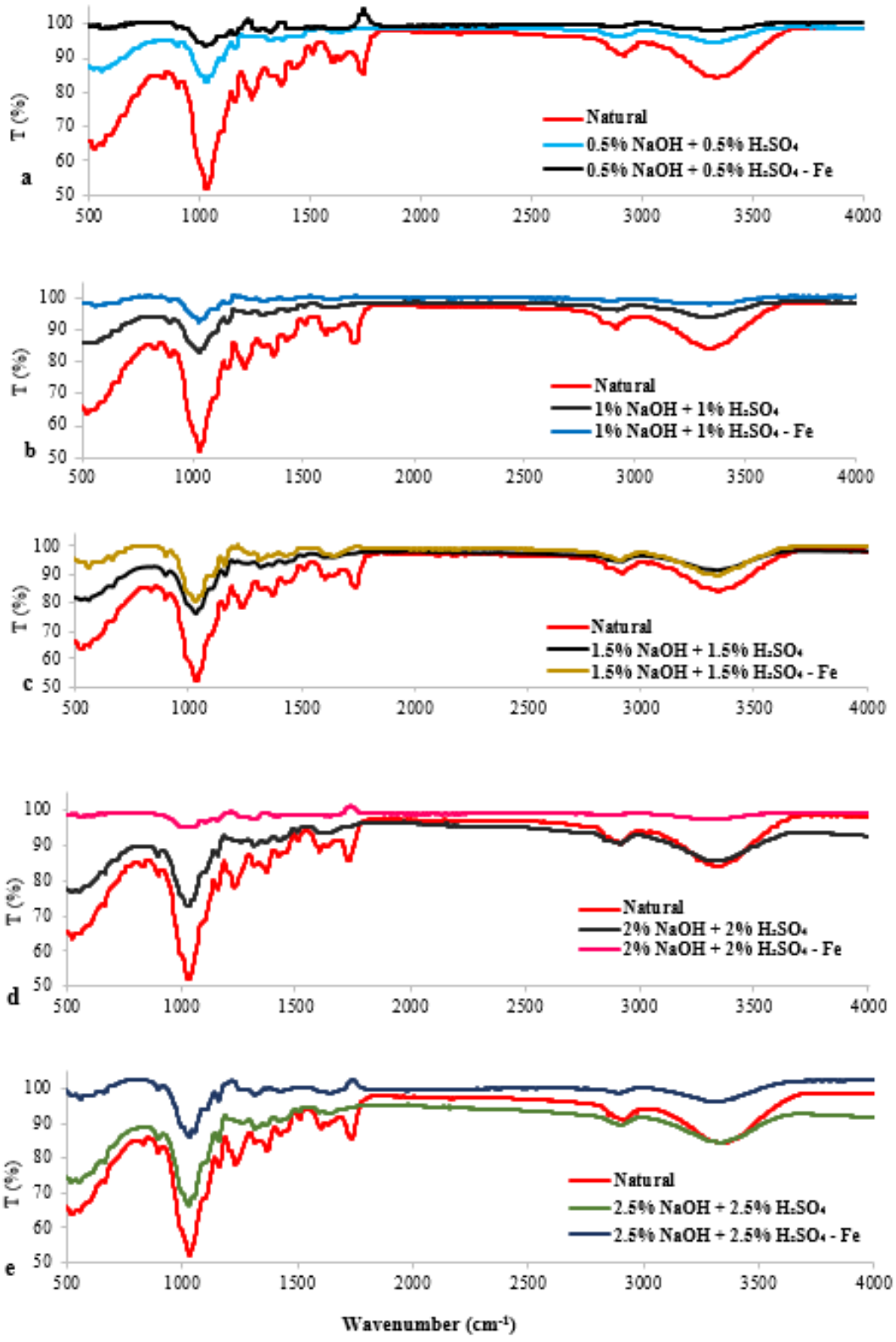

Figure 4.26: The FTIR spectra for the combined-pretreated biosorbents

Following the Fe^{2+} biosorption, an FTIR analysis was conducted to look for any potential alterations in the structural makeup of the original and modified bagasse. These adsorbents' FTIR spectra are displayed in Figures 4.24, 4.25, and 4.26. Following Fe^{2+} adsorption, a significant band shift and percentage increase in transmittance are seen in the FTIR spectra. These variations in the bands and transmittance imply a drop in intensity. It is important to note that after the adsorption of Fe^{2+}, the maxima of the bands in the 500–898 cm^{-1} range decreased for the alkali pretreatment, indicating that the functional groups present on these regions were involved in the adsorption of Fe^{2+}. Also seen are very angular peaks. After the adsorption of Fe^{2+} using various NaOH concentrations, extremely strong peaks can also be seen at 1220, 1375, and 1740cm^{-1}.

Following the adsorption of Fe^{2+} onto the natural and modified sugarcane bagasse, a drop in intensity is seen in the region of the hydroxyl groups (3175-3490 cm^{-1}), which shows that hydroxyl groups also played a role in the process.

After Fe^{2+} biosorption, a discernible change in peak intensities is seen on the spectra of acid pretreatment, with larger alterations seen at 1217, 1606, and 1745 cm^{-1}. The spectra of combination pretreatment employing alkali and acid pretreatment show a higher change. It is evident that with combined pretreatments, the majority of the peaks and their intensities dropped. The rise in hydroxyl and carbonyl group concentrations after pretreatments led to the lignin's hydrophilicity. Following the adsorption of Fe^{2+}, the results of all the spectra demonstrate that the carbonyl, silanol, and hydroxyl functional groups were crucial in the biosorption of Fe^{2+}.

4.6.2 X-Ray Diffraction (XRD)

Figures 4.27 to 4.29 display the X-ray diffractograms of sugarcane bagasse in its natural and modified forms. The cellulose-I structure is often represented by three primary distinctive peaks at 2theta values of 18.5, 22.5, and 34.5°, which were visible in the diffractograms of sugarcane bagasse in both its native and modified forms. While the greater intensity peak at 22.5° reflects $I_{(002)}$ of the crystalline material in cellulosic fibers, the low 2° angle reflection at 18.5° was of low intensity and represents $I_{(am)}$ of amorphous material. Numerous other people also made similar observations (Ray and Sarkar 2001; Wang, Koo and Kim 2003).

The XRD results illustrated in Figure 4.27 to Figures 4.29 revealed that the structure of sugarcane bagasse was of native cellulose with chemical formula $C_6H_{12}O_6$ that contains semi-crystalline cellulose, amorphous hemicellulose and amorphous lignin. The degree of cellulose crystallinity is regarded as one of the most important parameters of the structure and is dependent on the ratio of the crystalline to amorphous regions (Kumar *et al.* 2014a).

The deconvolution of the diffractograms using the Gaussian profiles yielded the intensities of the diffraction bands. It can be seen from the Gaussian profile that peak intensities and peak broadening vary, with more pronounced variations occurring at the peak range of 18.5°, 22.5°, and 34.5° of 2 reflection assigned to the crystallographic planes of 110°, 002°, and 004, respectively (Johar, Ahmad and Dufresne 2012). The fraction of crystalline to amorphous components in a material is indicated by the term "Crystallinity Index" (CI). In order to determine the crystallinity index (CI), the amorphous subtraction approach was used (Park *et al.* 2010).

$$CI\ (\%) = \frac{I_{002} - I_{am}}{I_{002}} * 100$$

After chemical pretreatments with alkali, acid, and combination pretreatment, more stronger crystalline peaks were seen. The increase in peak intensity was used as another way to estimate the degree of crystallinity creation caused by the sodium hydroxide pretreatment. Figure 4.27 shows that when the natural sugarcane bagasse was pretreated with different concentrations of sodium hydroxide ranging between 0.5 and 2.5%, the strength of the peaks increased. After alkali pretreatments, Table 4.11 demonstrated that the degree of crystallinity increased. The removal of the amorphous components (lignin and hemicellulose) that separated the cellulose chains may have caused the cellulose chains to pack more tightly, explaining why there has been such an increase.

The natural sugarcane bagasse's high concentration of amorphous lignin and amorphous hemicellulose resulted in a crystallinity index of 39, 04% (Xu *et al.* 2007). The crystallinity index increased from 39.04% to 51.61 and 66.85% when sugarcane bagasse was chemically pretreated with sodium hydroxide concentrations of 0.5% to 1%, as shown in Table 4.11 (due to the removal of lignin and hemicellulose). As the sodium hydroxide concentration exceeded 1%, the crystallinity index decreased quickly. This decrease in crystallinity index suggested that the cellulose was degrading molecularly (Das and Chakraborty 2008).

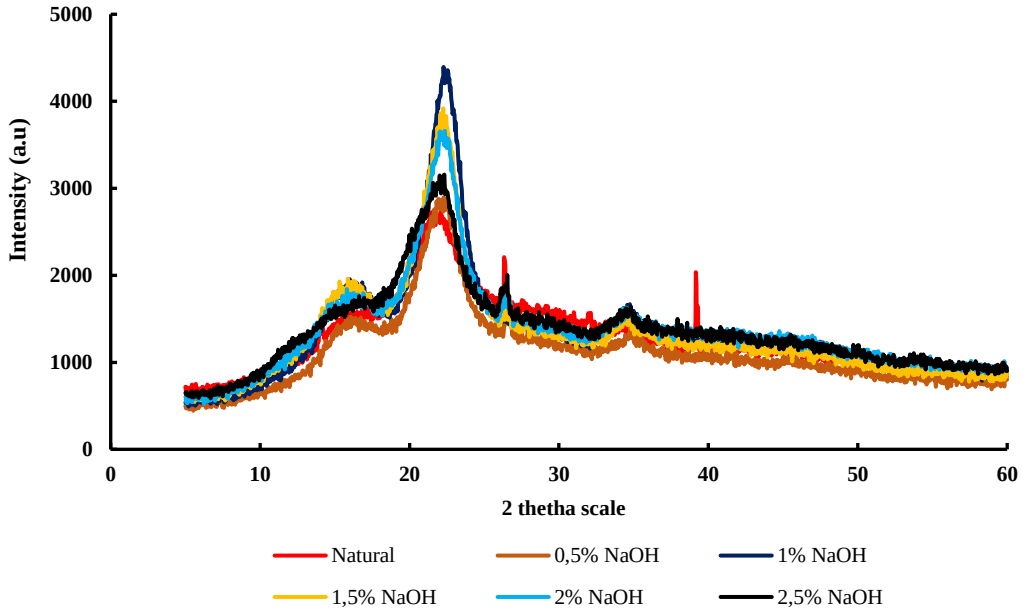

Figure 4.27: The X-Ray Diffractograms of the alkali-pretreated biosorbents

Table 4.11: Crystallinity Index for the natural and alkali-pretreated biosorbents

	CI (%)
Natural	39,04
0.5% NaOH	51,61
1% NaOH	66,85
1.5% NaOH	57,01
2% NaOH	53,67
2.5% NaOH	43,46

The diffractograms of both the native and modified forms of sugarcane bagasse still displayed three main distinctive peaks at 2theta values of 18.5, 22.5, and 34.5° after the sugarcane bagasse had undergone chemical pretreatment with various concentrations of sulphuric acid. When the sugarcane bagasse was chemically pretreated with varied concentrations of sulphuric acid ranging from 0.5 to 2.5%, a different trend with regard to the peaks was noticed. The peaks at the higher intensities (I_{002}) were inversely related to the sulphuric acid content. Table 4.12 shows that for pretreated sugarcane bagasse from 0.5 to 2.5%, the crystallinity index increased from 55.2% to 57.4. (Saïd Azizi Samir *et al.* 2004) also noted the rise in crystallinity index following acid treatments.

.

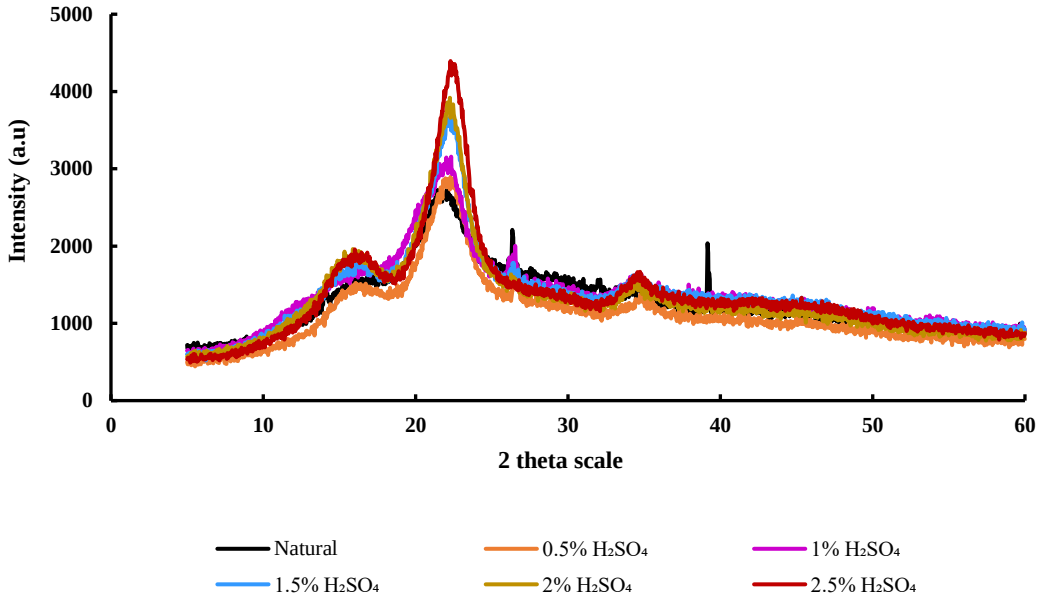

Figure 4.28: The X-Ray Diffractograms of the acid-pretreated biosorbents

Table 4.12: Crystallinity Index of the natural and acid-pretreated biosorbents

	CI (%)
Natural	39,04
0.5% H_2SO_4	55,82
1.0% H_2SO_4	57,13
1.5% H_2SO_4	56,94
2.0% H_2SO_4	57,37
2.5% H_2SO_4	57.47

The combination pretreatment was used to remove the lignin and the hemicellulose, two amorphous components, leaving behind a more crystalline cellulose. However, it was clearly shown in Figure 4.28 that as sulphuric acid concentration increased, the strength of the peaks in the I_{002} zone reduced. Table 4.12 shows that when the concentration of the combined pretreatment increased from (0.5% NaOH + 0.5% H_2SO4) to (2.5% NaOH + 2.5% H_2SO_4), the crystallinity index of the cellulose structure declined from 57.92 to 50.82%.

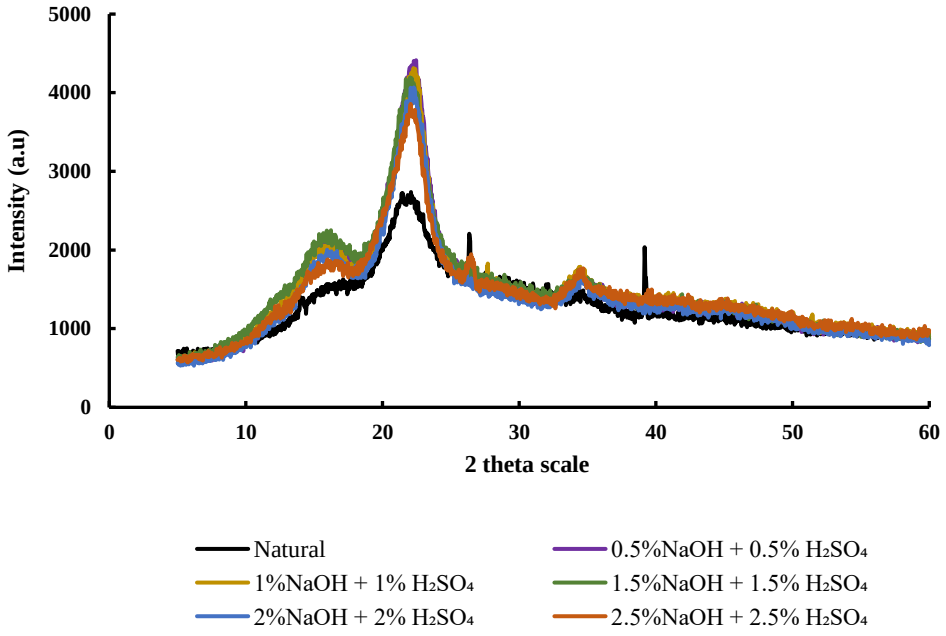

Figure 4.29: The X-Ray Diffractograms for the combined-pretreated biosorbents

Table 4.13: Crystallinity Index for the natural and combined-pretreated biosorbents

	CI (%)
Natural	39,04
0.5% NaOH + 0.5% H_2SO_4	57,92
1% NaOH + 1% H_2SO_4	54,05
1.5% NaOH + 1.5% H_2SO_4	50,99
2% NaOH + 2% H_2SO_4	50,9
2.5% NaOH + 2.5% H_2SO_4	50,82

The concentration of the acid pretreatment had a direct impact on the crystallinity index. As shown in Table 4.13 the sugarcane bagasse's amorphous hemicellulose and amorphous lignin were largely eliminated, which enhanced the crystallinity index as the sulphuric acid concentration rose from 0.5% to 2.5%. The rise in crystallinity was due to the reaction of sulphuric acid with the amorphous portion of sugarcane bagasse during acid pretreatment. The hydrolytic breakage of glycosidic links caused by this reaction resulted in the creation of the monocrystals.

The pretreatment of the bagasse produced the highest crystallinities for the alkali, acid, and combined pretreatments, measuring 66.85%, followed by the mixed pretreatment's 57.92% and the acid pretreatment's (57.47%), according to the peaks attained for the pretreated bagasse.

However, it is feasible to see a decrease in crystallinity indices at concentrations exceeding (1% NaOH) and (0.5% NaOH + 0.5% H_2SO_4). This modification of the cellulose, which transformed its orderly crystal regions into chaotic amorphous ones, was responsible for this shift. The hydrogen bonds required to preserve the crystalline structure were consequently shattered.

To determine if the structures of the adsorbents loaded with Fe^{2+} ions had changed after the adsorption of Fe^{2+}, only the adsorbents with the greatest crystallinity index (1% NaOH; 2.5% H_2SO_4; (0.5% NaOH + 0.5%H_2SO_4)) were submitted to XRD to see if the structure of the adsorbents had changed. The X-Ray diffractograms of the chemically pretreated adsorbents loaded with Fe^{2+} ions are shown in Figure 4.30 (after biosorption experiments). Figure 4.30 shows that following the biosorption, the intensity on the peaks of the X-Ray diffractograms significantly increased, with the largest peak being produced by 1% NaOH, followed by the combination pretreatment and finally the acid pretreatment. The Fe^{2+} that had been adsorbed on the structures of the pretreatment adsorbents was what caused the increase in peak intensities.

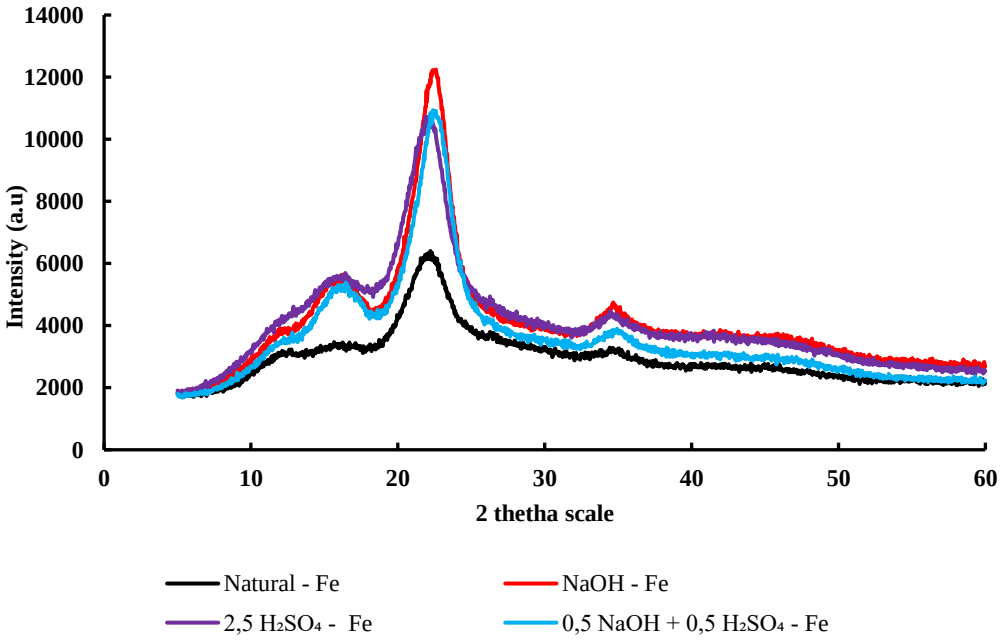

Figure 4.30: The X-Ray Diffractograms after the biosorption on Fe^{2+}

4.6.3 Scanning Electron Morphology (SEM)

Electron Scanning (Figure 4.31) displays micrographs of natural (natural) and modified (acid and alkali pretreatments fibers at various concentrations). The presence of lignin and hemicellulose was found to give the untreated fibers a semi-crystalline structure. The structure also demonstrated the existence of pores, which is crucial for greater adsorption capabilities. Major and moderate differences were seen when sugarcane bagasse was subjected to different sulphuric acid and sodium hydroxide concentrations. After the fiber surfaces underwent the acid pretreatment, the natural fiber's surface residue was no longer present.

After the acid treatments, the parallel stripes were easier to see. Additionally, it was noted that as the stripes became more visible, the acid pretreatment concentration rose. The morphology of the bagasse, particularly the bundles, was significantly altered by alkali pretreatment.

Figure 4.31's depictions of the alkali, acid, and combination pretreatments demonstrate how the removal of the glue agent caused the sugarcane bagasse fibers to begin to separate from one another when the sodium hydroxide concentration was increased (lignin). The twisted and curled look of the separated bundles gave the impression of greater flexibility. Additionally, it was observed that the removal of hemicellulose, lignin, and other impurities caused the roughness of the surface to rise with increasing concentrations of sodium hydroxide, sulphuric acid, and combination pretreatment.

The bundles became even more unstructured at higher NaOH concentrations. Because of this, chemical pretreatment caused noticeable morphological changes in the sugarcane bagasse, which in turn caused an increase in crystallinity index as seen in the XRD results. These modifications show how different pretreatments affect sugarcane bagasse when hemicellulose and lignin are more or less solubilized during chemical pretreatment operations.

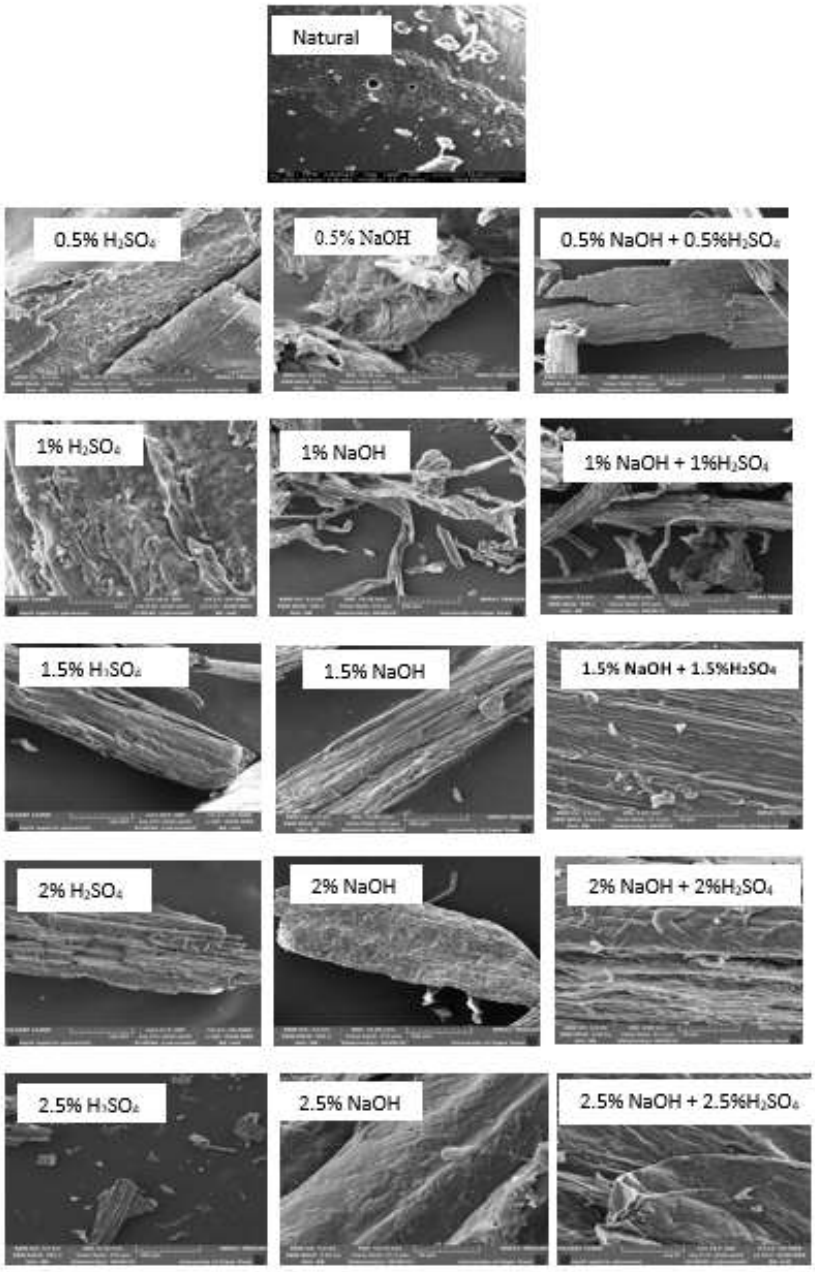

Figure 4.31: Scanning Electron Morphology (SEM) of the natural and modified biosorbents

The structure of the biomass was significantly altered by the combination treatments. It was observed that the bundles disassembled even more than the alkali and acid prepared adsorbent when the combination pretreatment of (0.5% NaOH + 0.5% H_2SO_4) and (1% NaOH + 1% H_2SO_4) was applied. When the combined pretreatment of 0.5% was employed, the fiber bundles were considerably more obvious. It was noted that the bundle structure began to deteriorate at combined concentrations greater than 1.0%.

4.6.3.1 Energy Dispersive X-Ray Spectroscopy (EDS)

A chemical microanalysis method called Energy Dispersive X-Ray Spectroscopy (EDS) is used in conjunction with scanning electron microscopy to characterize the elemental composition of the examined volume by detecting x-rays released from the sample during irradiation by an electron beam. According to Table 4.14, the elemental analysis of sugarcane bagasse in the current study included 0.23 wt% elemental silicon impurity in addition to 56.45 wt% C and 43.32 wt% O as primary components.

Table 4.14: Elemental composition for the natural and pretreated biosorbents before the biosorption of Fe^{2+}

	C	O	Si	Ca	S
Natural	56,45	43,32	0,23		
0,5% NaOH	50,06	49,34	0,38	0,22	
1% NaOH	59,43	39,14	1	0,43	
1,5% NaOH	50,67	48,97	0,07	0,29	
2% NaOH	54,38	44,63	0,49	0,5	
2,5% NaOH	51,05	48,11	0,62	0,22	
0,5% H_2SO_4	53,89	45,19			0,92
1% $H2SO_4$	54,27	45,73			
1,5% H_2SO_4	54,8	43,69	1,51		
2% H_2SO_4	51,26	48,74			
2,5% H_2SO_4	56,43	43,18	0,39		
0,5% NaOH + 0,5% H_2SO_4	57,36	42,44	0,19		
1% NaOH + 1% H_2SO_4	51,68	47,8		0,52	
1,5% NaOH + 1,5% H_2SO_4	52,76	46,88	0,35		
2% NaOH + 2% H_2SO_4	51,41	48,59			
2,5% NaOH + 2,5% H_2SO_4	51,34	48,66			

Following chemical pretreatment with various sodium hydroxide concentrations, it was discovered that the % of carbon decreased from 56.45% to 50.06% as the sodium hydroxide concentration increased from 0.5 to 1.0%. The breakage of the carbon-carbon bonds during the delignification process was the cause of this drop in carbon concentration. Additionally, it was noted that the silicon and oxygen contents had increased. When sodium hydroxide was used as a pretreatment for sugarcane bagasse, calcium was found. The calcium content that was found was thought to be an impurity. Ca content increased from 0.22% to 0.5% when sodium hydroxide concentration increased from 0.5% to 2% NaOH; however, it decreased to 0.22 wt% at 2.5% NaOH.

The carbon content increased from 50.06 to 59.43 wt% when the sodium hydroxide concentration was increased from 0.5% to 1.5% NaOH, whereas the oxygen content declined from 49.34 to 39.14% and the calcium content likewise increased from 0.22 to 0.43%. After pretreatment with various doses of sulphuric acid, the discovery of another new impurity, S, was made. This elemental contamination resulted from the cellulose fibers' acid hydrolysis. The initial carbon content of sugarcane bagasse was 43.32%; after pretreatment with sulphuric acid at concentrations of 0.5%, 1%, 1.5%, 2%, and 2.5%, it increased to 45.19; 45.73; 43.18; 48.74; and 43.69%, respectively.

The carbon content for the combined pretreatments only increased for the concentration of (0.5% NaOH and 0.5% H_2SO_4) from 56.45 to 57.36%, and then declined for the combined pretreatment concentrations of (1% NaOH + 1% H_2SO_4) to (2.5% NaOH + 2.5% H_2SO_4).

. **Table 4.15: Elemental composition of the natural and modified biosorbents after the biosorption of Fe^{2+}**

	C	**O**	**Si**	**Fe^{2+}**
Natural	52,77	45,61	0,85	0,77
1% NaOH	48,61	41,91	1,59	7,89
2,5% H_2SO_4	52,91	44,89	0,57	1,63
0,5% NaOH + 0,5% H_2SO_4	54,77	40,51	0,92	3,8

Table 4.15 depicts the elemental analysis of both the natural and pretreated sugarcane bagasse after adsorption experiments of Fe^{2+}. It can be seen from the results that the natural, 1% NaOH, 2.5% H_2SO_4 and combined pretreatment of alkaline and acid were loaded with 0.77wt%; 7.89 wt%; 1.63wt%; 3.8 wt% of Fe^{2+} ions; respectively.

4.6.4 BET Analysis

The BET analysis is the measurement of surface area, pore volume, and pore size. Table 4.16 shows the results of a BET study of both natural and modified sugarcane bagasse. The natural sugarcane bagasse was found to have a surface area and pore size of 0.904 cm^3/g and 56.33 ˚A, respectively.

Table 4.16: BET results for the natural and modified biosorbents

	Surface Area (cm^3/g)	**Pore size (˚A)**
Natural	0,904	56,33
0,5% NaOH	1.160	75,621
1% NaOH	1.503	99,632
1,5% NaOH	1.068	92,205
2% NaOH	0.755	82,712
2,5% NaOH	0.627	76,324
0,5% H_2SO_4	0.934	60.225
1% H_2SO_4	0,950	63.589
1,5% H_2SO_4	1.134	66.220
2% H_2SO_4	1,184	90.240
2,5% H_2SO_4	1,233	93.680
0,5% NaOH + 0,5% H_2SO_4	1.376	99.100
1% NaOH + 1% H_2SO_4	1.194	97.232
1,5% NaOH + 1,5% H_2SO_4	1.056	98.22
2% NaOH + 2% H_2SO_4	0.376	90.44
2,5% NaOH + 2,5% H_2SO_4	0.242	92.252

The surface area and pore size increased from 1.160 to 1.503 cm^3/g and 75.621 to 99.632 ˚A, respectively, during the alkali treatments of 0.5 and 1% NaOH. The surface area and pore size after acid pretreatment were directly correlated with the acid concentration, with 0,934 and 1.233 cm^3/g for 0.5% H_2SO_4 and 60.225 and 93.680 ˚A for 2.5% H_2SO_4, respectively.

The surface area and pore size of the sugarcane bagasse increased when combined pretreatment of alkali and acid was applied, but they reduced as the concentration of the combined pretreatment increased to (2.5% NaOH + 2.5% H_2SO_4). This is due to the possibility that the pretreatment's high concentration causing the sugarcane bagasse's structure to collapse, resulting in a reduction in surface area and pore size.

CHAPTER 5

5.1 Conclusion

Sugarcane comprises of cellulose, hemicellulose and lignin. Lignin is defined as the substance that binds the fibers together. In order to determine the adsorptive performance of the cellulose, cellulose-lignin and cellulose-hemicellulose, sugarcane bagasse was modified with different concentrations of sodium hydroxide + sulphuric acid, sodium hydroxide and sulphuric acid, respectively. Upon chemical pretreatments with alkali, the content of lignin decreased from 22.30 to 7.56%, for acid pretreatment, the content of hemicellulose decreased from 24.30% to 13.63%.

Biosorption studies were performed in order to investigate the performance of the natural and pretreated sugarcane bagasse in the adsorption of Fe^{2+}. The present study on removal of Fe^{2+} from aqueous solutions using natural and modified sugarcane bagasse was carried out in batch experiments. Sugarcane comprises of cellulose, hemicellulose and lignin. The material that holds the fibers together is known as lignin. Sugarcane bagasse was pretreated with various concentrations of (sodium hydroxide + sulphuric acid), sodium hydroxide, and sulphuric acid, respectively, to test the adsorptive efficacy of the cellulose, cellulose-lignin, and cellulose-hemicellulose. Lignin level dropped from 22.30 to 7.56% after chemical pretreatment with alkali, and hemicellulose content dropped from 24.30% to 13.63% after pretreatment with acid.

By using biosorption experiments, the efficacy of the raw/natural and pretreated/ modified sugarcane bagasse in the biosorption of Fe^{2+} was evaluated. In the current investigation, natural and modified sugarcane bagasse were employed in batch experiments to remove Fe^{2+} from aqueous solutions. The operational parameters such as the initial concentration, pH, contact time, adsorbent dose had a significant effect on the Fe^{2+} removal efficiency.

The initial concentration, pH, contact time, and adsorbent dosage were all operational factors that significantly impacted the removal efficiency of Fe^{2+}. For the concentration variation using alkali pretreatment, it was found that the maximum removal of Fe^{2+} was obtained at 1% NaOH when initial sorbate concentration was varied from 1 mg/L to 30 mg/L. As the severity of the alkali pretreatment increased, the adsorption capacity of the adsorbent decreased. The percentage removal of Fe^{2+} increased as the adsorbent dosage increased, for all pretreatments studied; with

1% NaOH increasing from 38.30% to 66.03%, 2.5% H_2SO_4 increasing from 12.97% to 45.78% while (0.5%NaOH + 0.5% H_2SO_4) increased from 10.30% to 62.39% using 0.2g and 1gram, respectively. Above an adsorbent dosage of 1 g, the percentage removal of Fe^{2+} did not show any noticeable increase, this was due to the saturation of active sites of the adsorbent.

Therefore, one gram of both natural and pretreated bagasse was found to be the optimum adsorbent dosage. The maximum removal of Fe^{2+} was found to increase with increasing pH ranging between 2-7, with optimum pH of 6. The batch adsorption results showed that 1% sodium hydroxide had a better biosorption performance, followed by the combined pretreatment of (0.5% NaOH + 0.5% H_2SO_4) then the 2.5% of sulphuric acid (H_2SO_4). In order to examine the mechanism responsible for the adsorption process, the Langmuir and Freundlich kinetic isotherms were used. For both the natural and modified sugarcane bagasse, a good correlation coefficient (>0.95) was obtained using both the Langmuir and Freundlich isotherms. The pseudo second order kinetic model best described the adsorption of Fe^{2+} onto the natural and pretreated adsorbent.

According to the results, it was inferred that both homogeneous and heterogeneous surfaces of the natural and pretreated bagasse experienced physical and chemical adsorption of Fe^{2+}. The outcomes also demonstrate that, due to improved crystallinity, the cellulose that was left behind after the removal of the useful components (lignin and hemicellulose) had a good ability to remove Fe^{2+} ions.

The natural and processed bagasse underwent characterization tests using FTIR, XRD, BET, and SEM. The pretreated adsorbent's surface characteristics had changed, according to the FTIR data. The results, when analyzed, revealed that Fe^{2+} was biosorbed onto the natural and processed bagasse on both homogeneous and heterogeneous surfaces through physical and chemical adsorption. The outcomes also demonstrate that, due to improved crystallinity, the cellulose that was left behind after the removal of the useful components (lignin and hemicellulose) had a good ability to remove Fe^{2+} ions.

The FTIR spectra after the alkali pretreatment using 1% NaOH, 2.5% H_2SO_4 and (0.5% NaOH + 0.5% H_2SO_4) showed intense peaks in the regions of the hydroxyl, carbonyl and carboxyl groups, which were responsible for the adsorption process.

The hydroxyl, carbonyl, and carboxyl groups, which were in charge of the adsorption process, showed up as highly intense peaks in the regions of the FTIR spectra following the alkali pretreatment using 1% NaOH, 2.5% H_2SO_4, and (0.5% NaOH + 0.5% H_2SO_4).

According to the XRD results, the chemical pretreatments were successful in removing the amorphous areas of the bagasse and leaving a crystalline structure behind. Crystalline indices for the alkali modification increased for 0.5% and 1% NaOH concentrations and dropped above those levels. The crystalline indices for the sulphuric acid pretreatment were inversely correlated with the sulphuric acid concentration. This was because the lignin rendered the adsorbent more resistant to pretreatment, necessitating larger doses of sulphuric acid to overcome this resistance. The crystalline indices dropped as the combined pretreatment's concentration rose. Adsorbents with higher crystallinity indices demonstrated better Fe^{2+} adsorption capacity.

5.2 Recommendations

The current study looked at utilizing natural and pretreated sugarcane bagasse to remove heavy metals. The study only focused on batch adsorption configuration. As a recommendation, the current investigated adsorbent proved to be significant in enhancing the metal uptake performance of the Fe^{2+} ions. Hence, taking the same procedure/pretreatments and use them in dynamic adsorption to incorporate scaling up requirements. It is also recommended to take into account economic feasibility studies when using biomaterials as feedstock or catalyst. Economic feasibility studies assist in visualizing the possibility of commercializing the idea. With 4IR underway, all environmental studies need to incorporate computer modelling and designing of predictive interfaces based on feedstock type, pretreatments, adsorbates etc., in order to mitigate human error and smooth process.

6. APPENDICES

A: Linear plots of Langmuir isotherms for natural sugarcane bagasse and alkali-pretreated biosorbents

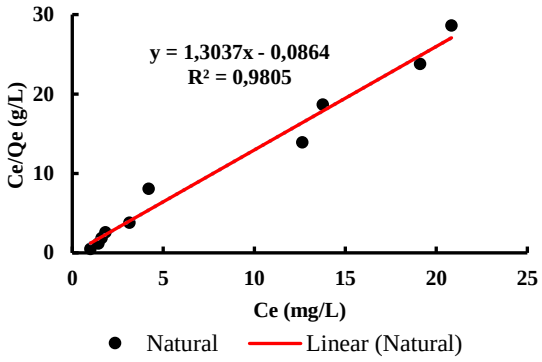

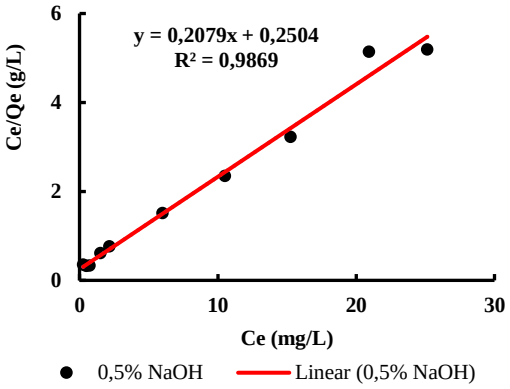

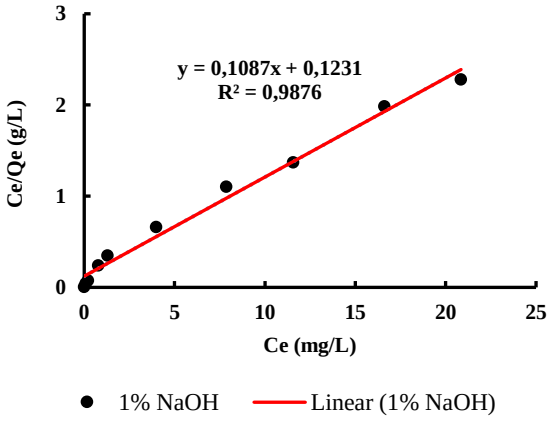

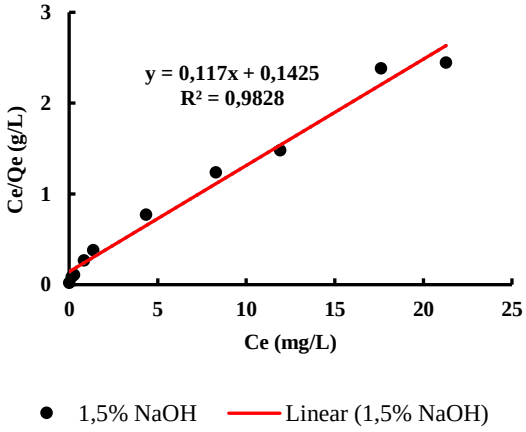

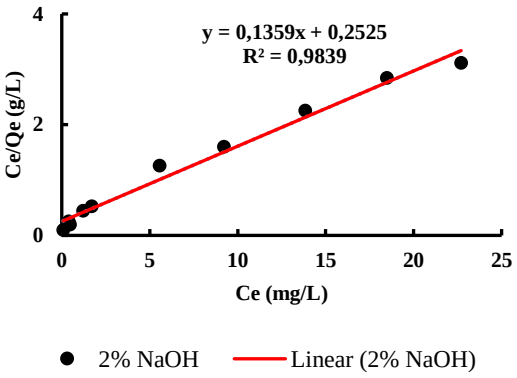

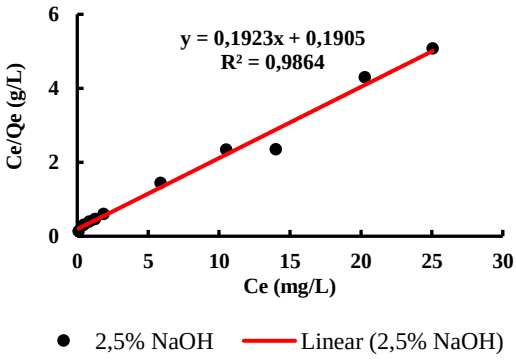

B: Linear plots of Langmuir isotherms for natural sugarcane bagasse and acid-pretreated biosorbents

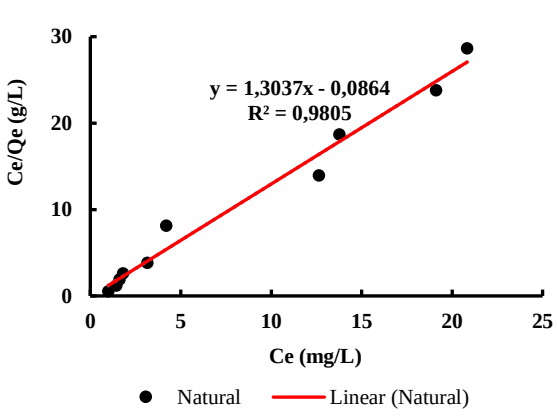

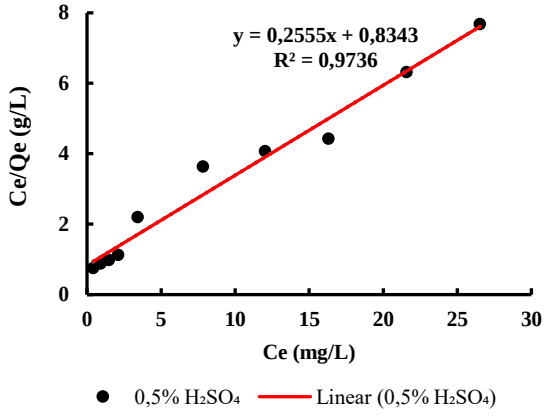

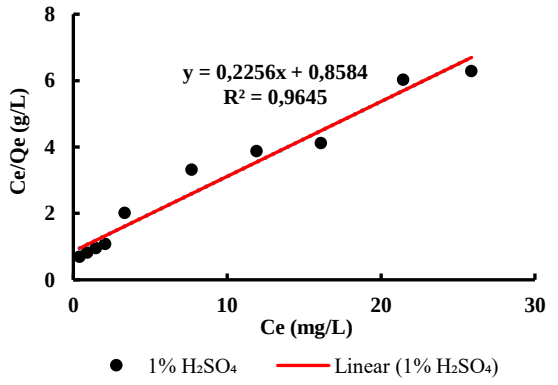

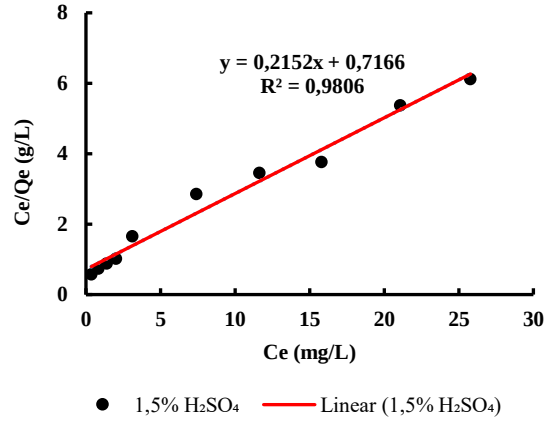

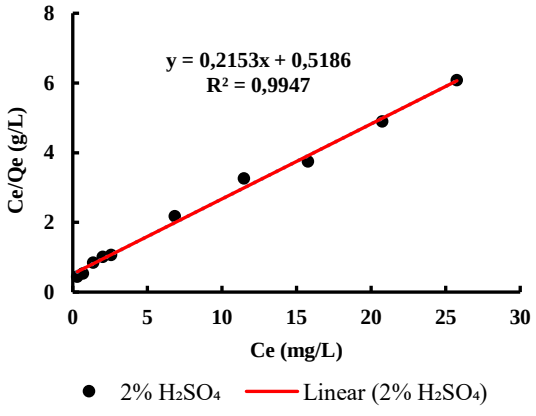

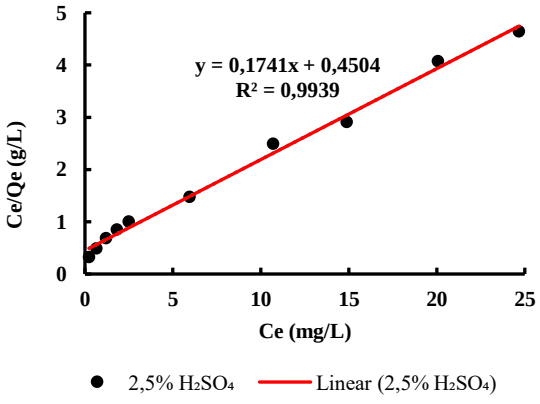

C: Linear plots of Langmuir isotherms for natural sugarcane bagasse and combined-pretreated biosorbents

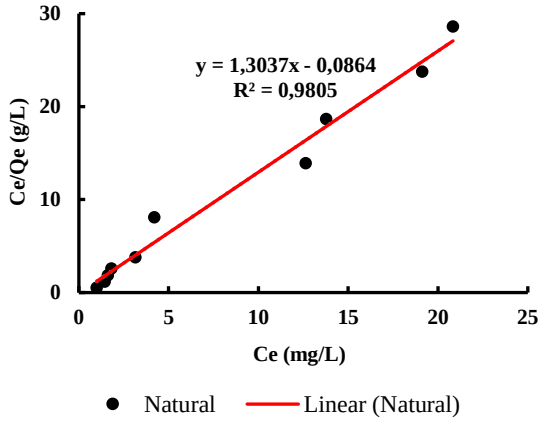

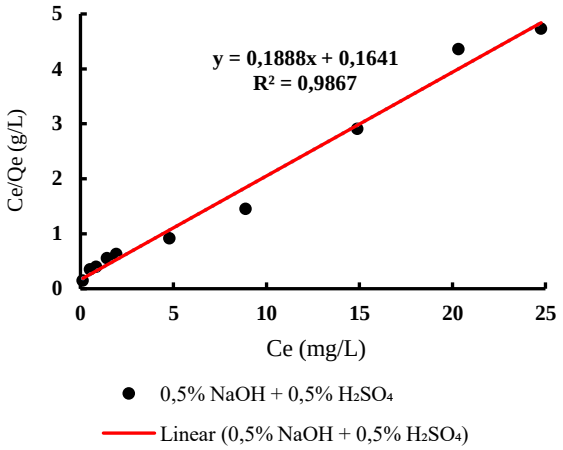

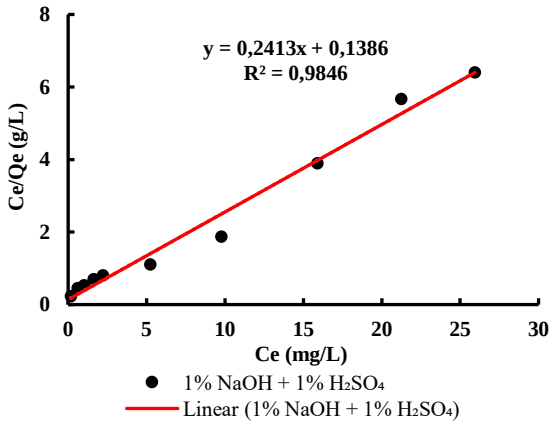

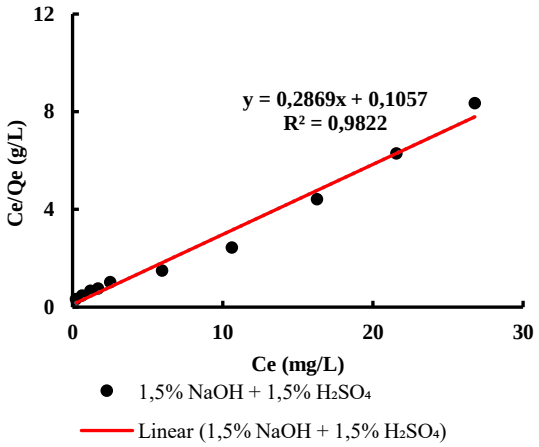

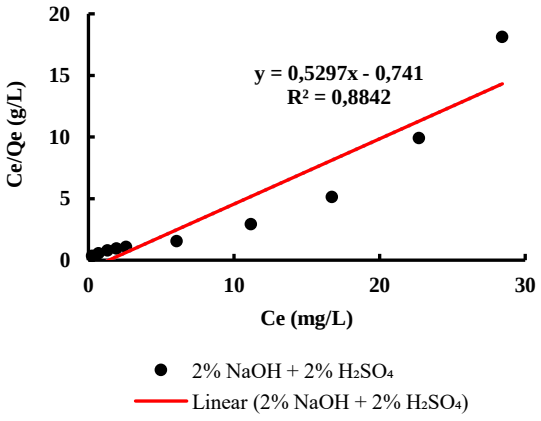

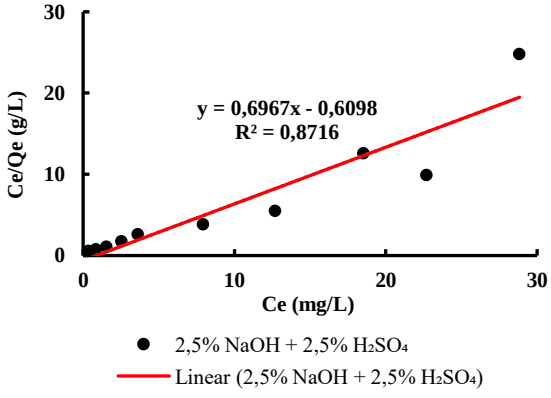

D: Linear plots of Freundlich isotherms for natural sugarcane bagasse and alkali-pretreated biosorbents

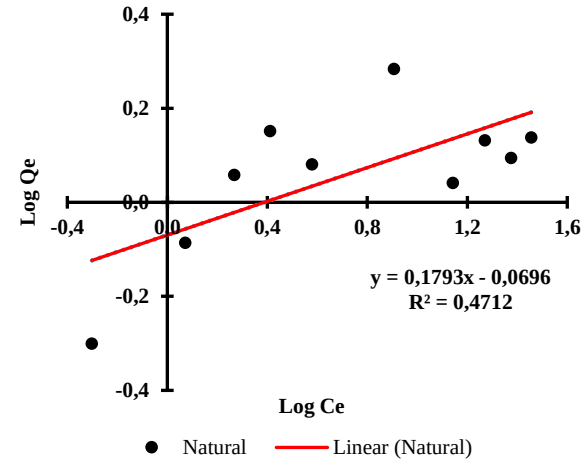

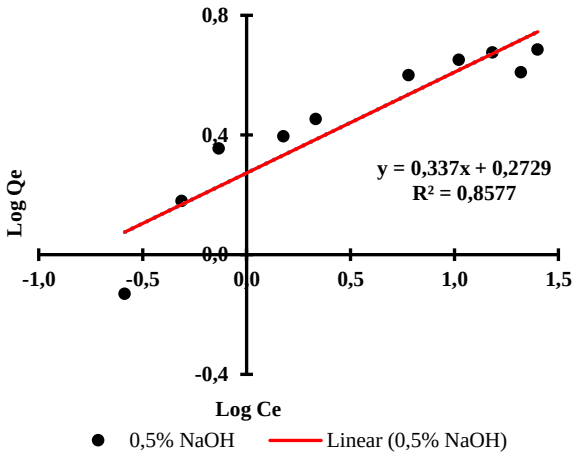

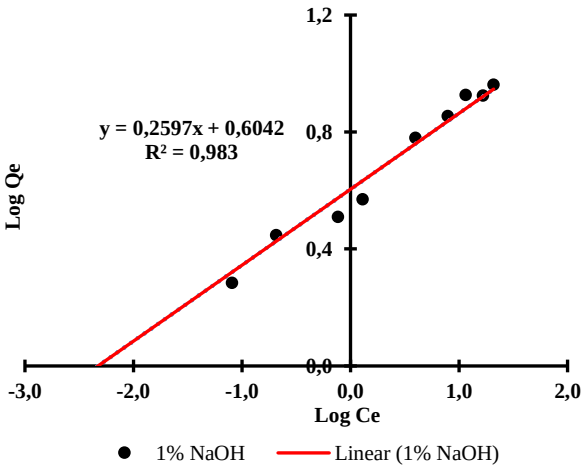

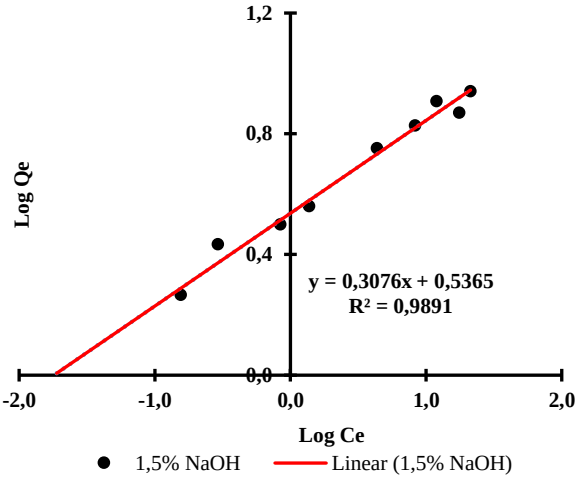

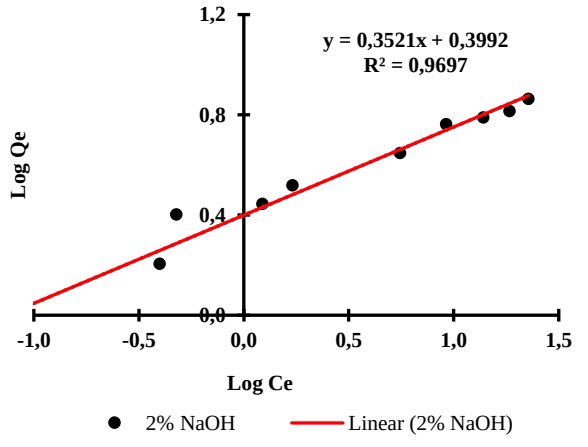

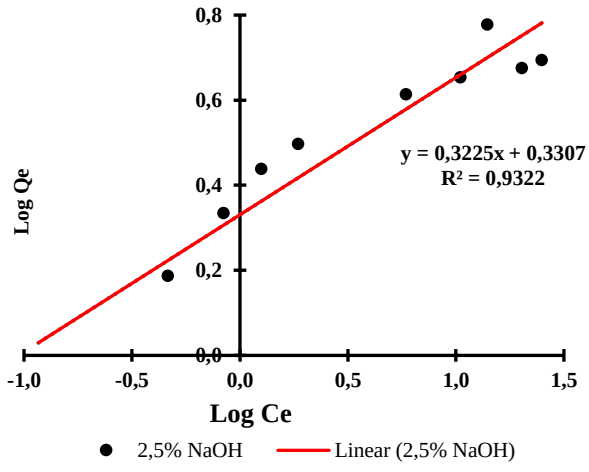

E: Linear plots of Freundlich isotherms for natural sugarcane bagasse and acid-pretreated biosorbents

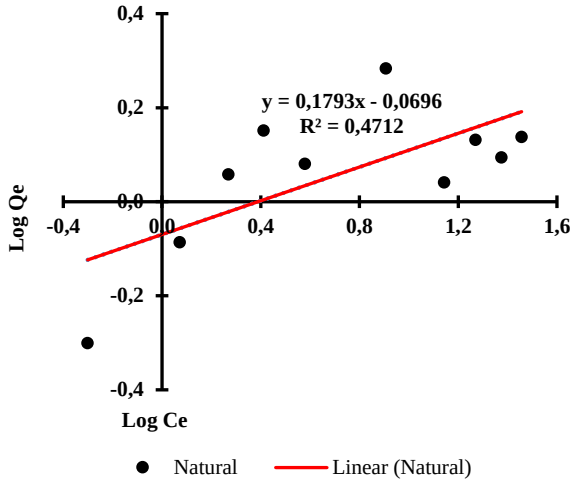

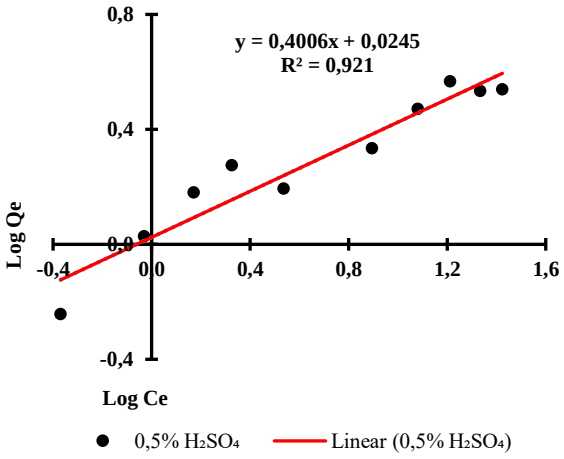

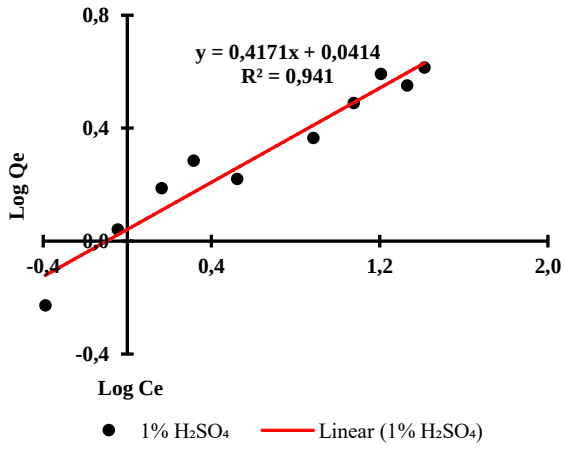

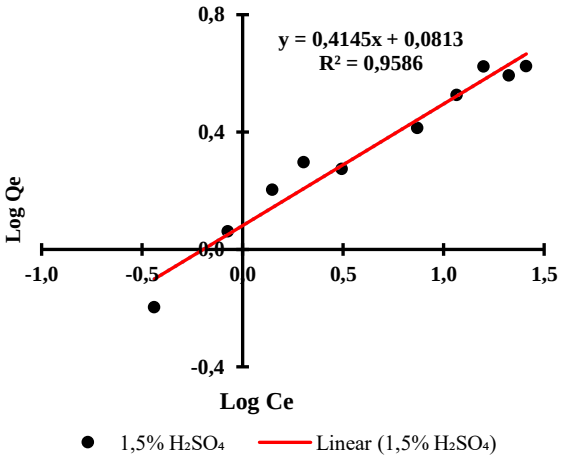

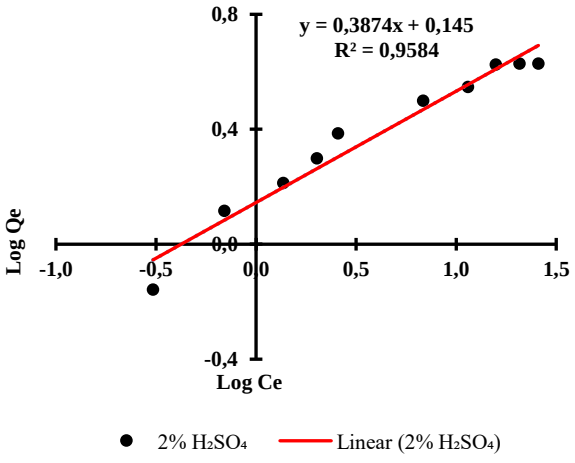

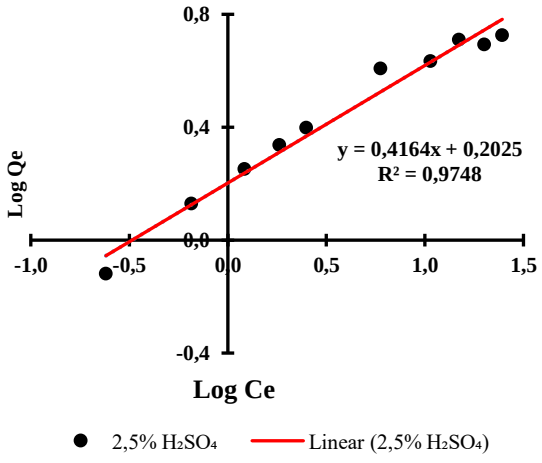

F: Linear plots of Freundlich isotherms for natural sugarcane bagasse and combined-pretreated biosorbents

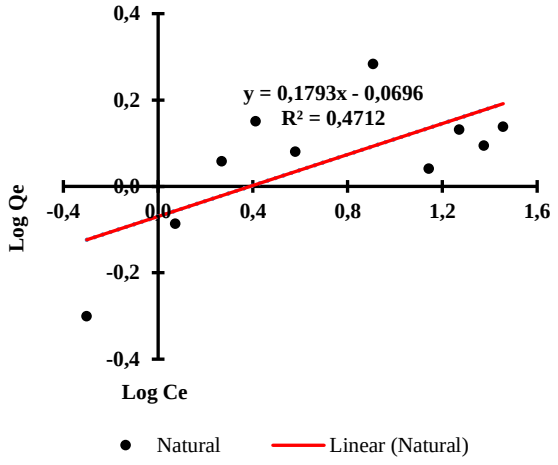

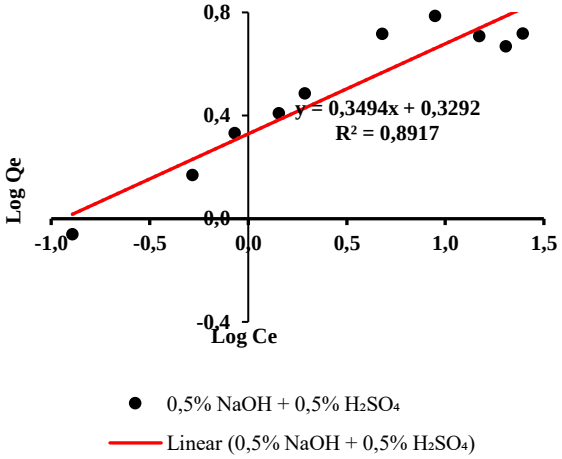

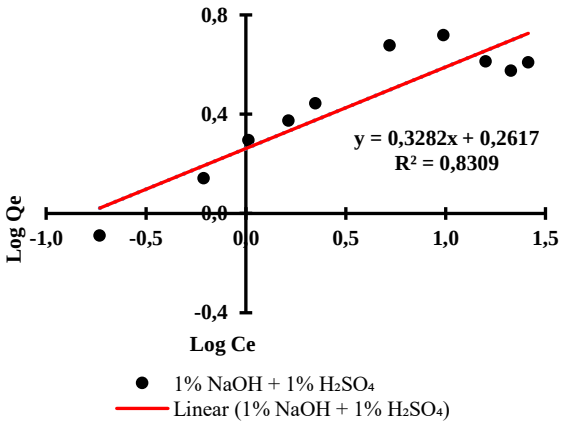

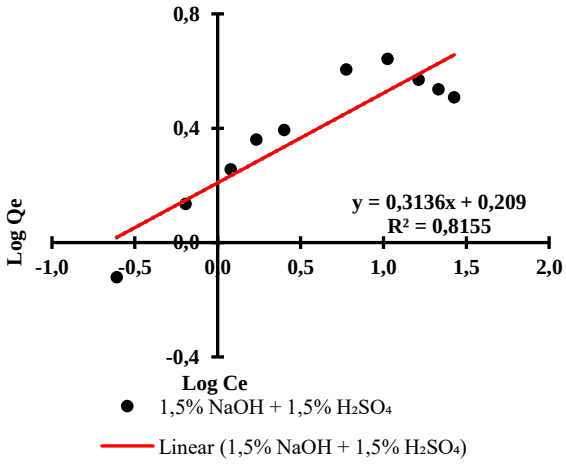

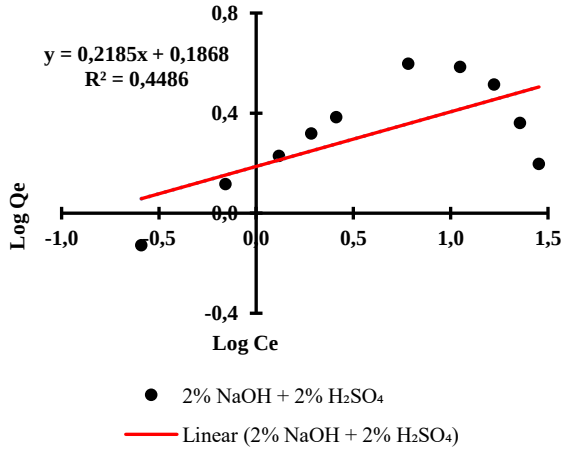

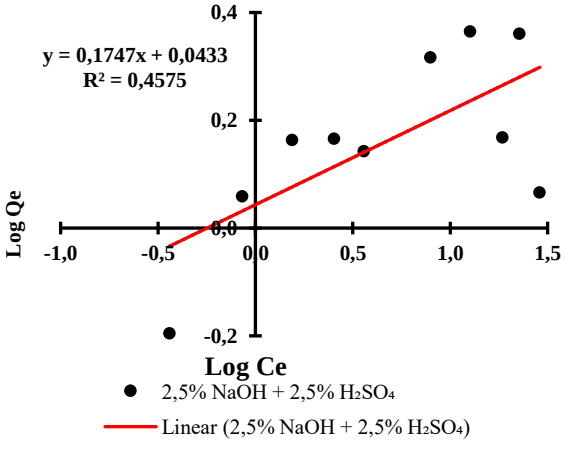

G: Pseudo 1st order kinetics of (1) alkali, (2) acid, (3) combined pretreated adsorbents

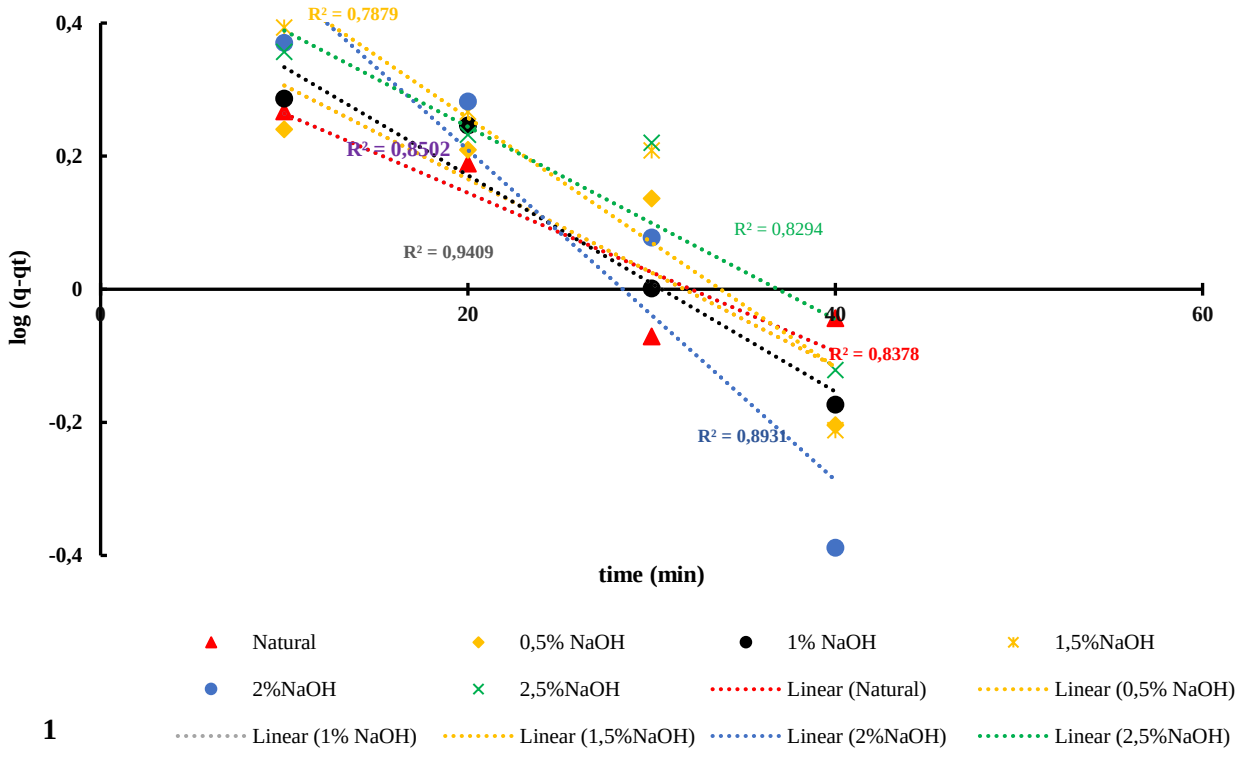

1

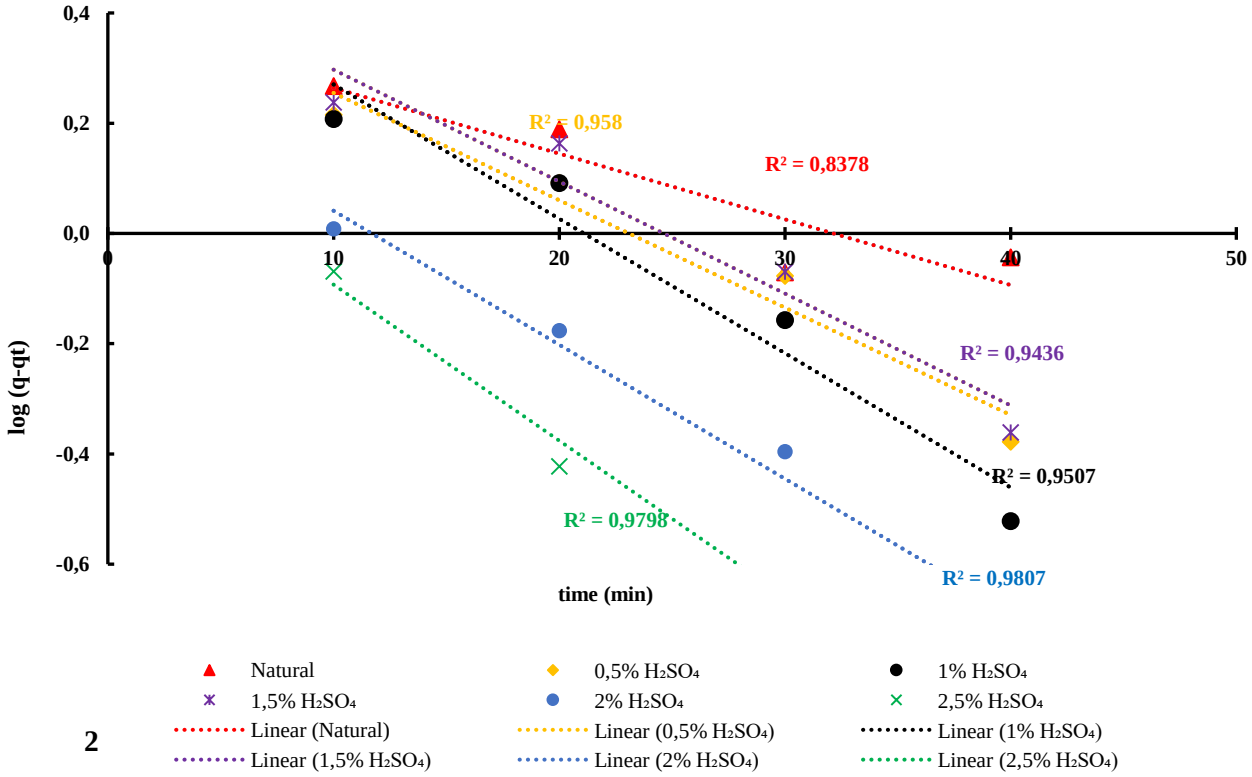

2

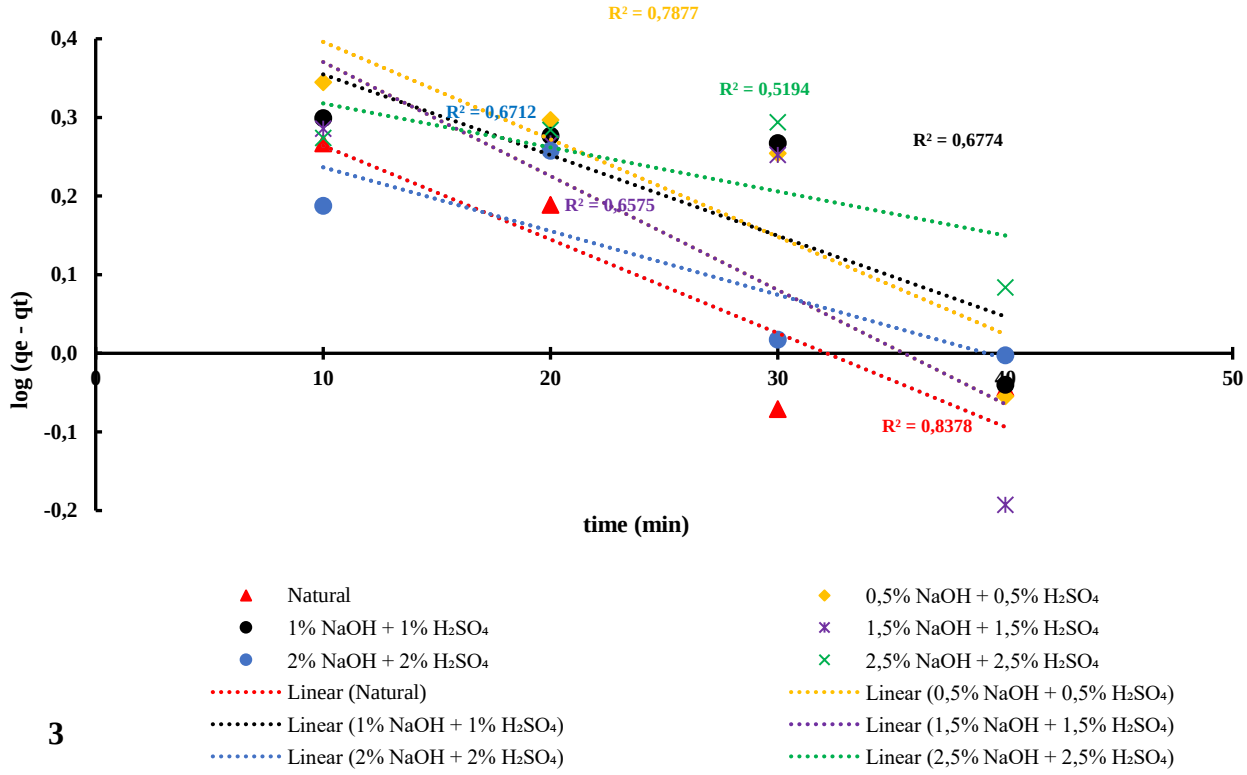
R² = 0,7877
R² = 0,5194
R² = 0,6712
R² = 0,6774
R² = 0,6575
R² = 0,8378
0,4
0,3
0,2
0,1
0,0
-0,1
-0,2
log (qe - qt)
10
20
30
50
time (min)
Natural
1% NaOH + 1% H₂SO₄
2% NaOH + 2% H₂SO₄
Linear (Natural)
Linear (1% NaOH + 1% H₂SO₄)
Linear (2% NaOH + 2% H₂SO₄)
0,5% NaOH + 0,5% H₂SO₄
1,5% NaOH + 1,5% H₂SO₄
2,5% NaOH + 2,5% H₂SO₄
Linear (0,5% NaOH + 0,5% H₂SO₄)
Linear (1,5% NaOH + 1,5% H₂SO₄)
Linear (2,5% NaOH + 2,5% H₂SO₄)

3

H: Pseudo 2nd order kinetics of (1) alkali, (2) acid, (3) combined pretreated adsorbents.

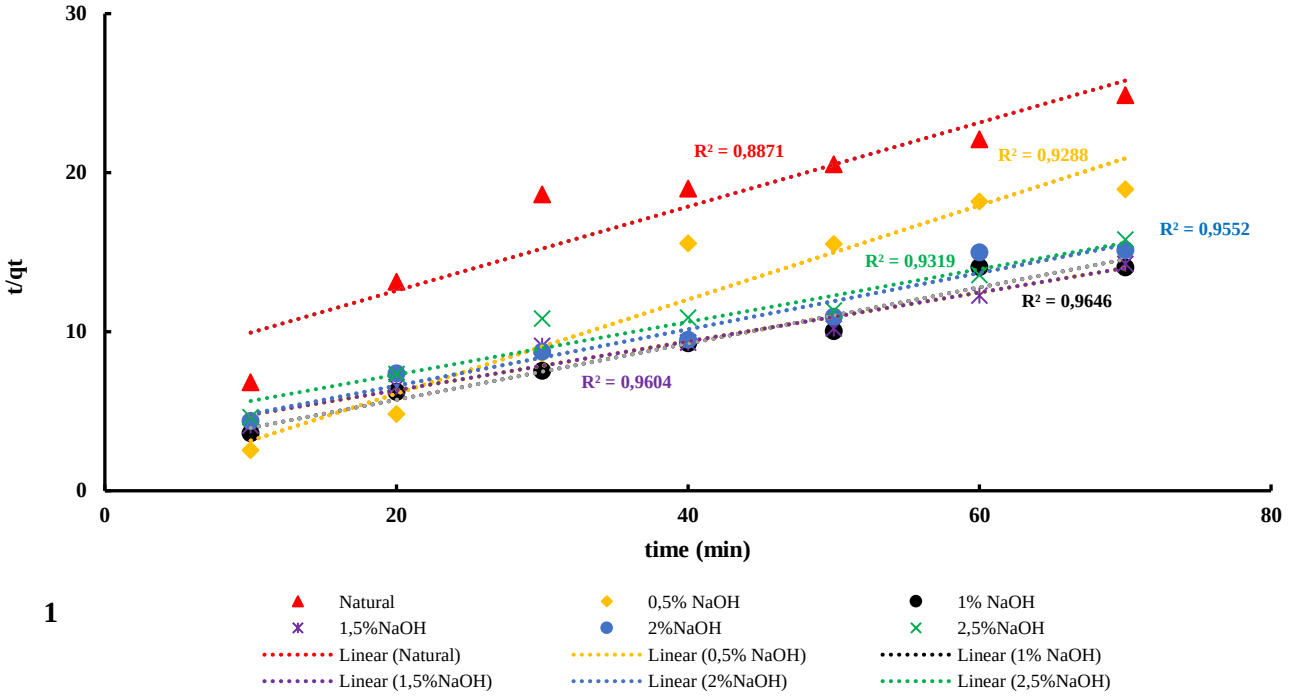

1

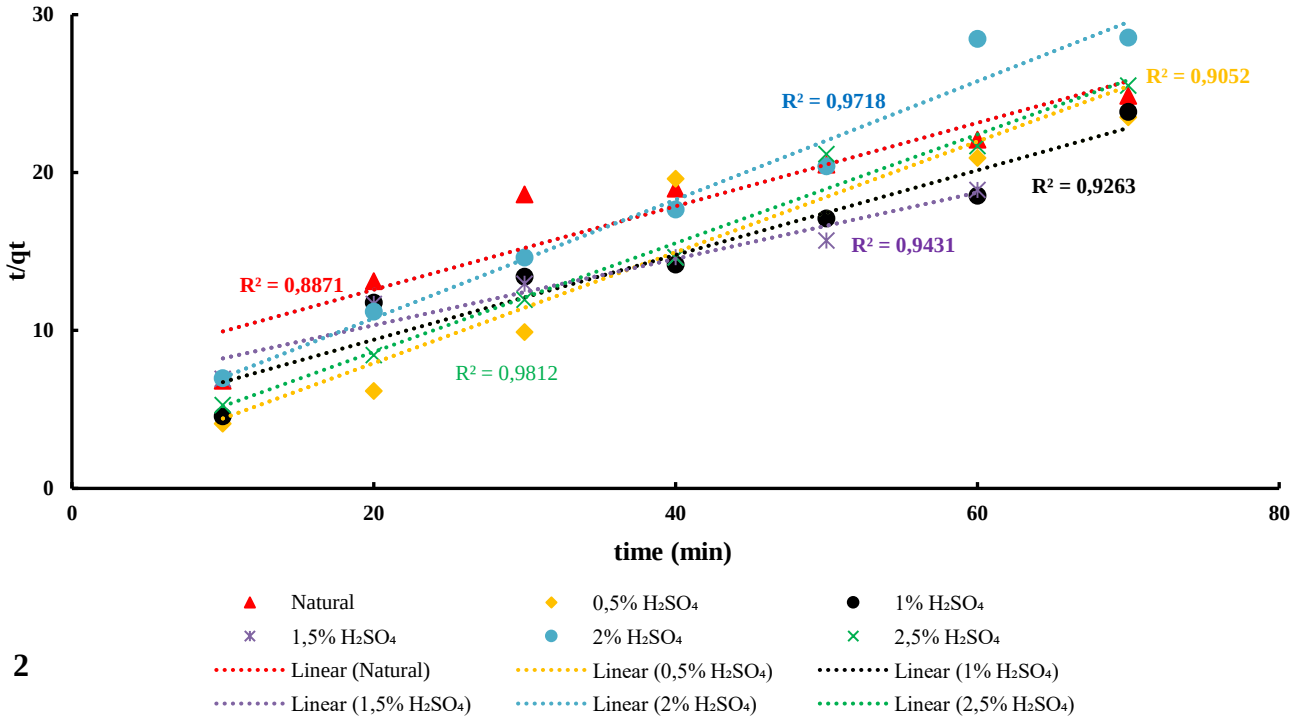

2

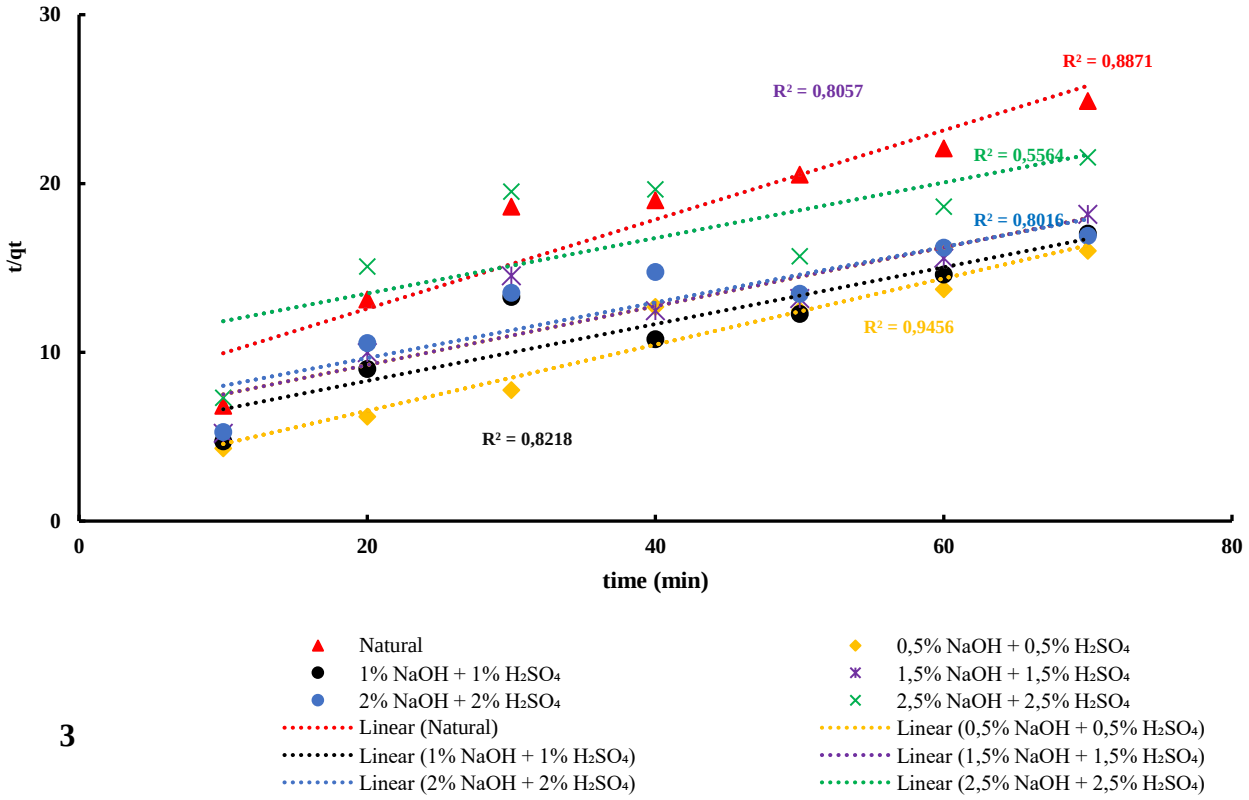
30
20
10
0
t/qt
0
20
40
60
80
time (min)
R² = 0,8871
R² = 0,8057
R² = 0,5564
R² = 0,8016
R² = 0,9456
R² = 0,8218
Natural
1% NaOH + 1% H2SO4
2% NaOH + 2% H2SO4
Linear (Natural)
Linear (1% NaOH + 1% H2SO4)
Linear (2% NaOH + 2% H2SO4)
0,5% NaOH + 0,5% H2SO4
1,5% NaOH + 1,5% H2SO4
2,5% NaOH + 2,5% H2SO4
Linear (0,5% NaOH + 0,5% H2SO4)
Linear (1,5% NaOH + 1,5% H2SO4)
Linear (2,5% NaOH + 2,5% H2SO4)

3

REFERENCES

Ahalya, N., Ramachandra, T. and Kanamadi, R. 2003. Biosorption of heavy metals. *Res. J. Chem. Environ*, 7 (4): 71-79.

Aklil, A., Mouflih, M. and Sebti, S. 2004. Removal of heavy metal ions from water by using calcined phosphate as a new adsorbent. *Journal of hazardous materials*, 112 (3): 183-190.

Ansari, K. B. and Gaikar, V. G. 2014. Green hydrotropic extraction technology for delignification of sugarcane bagasse by using alkybenzene sulfonates as hydrotropes. *Chemical Engineering Science*, 115: 157-166.

Babel, S. and Kurniawan, T. A. 2003. Low-cost adsorbents for heavy metals uptake from contaminated water: a review. *Journal of hazardous materials*, 97 (1-3): 219-243.

Betancur, G. J. V. and Pereira Jr, N. 2010. Sugar cane bagasse as feedstock for second generation ethanol production: Part II: Hemicellulose hydrolysate fermentability. *Electronic Journal of Biotechnology*, 13 (5): 14-15.

Bhattacharya, A., Mandal, S. and Das, S. 2006. Adsorption of Zn (II) from aqueous solution by using different adsorbents. *Chemical Engineering Journal*, 123 (1-2): 43-51.

Brígida, A., Calado, V., Gonçalves, L. and Coelho, M. 2010. Effect of chemical treatments on properties of green coconut fiber. *Carbohydrate Polymers*, 79 (4): 832-838.

Brownell, H. H. and Saddler, J. N. 1987. Steam pretreatment of lignocellulosic material for enhanced enzymatic hydrolysis. *Biotechnology and bioengineering*, 29 (2): 228-235.

Calace, N., Di Muro, A., Nardi, E., Petronio, B. and Pietroletti, M. 2002. Adsorption isotherms for describing heavy-metal retention in paper mill sludges. *Industrial & engineering chemistry research*, 41 (22): 5491-5497.

Cannon, F. S. 1997. 28 ENHANCED METAL REMOVAL FROM WASTEWATER BY COAGULANT ADDITION. In: Proceedings of *Proceedings of the 50th Industrial Waste Conference May 8, 9, 10, 1995*. CRC Press, 259.

Chai, W. S., Cheun, J. Y., Kumar, P. S., Mubashir, M., Majeed, Z., Banat, F., Ho, S.-H. and Show, P. L. 2021. A review on conventional and novel materials towards heavy metal adsorption in wastewater treatment application. *Journal of Cleaner Production*, 296: 126589.

Chang, V. S. and Holtzapple, M. T. 2000. Fundamental factors affecting biomass enzymatic reactivity. In: Proceedings of *Twenty-first symposium on biotechnology for fuels and chemicals*. Springer, 5-37.

Chen, Y., Sharma-Shivappa, R. R., Keshwani, D. and Chen, C. 2007. Potential of agricultural residues and hay for bioethanol production. *Applied biochemistry and biotechnology*, 142 (3): 276-290.

Crist, R. H., Martin, J. R. and Crist, D. R. 1999. Interaction of metal ions with acid sites of biosorbents peat moss and Vaucheria and model substances alginic and humic acids. *Environmental science & technology*, 33 (13): 2252-2256.

Das, M. and Chakraborty, D. 2008. Evaluation of improvement of physical and mechanical properties of bamboo fibers due to alkali treatment. *Journal of applied polymer science*, 107 (1): 522-527.

Davis, T. A., Volesky, B. and Mucci, A. 2003. A review of the biochemistry of heavy metal biosorption by brown algae. *Water research*, 37 (18): 4311-4330.

Devnarain, P., Arnold, D. and Davis, S. 2002. Production of activated carbon from South African sugarcane bagasse. In: Proceedings of *Proc S Afr. Sug. Technol. Ass*. Citeseer, 477-489.

Dialynas, E. and Diamadopoulos, E. 2009. Integration of a membrane bioreactor coupled with reverse osmosis for advanced treatment of municipal wastewater. *Desalination,* 238 (1-3): 302-311.

Duranoğlu, D., Trochimczuk, A. W. and Beker, U. 2012. Kinetics and thermodynamics of hexavalent chromium adsorption onto activated carbon derived from acrylonitrile-divinylbenzene copolymer. *Chemical Engineering Journal*, 187: 193-202.

El-Naas, M. H. and Alhaija, M. A. 2011. Modelling of adsorption processes. *Mathematical Modelling*: 1-22.

Fernández, Y., Maranon, E., Castrillón, L. and Vázquez, I. 2005. Removal of Cd and Zn from inorganic industrial waste leachate by ion exchange. *Journal of hazardous materials,* 126 (1-3): 169-175.

Foo, K. Y. and Hameed, B. H. 2010. Insights into the modeling of adsorption isotherm systems. *Chemical engineering journal*, 156 (1): 2-10.

Fortunati, E., Puglia, D., Monti, M., Peponi, L., Santulli, C., Kenny, J. and Torre, L. 2013. Extraction of cellulose nanocrystals from Phormium tenax fibres. *Journal of Polymers and the Environment,* 21 (2): 319-328.

Freundlich, H. 1906. Over the adsorption in solution. *J. Phys. chem,* 57 (385471): 1100-1107.

Garside, P. and Wyeth, P. 2003. Identification of cellulosic fibres by FTIR spectroscopy-thread and single fibre analysis by attenuated total reflectance. *Studies in conservation,* 48 (4): 269-275.

Gourdon, R., Bhende, S., Rus, E. and Sofer, S. S. 1990. Comparison of cadmium biosorption by Gram-positive and Gram-negative bacteria from activated sludge. *Biotechnology letters*, 12 (11): 839-842.

Ho, Y.-S. and McKay, G. 1999. Pseudo-second order model for sorption processes. *Process biochemistry*, 34 (5): 451-465.

Jackson, M. 1977. The alkali treatment of straws. *Animal Feed Science and Technology*, 2 (2): 105-130.

Johar, N., Ahmad, I. and Dufresne, A. 2012. Extraction, preparation and charactrization of cellulose fibres and nanocrystals from rice husk. *Ind. Crops Prod.*, 37 (1): 93-99.

Kadirvelu, K. and Namasivayam, C. 2003. Activated carbon from coconut coirpith as metal adsorbent: adsorption of Cd (II) from aqueous solution. *Advances in Environmental Research*, 7 (2): 471-478.

Kalyani, S., Priya, J. A., Rao, P. S. and Krishnaiah, A. 2003. Adsorption of nickel on flyash in natural and acid treated forms. *Indian Journal of Environmental Health*, 45 (3): 163-168.

Kandah, M. I. 2004. Zinc and cadmium adsorption on low-grade phosphate. *Separation and Purification Technology*, 35 (1): 61-70.

Kumar, A., Negi, Y. S., Choudhary, V. and Bhardwaj, N. K. 2014a. Characterization of cellulose nanocrystals produced by acid-hydrolysis from sugarcane bagasse as agro-waste. *Journal of Materials hysics and Chemistry*, 2 (1): 1-8.

Kumar, A., Negi, Y. S., Choudhary, V. and Bhardwaj, N. K. 2014b. Characterization of cellulose nanocrystals produced by acid-hydrolysis from sugarcane bagasse as agro-waste. *Journal of materials physics and chemistry*, 2 (1): 1-8.

Lagergren, S. K. 1898. About the theory of so-called adsorption of soluble substances. *Sven. Vetenskapsakad. Handingarl*, 24: 1-39.

Lasheen, M., Sharaby, C., El-Kholy, N., Elsherif, I. and El-Wakeel, S. 2008. Factors influencing lead and iron release from some Egyptian drinking water pipes. *Journal of hazardous materials*, 160 (2-3): 675-680.

Latour, R. A. 2015. The Langmuir isotherm: a commonly applied but misleading approach for the analysis of protein adsorption behavior. *Journal of biomedical materials research part A*, 103 (3): 949-958.

Le Troedec, M., Sedan, D., Peyratout, C., Bonnet, J. P., Smith, A., Guinebretiere, R., Gloaguen, V. and Krausz, P. 2008. Influence of various chemical treatments on the composition and structure of hemp fibres. *Composites Part A: Applied Science and Manufacturing*, 39 (3): 514-522.

Malkoc, E. and Nuhoglu, Y. 2005. Investigations of nickel (II) removal from aqueous solutions using tea factory waste. *Journal of hazardous materials*, 127 (1-3): 120-128.

Mckay, G., Blair, H. and Gardner, J. 1982. Adsorption of dyes on chitin. I. Equilibrium studies. *Journal of applied polymer science*, 27 (8): 3043-3057.

Mebrahtu, G. and Zerabruk, S. 2011. Concentration and health implication of heavy metals in drinking water from urban areas of Tigray region, Northern Ethiopia. *Momona Ethiopian Journal of Science*, 3 (1): 105-121.

Mirbagheri, S. A. and Hosseini, S. N. 2005. Pilot plant investigation on petrochemical wastewater treatmentfor the removal of copper and chromium with the objective of reuse. *Desalination*, 171 (1): 85-93.

Mohsen-Nia, M., Montazeri, P. and Modarress, H. 2007. Removal of Cu2+ and Ni2+ from wastewater with a chelating agent and reverse osmosis processes. *Desalination*, 217 (1-3): 276-281.

Mosier, N., Wyman, C., Dale, B., Elander, R., Lee, Y., Holtzapple, M. and Ladisch, M. 2005. Features of promising technologies for pretreatment of lignocellulosic biomass. *Bioresource technology*, 96 (6): 673-686.

Moubasher, A. H., Abdel-Hafez, S. I. I., Abdel-Fattah, H. M. and Moharram, A. M. 1982. Fungi of wheat and broad-bean straw composts. *Mycopathologia*, 78 (3): 161-168.

Muhamad, H., Doan, H. and Lohi, A. 2010. Batch and continuous fixed-bed column biosorption of Cd2+ and Cu2+. *Chemical Engineering Journal*, 158 (3): 369-377.

Murphy, V., Hughes, H. and McLoughlin, P. 2007. Cu (II) binding by dried biomass of red, green and brown macroalgae. *Water research*, 41 (4): 731-740.

Ngah, W. W. and Hanafiah, M. M. 2008. Removal of heavy metal ions from wastewater by chemically modified plant wastes as adsorbents: a review. *Bioresource technology*, 99 (10): 3935-3948.

Niu, X., Zheng, L., Zhou, J., Dang, Z. and Li, Z. 2014. Synthesis of an adsorbent from sugarcane bagass by graft copolymerization and its utilization to remove Cd (II) ions from aqueous solution. *Journal of the Taiwan Institute of Chemical Engineers*, 45 (5): 2557-2564.

Pagano, M., Petruzzelli, D., Tiravanti, G. and Passino, R. 2000. Pb/Fe separation and recovery from automobile battery wastewaters by selective ion exchange. *Solvent extraction and ion exchange*, 18 (2): 387-399.

Pandey, A., Soccol, C. R., Nigam, P. and Soccol, V. T. 2000. Biotechnological potential of agro-industrial residues. I: sugarcane bagasse. *Bioresource technology*, 74 (1): 69-80.

Park, S., Baker, J. O., Himmel, M. E., Parilla, P. A. and Johnson, D. K. 2010. Cellulose crystallinity index: measurement techniques and their impact on interpreting cellulase performance. *Biotechnology for biofuels*, 3 (1): 1-10.

Puranik, P., Modak, J. and Paknikar, K. 1999. A comparative study of the mass transfer kinetics of metal biosorption by microbial biomass. *Hydrometallurgy*, 52 (2): 189-197.

Ray, D. and Sarkar, B. 2001. Characterization of alkali-treated jute fibers for physical and mechanical properties. *Journal of Applied Polymer Science*, 80 (7): 1013-1020.

Reategui, M., Maldonado, H., Ly, M. and Guibal, E. 2010. Mercury (II) biosorption using Lessonia sp. kelp. *Applied biochemistry and biotechnology*, 162 (3): 805-822.

Rezende, C. A., De Lima, M. A., Maziero, P., deAzevedo, E. R., Garcia, W. and Polikarpov, I. 2011. Chemical and morphological characterization of sugarcane bagasse submitted to a delignification process for enhanced enzymatic digestibility. *Biotechnology for biofuels*, 4 (1): 1-19.

Ristolainen, M., Alén, R., Malkavaara, P. and Pere, J. 2002. Reflectance FTIR microspectroscopy for studying effect of xylan removal on unbleached and bleached birch kraft pulps.

Saïd Azizi Samir, M. A., Alloin, F., Paillet, M. and Dufresne, A. 2004. Tangling effect in fibrillated cellulose reinforced nanocomposites. *Macromolecules*, 37 (11): 4313-4316.

Sain, M. and Panthapulakkal, S. 2006. Bioprocess preparation of wheat straw fibers and their characterization. *Industrial crops and products*, 23 (1): 1-8.

Sankhla, M. S., Kumari, M., Nandan, M., Kumar, R. and Agrawal, P. 2016. Heavy metals contamination in water and their hazardous effect on human health-a review. *Int. J. Curr. Microbiol. App. Sci (2016)*, 5 (10): 759-766.

Siqueira, G., Milagres, A. M., Carvalho, W., Koch, G. and Ferraz, A. 2011. Topochemical distribution of lignin and hydroxycinnamic acids in sugar-cane cell walls and its correlation with the enzymatic hydrolysis of polysaccharides. *Biotechnology for biofuels*, 4 (1): 1-9.

Srilatha, H., Nand, K., Babu, K. S. and Madhukara, K. 1995. Fungal pretreatment of orange processing waste by solid-state fermentation for improved production of methane. *Process Biochemistry*, 30 (4): 327-331.

Stephenson, E., Nathoo, N., Mahjoub, Y., Dunn, J. F. and Yong, V. W. 2014. Iron in multiple sclerosis: roles in neurodegeneration and repair. *Nature Reviews Neurology*, 10 (8): 459-468.

Sud, D., Mahajan, G. and Kaur, M. 2008. Agricultural waste material as potential adsorbent for sequestering heavy metal ions from aqueous solutions–A review. *Bioresource technology*, 99 (14): 6017-6027.

Sun, F. and Chen, H. 2007. Evaluation of enzymatic hydrolysis of wheat straw pretreated by atmospheric glycerol autocatalysis. *Journal of Chemical Technology & Biotechnology: International Research in Process, Environmental & Clean Technology*, 82 (11): 1039-1044.

Swatloski, R. P., Spear, S. K., Holbrey, J. D. and Rogers, R. D. 2002. Dissolution of cellose with ionic liquids. *Journal of the American chemical society*, 124 (18): 4974-4975.

Tao, H.-C., Zhang, H.-R., Li, J.-B. and Ding, W.-Y. 2015. Biomass based activated carbon obtained from sludge and sugarcane bagasse for removing lead ion from wastewater. *Bioresource technology*, 192: 611-617.

Üçer, A., Uyanık, A., Cay, S. and Özkan, Y. 2005. Immobilisation of tannic acid onto activated carbon to improve Fe (III) adsorption. *Separation and Purification Technology*, 44 (1): 11-17.

Wang, H., Xu, J.-Z., Zhu, J.-J. and Chen, H.-Y. 2002. Preparation of CuO nanoparticles by microwave irradiation. *Journal of crystal growth*, 244 (1): 88-94.

Wang, J. and Chen, C. 2006. Biosorption of heavy metals by Saccharomyces cerevisiae: a review. *Biotechnology advances*, 24 (5): 427-451.

Wang, W.-m., Cai, Z.-s., Yu, J.-y. and Xia, Z.-p. 2009. Changes in composition, structure, and properties of jute fibers after chemical treatments. *Fibers and Polymers*, 10 (6): 776-780.

Wang, Y.-S., Koo, W.-M. and Kim, H.-D. 2003. Preparation and properties of new regenerated cellulose fibers. *Textile Research Journal*, 73 (11): 998-1004.

Xu, Z., Cai, J.-g. and Pan, B.-c. 2013. Mathematically modeling fixed-bed adsorption in aqueous systems. *Journal of Zhejiang University SCIENCE A*, 14 (3): 155-176.

Xu, Z., Wang, Q., Jiang, Z., Yang, X.-x. and Ji, Y. 2007. Enzymatic hydrolysis of pretreated soybean straw. *Biomass and Bioenergy*, 31 (2-3): 162-167.

Zhang, Y. H. P. and Lynd, L. R. 2004. Toward an aggregated understanding of enzymatic hydrolysis of cellulose: noncomplexed cellulase systems. *Biotechnology and bioengineering*, 88 (7): 797-824.